STABILIZATION OF EXPANSIVE SOILS BY USING RED MUD

A THESIS SUBMITTED TO
THE GRADUATE SCHOOL OF NATURAL AND APPLIED SCIENCES
OF
MIDDLE EAST TECHNICAL UNIVERSITY

BY

CEMRE ÇAĞLAR

IN PARTIAL FULFILLMENT OF THE REQUIREMENTS
FOR
THE DEGREE OF MASTER OF SCIENCE
IN
CIVIL ENGINEERING

SEPTEMBER 2019

Approval of the thesis:

STABILIZATION OF EXPANSIVE SOILS BY USING RED MUD

submitted by **CEMRE ÇAĞLAR** in partial fulfillment of the requirements for the degree of **Master of Science in Civil Engineering Department, Middle East Technical University** by,

Prof. Dr. Halil Kalıpçılar
Dean, Graduate School of **Natural and Applied Sciences** _____

Prof. Dr. Ahmet Türer
Head of Department, **Civil Engineering** _____

Prof. Dr. Erdal Çokça
Supervisor, **Civil Engineering, METU** _____

Examining Committee Members:

Prof. Dr. Tamer Topal
Geological Engineering, METU _____

Prof. Dr. Erdal Çokça
Civil Engineering, METU _____

Assoc. Prof. Dr. Nejan Huvaj Sarıhan
Civil Engineering, METU _____

Assoc. Prof. Dr. Zeynep Gülerce
Civil Engineering, METU _____

Assoc. Prof. Dr. Abdullah Sandıkkaya
Civil Engineering, Hacettepe University _____

Date: 06.09.2019

I hereby declare that all information in this document has been obtained and presented in accordance with academic rules and ethical conduct. I also declare that, as required by these rules and conduct, I have fully cited and referenced all material and results that are not original to this work.

Name, Surname: Cemre Çağlar

Signature:

ABSTRACT

STABILIZATION OF EXPANSIVE SOILS BY USING RED MUD

Çağlar, Cemre
Master of Science, Civil Engineering
Supervisor: Prof. Dr. Erdal Çokça

September 2019, 113 pages

Expansive soils are generally existing in semi-arid and arid regions of the world. This type of soils expands when they absorb water and shrink when they dry out. Expansive soils are causing problems to the lightweight structures. The purpose of the study is to suggest a cost-effective alternative method for coping with these problems. The widely used traditional method is the stabilization of the soil with the chemical admixtures. In this study; waste red mud and waste fly ash were used as stabilizers. The expansive soil is prepared in the laboratory conditions, as a mixture of the kaolinite and bentonite. In the previous studies; fly ash, lime and cement are used for improving the swelling and strength properties of the soil. This study examines the effect of red mud as a stabilization material for soil. The admixtures were added to the soil in different percentages and separately to compare the effect of the admixtures. Grain size distributions, consistency limits, swelling percentage, rate of swell, uniaxial compressive strengths, direct and split tensile strengths of the samples were determined. Specimens were evaluated by their swelling percentages, swelling rates, undrained shear strengths and tensile strengths. These criteria show the effectiveness of the stabilizers. The results of the study prove that undrained shear strength is increased to 4 times of Sample A's value, while swelling potential decreased to 1/3 times and rates decreased 1/4 times of it, with addition of red mud, fly ash and cement.

Keywords: Cement, Lime, Swelling Potential, Swelling Soils, Soil Stabilization, Waste Fly Ash, Waste Red Mud

ÖZ

ŞİŞEN KİLLİ ZEMİNLERİN KIZIL ÇAMUR İLE STABİLİZASYONU

Çağlar, Cemre
Yüksek Lisans, İnşaat Mühendisliği
Tez Danışmanı: Prof. Dr. Erdal Çokça

Eylül 2019, 113 sayfa

Şişen killi zeminler genellikle Dünya'nın kurak ve yarı kurak iklimlerinde bulunmaktadır. Bu tip zeminler su aldığında şişip, içerisindeki suyu dışarı attığında büzüşmektedir. Şişen zeminler hafif yapılarda sorunlara neden olmaktadır. Bu çalışmanın amacı, bu problemlerle başa çıkmak için, ekonomik açıdan uygun alternatif bir yöntem önermektir.. Geleneksel ve yaygın olarak kullanılan yöntem, zeminin çeşitli katkı maddeleri ile iyileştirmesi yöntemidir. Bu araştırmada, kızıl çamur ve atık uçucu kül iyileştirici katkı maddeleri olarak kullanılmıştır. Şişen killi zemin, kaolin ve bentonit karıştırılarak, laboratuvar ortamında hazırlanmıştır. Daha önce yapılan çalışmalarda; uçucu kül, kireç ve çimento zeminin şişme ve dayanıklılık özelliklerinin iyileştirilmesi için kullanılmıştır. Bu çalışmada kızıl çamurun zemin iyileştirmesi amacıyla kullanımının etkileri incelenmiştir. Katkı maddeleri zemine farklı yüzdelerde ve ayrı ayrı eklenerek karışımların etkileri gözlenmiştir. Hazırlanan numunelerin tane boyutu dağılımları, kıvam limitleri, şişme yüzdeleri, şişme hızları, tek eksenli basınç dayanımları, direkt ve yarma çekme dayanımları belirlenmiştir. Numuneler şişme yüzdeleri, şişme hızları, drenajsız kayma mukavemetleri ve çekme mukavemetlerine göre değerlendirilmiştir. Bu kriterler eklenen maddelerin etkilerini göstermektedir. Bu çalışmanın sonuçları; kızıl çamur, uçucu kül ve çimento eklenmesiyle, A numunesinin drenajsız kayma mukavemetinin 4 kat arttığını, şişme yüzdesinin 3 kat azaldığını ve şişme süresinin 4 kat azaldığını kanıtlamıştır.

Anahtar Kelimeler: Atık Kızıl Çamur, Atık Uçucu Kül, Çimento, Kireç, Şişen Zeminler, Şişme Potansiyeli, Zemin İyileştirmesi

To My Family

ACKNOWLEDGEMENTS

I wish to express my respectful gratitude to my supervisor Prof. Dr. Erdal Çokça for his patient, encouraging and supportive guidance during the research, and experiments and preparation of this thesis.

I would like to thank to my instructors in METU for their helpful approaches to improve my engineering notion throughout my engineering education.

My thankfulness goes to geological engineer Mr. Ulaş Nacar for his support on theory of the laboratory works. Also, I would like to thank to the METU Soil Mechanics Laboratory staff Mr. Kamber Bilgen for his support on application of the laboratory works.

I would like to thank to my family for encouraging me and giving valuable and endless support throughout the study.

I wish to gratefully acknowledge my friends, Şükrü Şadi Kahraman and Serkan Gökmener for their support throughout my life.

TABLE OF CONTENTS

LIST OF TABLES

TABLES

LIST OF FIGURES

FIGURES

LIST OF ABBREVIATIONS

ABBREVIATIONS

ACAA	: American Coal Ash Association
C	: Cement
ECOBA	: European Coal Combustion Products association
FA	: Fly ash
L	: Lime
LL	: Liquid Limit
MDD	: Maximum dry density
NLA	: National Lime Association
OMC	: Optimum moisture content
PI	: Plasticity Index
PL	: Plastic Limit
RM	: Red mud
S	: Swell percent
SL	: Shrinkage Limit
USCS	: Unified Soil Classification System
w	: Water content
XRF	: X-ray fluorescence

LIST OF SYMBOLS

SYMBOLS

Å	: Angstrom
ΔH	: change in the length
A_c	: Activity of clay
A_{neck}	: cross sectional area of the neck of the 8-shaped specimen
$F_{max,dt}$	: The maximum load that the 8-shaped specimen can carry
H	: initial length
c_u	: undrained shear strength
q_u	: maximum load in unconfined compression test
σ	: tensile stress at the cylindrical specimen
σ_{max}	: maximum tensile stress at the cylindrical specimen
$\sigma_{max,dt}$	: maximum direct tensile stress at the neck of the specimen

CHAPTER 1

INTRODUCTION

1.1. Objective of The Study

In the semi-arid and arid regions of the world; some partially saturated clays are showing different responses to the change of the water conditions. Such clays, expand when they absorb water and shrink when they dry out, called as “swelling soils”.

The effects of swelling can be observed in lightweight mat foundations (Figure 1-1 and Figure 1-2), pavements, railway and highway embankments (Figure 1-3), slab-on-grade members, and hydraulic water lines. Lightweight structures are very sensitive to even small changes of the volume of soil (Figure 1-4). The purpose of the study is coping with these problems by suggesting cost-effective alternative before the construction stage.

Red mud is a highly alkaline (pH > 11) industrial solid waste produced by aluminum factories during extraction of alumina using Bayer process. The unutilized red mud is stored either in slurry form or in dry stacking takes vast tract of usable land and has an adverse effect on the quality of ground water, surface water and also on animal and plantation. An attempt is made here to use red mud as an alternative additive material to stabilize expansive soils.

Figure 1-1. Cracked foundation (http://www.etc-web.com/screw-it/)

Figure 1-2. Expansive soils and foundation damage (https://www.njdrybasements.com/)

Figure 1-3. Soil and pavement cracks in swelling ground (https://www.geoengineer.org)

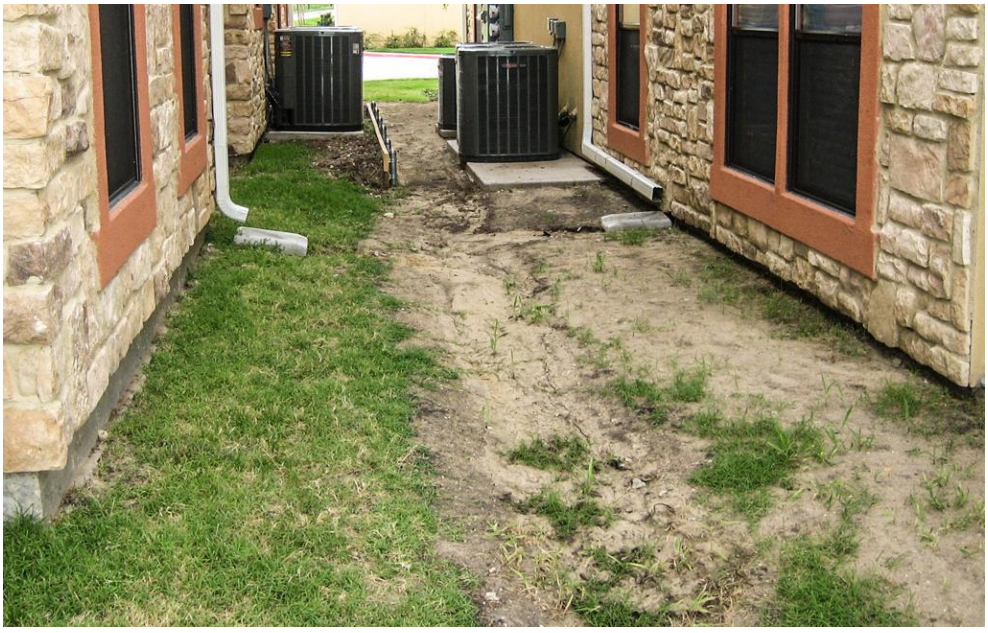

Figure 1-4. Expansive soil problem (https://mrconstructiondefectlaw.com)

The importance of swelling soils under the structures had not been considered before the latter part of 1930. By 1930, interest in swelling soils has increased by the

observation of The U. S. Bureau of Reclamation in the foundation damage of the steel siphon of Owyhee Project in Oregon. Today, the engineers from all over the world take the swelling soil into consideration (Chen, 1975).

The annual costs due to the cracks on the structures are exceeding the other natural disasters such as floods, hurricanes, earthquakes and tornados (Chen,1975), which is shown in Table 1.1. The early investigation of soils about swelling is very important. Although the precautions against swelling are costly, the repairing costs of the structures on the swelling soils are much more costly (Nelson, Chao, Overton, & Nelson, 2015). In order not to face with the after-construction costs, the swelling related problems are seriously considered at the investigation step of the projects.

Table 1.1. *Annual loss values due to swelling soils (Jones and Holtz, 1973)*

Construction Category	**Estimated average annual loss, millions of dollars**
Single-family homes	300
Commercial buildings	360
Multi-story buildings	80
Walks, drives, parking areas	110
Highway and streets	1,140
Underground utilities and service	100
Airports	40
Urban landslides	25
Others	100
TOTAL	2,255

Geotechnical engineers may improve the engineering properties of the swelling soils, by changing the chemical composition of the soil, when they face with them on the construction sites.

1.2. Scope of the Study

This study examines the effect of red mud and fly ash as stabilization materials for expansive soils. In addition to these waste materials, lime and cement were also used for increasing the stabilizing effect of the waste materials. The expansive soil is

prepared in the laboratory conditions, as a mixture of the kaolinite and bentonite. The admixtures are added to the soil in different percentages and separately to compare the effect of the admixtures. Grain size distributions, consistency limits, swelling percentages, rates of swell, permeabilities, optimum water contents, maximum dry densities, uniaxial compressive strengths, direct and split tensile strengths of the samples were determined. Specimens are evaluated by its swelling percentages, swelling rates, undrained shear strengths and tensile strengths.

1.3. General Information about Swelling Soils

Swelling soils are identified by its sensitivity to the changing water content. This type of soils expands in volume when they absorb water and shrinks when they dry out. This characteristic of the soil is hazardous for the structures on it due to the huge uplift forces caused by the volume expansion. The swelling mechanism of the soil is caused by its chemical structure.

The swelling of soils causes problems mostly for lightweight structures on them. Heavyweight structure loads are commonly bigger than the swelling pressure of the soil. (Marr, Gilbert, & Rauch, 2004). This situation reveals the importance of identifying the swelling soil and improving it.

There are many empirical correlations that are used to define the soil as “swelling” or not. The visual indications of the swelling soil are (Charlie, Osman, & Ali, 1984):

1- Wide and deep shrinkage cracks during dry periods
2- Soil “rock hard” when dry, but very sticky and soft when wet
3- Observed expansive soil damage to other structures in the area.

When the natural environmental conditions change, which results in the alteration of the water content in the soil, this type of soil shows large volume change. This type of soil is generally found in regions, which have tropical climate conditions (Dakshinamurthy & Raman, 1977). Additionally, these soils are encountered in different regions all over the World.

In order to identify the swelling soil, at present, there is no universally accepted simple procedure. For this reason, the Liquid Limit, Plasticity Index, and Shrinkage Index values have been tried to be used for determining the swelling characteristic of the soil (Dakshinamurthy & Raman, 1977).

1.4. Clay Mineralogy

Clay is a term that is used to describe a particle size (smaller than 2 μm) but it also describes mineral composition. The formation of the soil is the destructive process of rock by chemical or physical weathering of the rocks. Mostly the clays are formed by the chemical weathering due to the action of water of the parent rock. These clay particles are generally plate-like structures, whereas the long "needle-shaped particles can also occur but it is rare (Craig & Knappett, 2012).

Most clay minerals have basic structures that are formed by a silicon-oxygen tetrahedron and aluminum-hydroxyl octahedron (Figure 1-5(a)). Both units have valency imbalances and that results in a negative charge. Because of this, they combine to form a sheet structure. Silica sheets are formed by a combination of the tetrahedral units by sharing oxygen atoms, while gibbsite sheets are formed by a combination of the octahedral units by hydroxyl ions. The silica sheet has a net negative charge, but the gibbsite sheet stays electrically neutral. The sheet structures are represented symbolically in Figure 1-5 (Craig & Knappett, 2012).

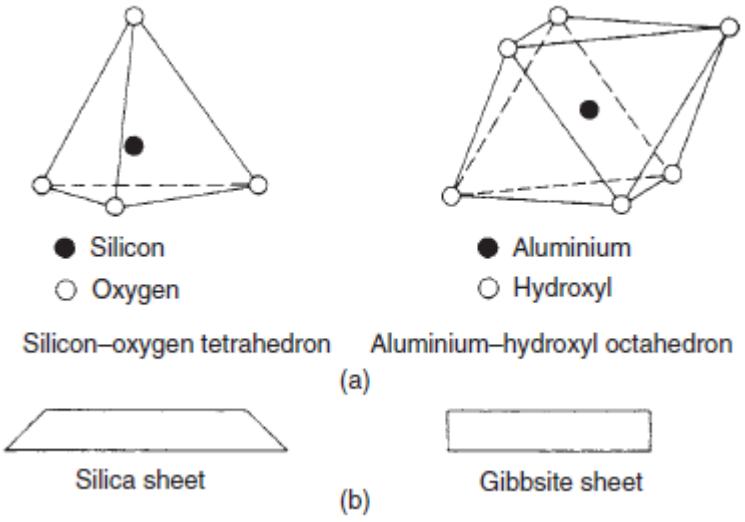

Figure 1-5. Basic units of the clay minerals (Craig & Knappett, 2012)

The layered structure of clay minerals is matching a gibbsite sheet and one or two silica sheet. The arrangement of the sheets is determining the type of clay. The symbolic representation of the minerals is shown in Figure 1-6. The kaolinite layers are consisting of one silica and one gibbsite sheet, while illite and montmorillonite sheets are consisting of one gibbsite sheet is squeezed by two silica sheets.

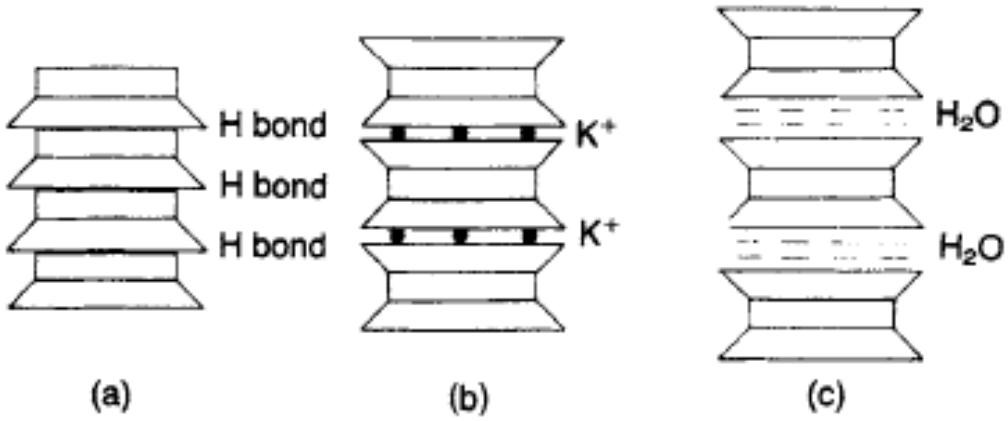

Figure 1-6. Clay minerals (a)kaolinite (b)illite (c)montmorillonite (Craig, 2004)

The structural unit of the kaolinite mineral is the combination of one silica and one gibbsite sheet (Grim, 1953). The layers are held together with the force of hydrogen

bonds between hydroxyl ions of the octahedral sheet of one layer and the oxygen ions of the tetrahedral sheet of the adjacent layer. The thickness of the layer is about 7.1 Å. The kaolinites have very stable lattices because the bonding force between the units does not allow the water to penetrate in them. Kaolinites are principally formed by weathering of feldspars, feldspathoids and muscovite under acidic conditions. It is the most stable clay mineral due to its chemical structure. Kaolinites are used in paints, paper and in pottery and pharmaceutical industries. The chemical formula of the kaolinite is $(OH)_8Al_4Si_4O_{10}$.

The structural unit of the illite mineral is the combination of one gibbsite sheet squeezed by two silica sheets (Grim, 1953) The interlayer cation in illite is potassium. The size and charge of the potassium fit it to the hexagonal ring of the oxygen atoms of the adjacent layers. Sharing Potassium atoms between the silica sheets produces strong bonds. This structure provides ionic bonds between layers, so water and other cations cannot easily fill the interlayer spaces (Grim, 1953). The thickness of the layer is about 10 Å. The chemical formula of the illite is $K_{0.65}Al_{2.0}[Al_{0.65}Si_{3.35}O_{10}](OH)_2$. The illite has stable lattices.

The structural unit of the montmorillonite has the same base structure as illite. The interlayer structure is different than illite. The exchangeable cations other than potassium and water molecules are occupying the space between the layers. Thus, the kaolinite and illite minerals exhibit less expansive behavior than montmorillonite (Grim et al.,1937) (Figure 1-6(c)). This situation results in weak bonding forces between the layers. The thickness of the layer is about 12-15 Å when air-dried and 10 Å when oven-dried. The montmorillonites form in an alkaline environment. The rocks, that do not contain alkali and alkaline earth, can only produce kaolinite type clay minerals (Grim, 1953). The chemical formula of the montmorillonite is $(OH)_4Al_4Si_8O_{20}\cdot nH_2O$. The montmorillonite is highly reactive clay mineral.

Bentonite is a special type of montmorillonite. Bentonite has very high plasticity and very high swelling potential. It is widely used for a variety of purposes, such as drilling

mud, slurry walls, and clarification of beer and wine, seepage barriers. It has LL of 500% or more (Mitchell & Soga, 2006). Bentonites are linked with the underground and slope stability problems by the presence of bentonite in joints and faults (Brekke & Selmer-Olsen, 1965).

1.5. Mechanism of Swelling

The swelling mechanism of the soil is directly linked with 3 factors (Popescu, 1986):

1- Potentially unstable and partially saturated clay
2- Critical increase in soil water content
3- The value of applied stress, which is lower than the soil's swelling pressure

When these 3 conditions are present, the swelling occurs. The water is filling the spaces between and in the layers of the clay structures. The repulsive forces are increasing, and the soil expands in volume.

The swelling mechanism of the soil is directly related to the hydration of adsorbed cations and osmotic attraction in clay micelle (Norrish, 1954). The clay micelle is a term that represents the negatively charged inner clay particle core, surrounded by positively charged cations with water of hydration and osmotic water that is held closely to the inner mineral core (Lambe & Whitman, 1969).

The thickness of the water and cations are primarily influenced by the type of cations and electrical surface charges on the particles. It is not influenced greatly by the thickness of the particles. Kaolinite and montmorillonite micelle thicknesses are described for w>LL in Figure 1-7(a), w=LL in Figure 1-7(b) and w<LL in Figure 1-7(c) (Lambe & Whitman, 1969). The micelle thickness increase with the water content is much higher in montmorillonite. So, the swelling of the montmorillonite is more critical in all other types of clays.

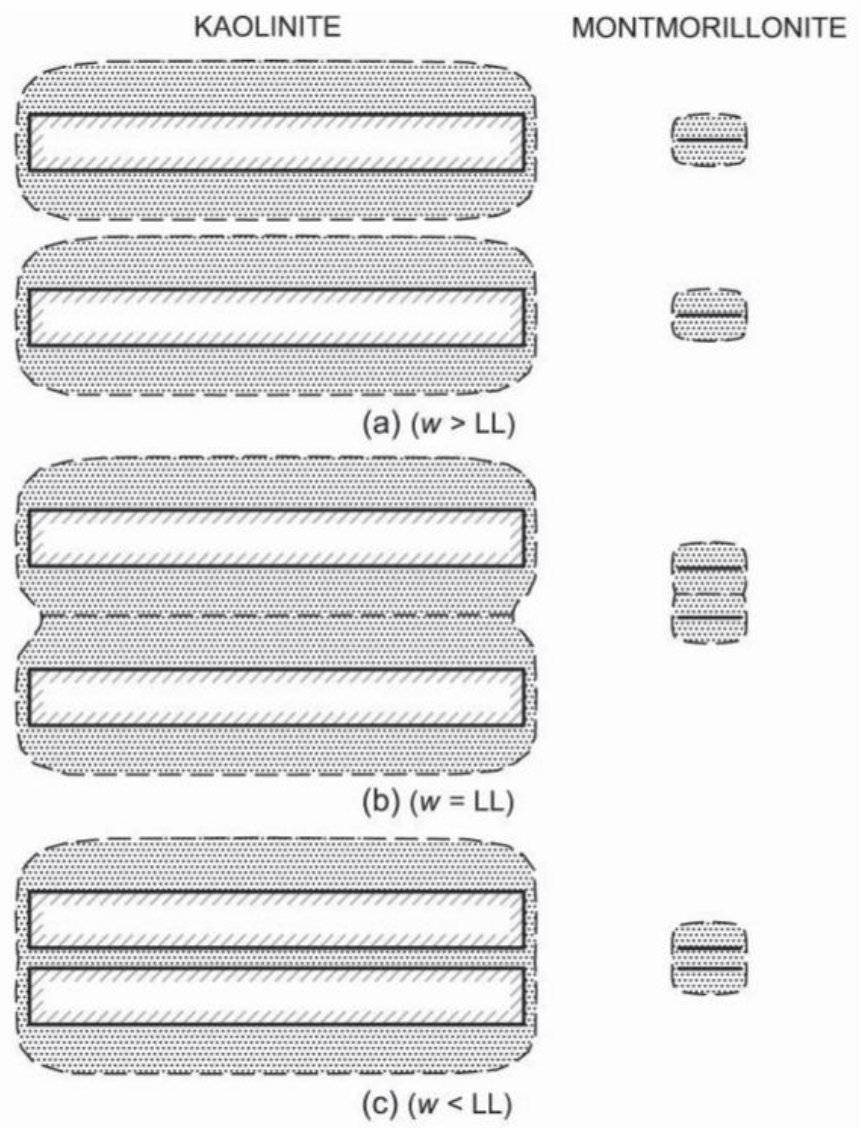

Figure 1-7. Kaolinite and montmorillonite micelles (a)w>LL (b)w=LL (c)w<LL (Lambe & Whitman, 1969)

The swelling of montmorillonite is taking place in two distinct ways, crystalline, and osmotic expansion. When the distance between the particles is smaller than 22 Å, the expansion is dependent on the hydration energy of the cation. When the distance between the particles is greater than 35 Å, the montmorillonite develops the rest of the expansion. Because of the hydration requires much more energy, the added water

firstly hydrating the cations and this phase is called “crystalline”. After that phase, subsequent swelling is called “osmotic” (Slade, Quirk, & Norrish, 1991).

One other suggestion is separating the intercrystalline swelling from intracrystalline swelling by hydration (Popescu, 1986). The two basic mechanisms of swelling by hydration:

1- Interparticle or intercrystalline swelling: This type of swelling can be observed in all type of clays. For the clay in the nearly dry state, the particles are held closely by the capillary tensions. When the water is added to the clay, the forces are relaxed, and the particles are moving away from other particles (Figure 1-8). The perpendicular short lines in Figure 1-8 represents the strong molecular bonds between the layers.
2- Intracrystalline swelling: This type of swelling can be observed in the montmorillonite type of clays mostly. The molecular bonds between the layers are weak due to the presence of cations. The water easily fills the spaces between the layers. The water enters in these clays between the layers, as well as between the particles (Figure 1-8), and makes up the crystalline structure.

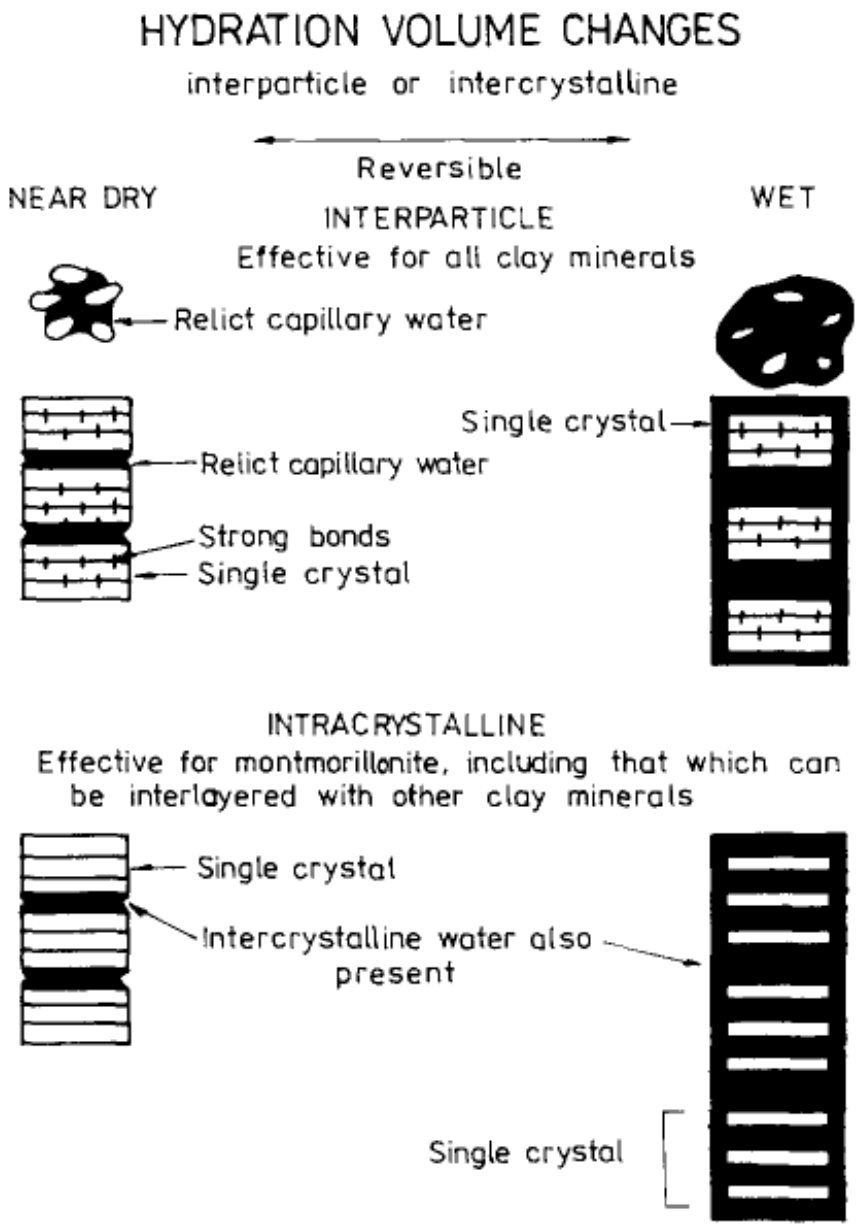

Figure 1-8. Mechanism of swelling by hydration (Popescu, 1986)

The interlayer cations are playing the most important role in intracrystalline swelling mechanism. The swelling of the montmorillonites is chiefly caused by the hydration of cations. As the cation density is increases in the micelle, the swelling potential increases. The clay micelle can contain monovalent and multivalent cations at the

same time. With the increasing valence number of cations, the required number of cations decrease to neutralize the net negative charge on the clay layer surfaces. So, the presence of multivalent cations in montmorillonite decreases its swelling potential (Benson & Meer, 2009).

There can be two reasons for the intracrystalline swelling in montmorillonites:

1- Clay particles have platelets, which are parallel to each other. The negative charges are present on their surfaces and while positive charges are on their edges (Figure 1-9). The positively charged cations are attracted by the surfaces of the clay. And these cations are creating repulsive forces between the layers of the clay particles and the plates are staying apart from the adjacent layers.

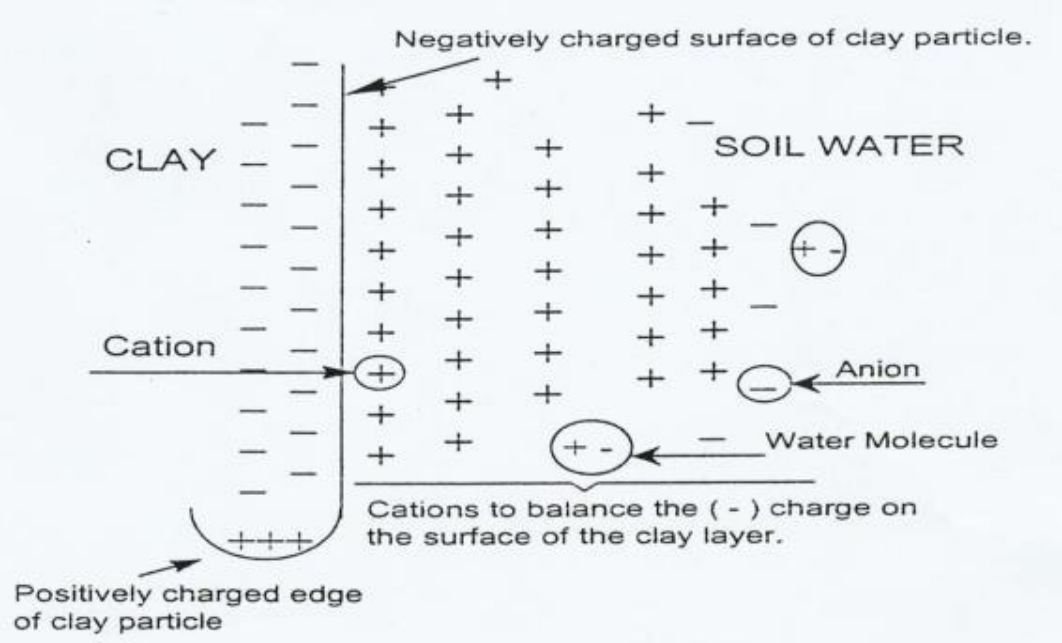

Figure 1-9. The electrochemical system of clay surface (Mitchell, 1976)

2- The other reason is also related to the cations attracted by the clay surface. The cations are creating osmotic pressure between the layers of clay. The cations are not moving outside of the spaces because of the attractive forces. In order to balance the osmotic pressure between the layers, water easily move into the spaces between the layers (Figure 1-10).

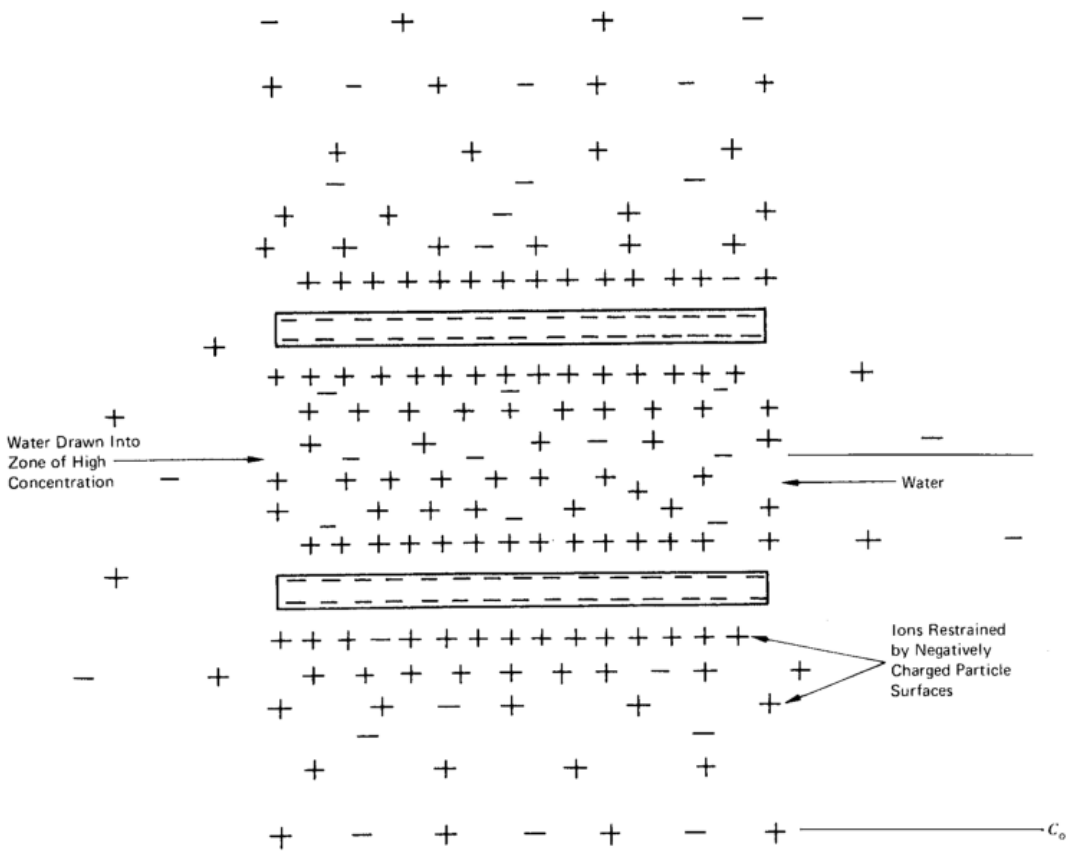

Figure 1-10. Mechanism of osmotic swelling pressure generation in clay (Mitchell and Soga, 2005)

1.6. Factors Affecting Swelling

Researches have been made to understand the mechanism of swelling, the factors that inhibit or trigger the swelling in the soil is determined.

The factors, that are affecting the swelling potential of the clay, can be classified as microscale and macroscale factors. These microscale factors include clay mineralogy, pore fluid chemistry, and soil structure; while macroscale factors, which are affected by the microscale factors, include plasticity, density, and water content (Nelson et al., 2015). In addition to these soil properties; environmental factors such as climate, groundwater, drainage, vegetation, and permeability have an effect on the swell percent of soil as well as the rate of the swell.

The factors that influence the shrink-swell potential of soil and their descriptions are summarized in Table 1-2 and Table 1-3 (Nelson & Miller, 1992).

Table 1-2. *Soil properties that influence shrink-swell potential (Nelson and Miller, 1992)*

Factor	Description
Clay mineralogy	The montmorillonites, vermiculites and some mixed-layer minerals are more susceptible than kaolinites and illites.
Soil water chemistry	The higher cation valence of the adsorbed cations, associated with less swelling.
Soil suction	The soil suction is a stress variable which is related to saturation, gravity, pore size and shape, and electrical and chemical characteristics of the soil particles. As the suction increase, the swell potential will increase.
Plasticity	Plasticity is an indicator of swell potential. The high LL and plasticity values directly linked with the higher swelling potential.
Soil structure and fabric	Flocculated clays tend to be more expansive than the dispersed clays. The aims of the compaction operation are the alteration of clay into a dispersed structure.
Dry density	Higher densities correspond to closer particle spacing and greater repulsive forces. The swelling potential of the clay is increasing with the dry density.

Table 1-3. *Environmental conditions that influence shrink-swell potential (Nelson and Miller, 1992)*

Factor	Description
1. Initial Moisture Condition	The initial moisture content of a soil related to the suction. The higher initial water content of the soil decreases its swelling potential.
2. Moisture Variations	The widest moisture variation in the soil is near the upper part, and the volume change occurs in this part of the soil.
a. Climate	The greatest seasonal heave occurs in semiarid climates, that have short wet periods.
b. Groundwater	Fluctuating water tables contribute more volume change, because of the change of the saturation of the soil.
c. Drainage and manmade water sources	Surface drainage features are the water sources and leakage from these sources are giving access of water to the soil at great depths.
d. Vegetation	The vegetative cover is taking the moisture from the soil and reduce the accessibility of the soil to the water.
e. Permeability	The permeability of the soil increases the accessibility of water to the soil and increases the rate of the swell.
1.1. Temperature	Increasing the temperature cause moisture to diffuse cooler areas under the structures and increase the swelling there.
2. Stress conditions	
2.1. Stress history	As the OCR of the soil increases, the soil regarded to be more expansive. Repeated wetting and drying of soil reduce its swelling potential until a certain number of cycles.
2.2. In situ conditions	The initial stress state is important for determining the volume change behavior of the soil with the effect of these conditions.
2.3. Loading	As the surcharge load on the swelling soil increases, the swelling percent of the soil decreases.
2.4. Soil Profile	The thickness of the expansive layer determines the amount of swelling of the soil. As the thickness increases, the swelling amount of the soil increases.

1.7. Oedometer Methods to Measure Swelling Properties

There are many methods available for predicting the heave of the expansive soils. Although; empirical relationships and suction techniques can be used, Oedometer methods are more practical and widely used methods (Dhowian, 1990).

To understand the behavior of the expansive clays, Oedometer test can be performed. The test procedures, which can be used for determination of the percent of swell, is described with the ASTM D4546-14^{E1} standard. The standard proposes three different methods for determination of the swell percent.

The swell percent, S, can be expressed as:

$$S(\%) = \frac{\Delta H}{H} * 100$$

where,

ΔH : change in the height of the specimen

H : initial height of the specimen

The detailed information about the tests are given in sections 3.4 and 3.5.1. For further information and limitations about the test (please see ASTM D4546-14).

1.7.1. Method A

The oedometer setup is prepared and the seating pressure is applied to the specimen. After the application of the pressure, the water will be added to the setup and the specimen is inundated. The specimen may be swelling or contracting under the constant seating pressure, regarding the type of soil. When the movement nearly remains the same, the swell percent or settlement is measured. This method can be referred to as “wetting-after-loading tests”.

By using this method:

- One-dimensional ground surface heave or settlement due to full wetting after fill construction.
- The swell pressure

can be measured.

The deformation vs. vertical stress graph of 4 specimens with different seating pressures is shown in Figure 1-11. Specimen 1 and 2 show the swelling soil behavior.

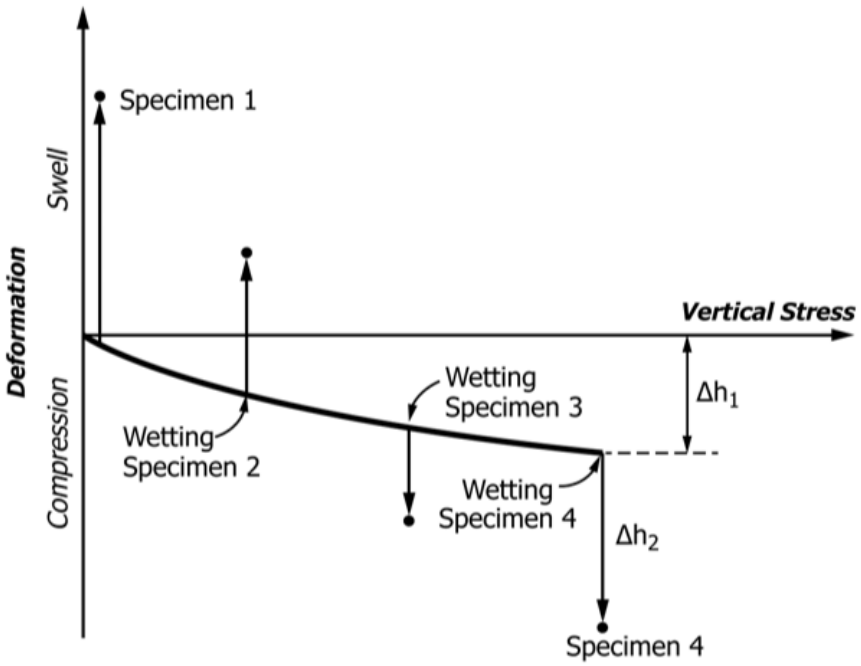

Figure 1-11. Deformation vs. vertical stress, test method A (ASTM D4546)

Δh_1 represents the initial settlement due to the seating pressure application, while Δh_2 is the volume change due to the wetting process in Figure 1-11.

1.7.2. Method B

The oedometer setup is prepared and the predicted in-situ vertical pressure is applied to the specimen corresponding to the sampling depth. After the application of the pressure, the water will be added to the setup and the specimen is inundated. The specimen may be swelling or contracting under the constant vertical in-situ pressure, regarding the type of soil. When the movement nearly remains the same, the swell

percent or settlement is measured. This method can be referred to as “single-point wetting-after-loading tests”.

By using this method:

- If intact specimens from various depths are tested, heave or settlement of the ground surface,
- If the same procedure is used as in Method A, the swell pressure

can be measured.

The deformation vs. vertical stress graph of a specimen for Method B is shown in Figure 1-12.

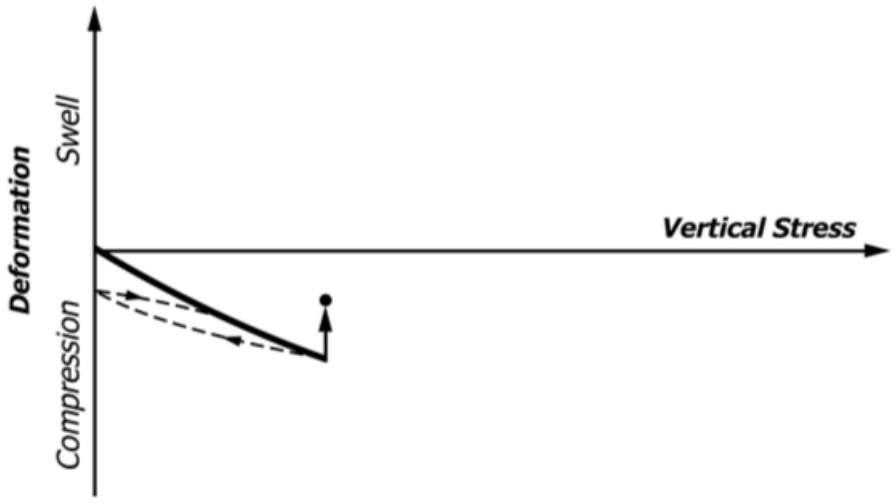

Figure 1-12. Deformation vs. vertical stress, single-point test method B (ASTM D4546)

1.7.3. Method C

The oedometer setup is prepared and the first phase of the experiment is the same as the Method A. The specimen may be swelling or contracting under the constant vertical in-situ pressure, regarding the type of soil. When the movement nearly remains the same, the swell percent or settlement is measured. After determination of the heave, the additional load is applied on the specimen in the same manner as in a consolidation test. This method can be referred to as “loading-after-wetting tests”.

By using this method; load-induced strains after wetting-induced swell or collapse can be measured.

The deformation vs. vertical stress graph of a specimen for Method C is shown in Figure 1-13.

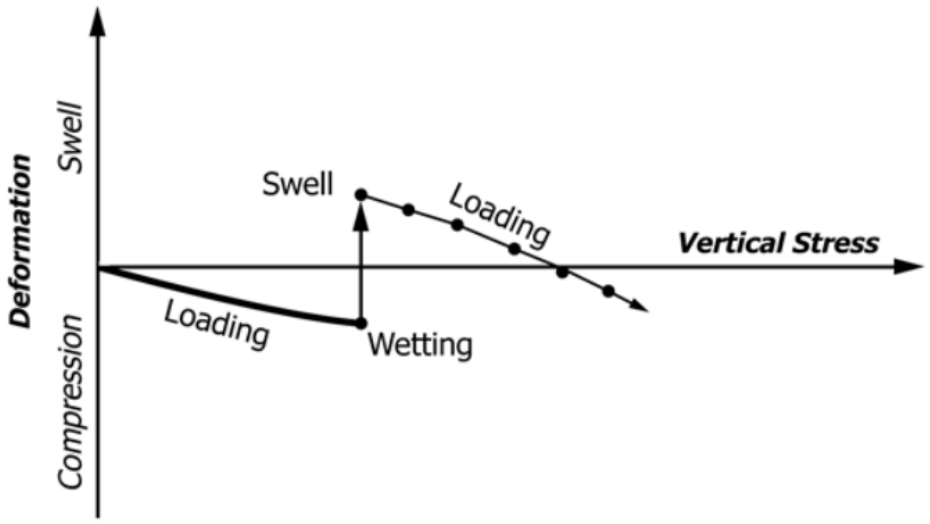

Figure 1-13. Deformation vs. vertical stress, loading-after-wetting test method C (ASTM D4546)

1.8. Determination of Rate of Swell

The only suggestion about the rate of swell determination in literature is, taking the time corresponding to half of the maximum swell occurs (Basma & Tuncer, 1991). Therefore, in this study rate of swell, t_{50}, will be used as an indicator of how rapidly the swelling takes place for specimens.

CHAPTER 2

SOIL STABILIZATION

2.1. General Information about Soil Stabilization

In geotechnical engineering practice, mostly the soil at the site may not be suitable for construction, because of various reasons. In such cases, two alternative methods can be used. The first alternative is designing the superstructure appropriate with the soil conditions at the site. The other alternative is improving the engineering properties of the soil to make it suitable for construction. With regarding the environmental factors, the second alternative may provide the most economical solution. Stabilization of the soil is usually done by mechanical or chemical stabilization. In recent years, thermal and electrical stabilization are also considered and applied (Craig & Knappett, 2012).

The swelling potential of an expansive clay is minimized or eliminated theoretically by using the following methods (Chen, 1975):

- Flooding the soil before construction stage (prewetting)
- Replacing the swelling soil with non-swelling soil (soil replacement)
- Changing the soil properties with chemical additives (chemical stabilization)
- Isolating the soil to prevent it from moisture changes

This study concentrates on the chemical stabilization of the expansive soils. Chemical stabilization is mixing with and injecting the chemical additives to the soil. The most commonly used chemical additives are lime, cement, fly ash, as well as calcium chloride, sodium chloride, and paper mill wastes. The additive type is chosen according to the type of soil, soil conditions, cost, availability, and workability.

In recent years, the usage of industrial waste materials instead of industrial products for stabilizing the swelling soils are taken into consideration seriously. The usage of

waste materials is decreasing the industrial products usage and storage costs of the waste materials (Kamon, Katsumi, & Nontananandh, 1991). This provides more economical solutions for soil stabilization.

In this study, fly ash and red mud were analyzed as waste materials along with industrial products such as lime and cement.

2.2. Stabilization with Lime

The most commonly used stabilization agent is lime for improving the engineering properties of the swelling soils, for a long time. Chinese have used the lime as a chemical stabilizer for centuries. In case the shear strength of the improved soil is not important, lime has been used as a chemical stabilizer (Chen, 1975).

Generally, from 3% to 8% by weight hydrated lime is mixed with the top layer of the expansive soil (Teng, Mattox, & Clisby, 1972).

The lime is not effective stabilizer for all types of soils. The soil with a minimum of 25% of it passes from the No. 200 sieve and PI>10% is regarded as a suitable soil type for lime stabilization (National Lime Association, 2004).

The effectiveness of the lime treatment is influenced by the following factors (Nelson et al., 2015):

- The soil has pH>7 reacts with lime effectively
- Organic carbons inhibiting the lime soil reactions
- Poor drainage increases the reactivity
- Calcareous soils react more rapidly
- Soluble sulfate salts presence is causing ettringite formation sourced heave.

There are two techniques that have been used for the stabilization of expansive clay. The lime column technique is used as a deep improvement of soil, while the lime mixture technique is used as a shallow improvement of soil (Tonoz, Gokceoglu, & Ulusay, 2006).

The lime column technique is applied as the powdered quicklime columns in the drilled holes through the ground. The columns can be drilled to the required depths (Rogers & Bruce, 1991). The stabilization process is mainly controlled by the migration of lime from the columns through the soil (Rogers & Glendinning, 1997).

The lime mixture technique is the direct mixing of the shallow clay layer under the roads, highway embankments, airports, and canal linings. The stabilization of the soil mixing it with lime has been researched by numerous groups (Bell, 1996; Indraratna, Balasubramanian, & Khan, 1995).

2.2.1. Chemical Composition of Lime

Many types of lime have been used as soil stabilizers and their mineralogical composition provides different improvement characteristics (Table 2.1). In some cases, the dolomitic lime has been used as a stabilizer. The magnesium in the dolomitic lime is effective on the increasing strength of the soil, while it requires more time to react than calcium (Nelson et al., 2015).

Table 2.1. *Lime materials used in soil stabilization (NLA, 2004)*

Type	**Formula**
Quicklime	CaO
Hydrated lime	$Ca(OH)_2$
Dolomitic lime	$CaO \cdot MgO$
Normal hydrated or monohydrated dolomitic lime	$Ca(OH)_2 \cdot MgO$
Pressure hydrated or dehydrated dolomitic lime	$Ca(OH)_2 \cdot Mg(OH)_2$

2.2.2. Chemical Reactions

The addition of lime to clay soil, many chemical reactions such as cation exchange, flocculation-aggregation, lime carbonation, and pozzolanic reaction occur. Because of this, the chemical theory of the reaction of lime with soil is complex (Thompson, 1966). As a result of this complexity, the soil types should be examined carefully, that the soil should not include sulfates, organics, and phosphates, in order to prevent the

soil from the adverse effects of the unexpected chemical reactions. Lime can be mixed with soil dry or in a lime slurry. The fastest way is the dry mixing of lime with soil. Also, enough water must be available in the soil for proper reactions to occur (Nelson & Miller, 1992).

Although lime is not a cementitious material, the pozzolanic reactions between the soil and lime with the presence of water provides the formation of insoluble gel-like material that forms by cement (Amu, Adeyeri, Oduma, & Fayokun, 2008).

Another reaction is the change of the divalent cations in the lime with the monovalent cations, which is present in the soil causing the swelling. Also, by flocculation and aggregation the structure of the soil changes.

By considering all the effects of the lime-soil reactions, the following benefits can be provided by lime stabilization:

- The decrease in the liquid limit and plasticity of the soil
- Decrease in the swelling potential of the soil
- Increase in the shrinkage limit of the soil
- Increase in workability
- Improvement of the soil strength and deformation properties of the soil.

2.3. Stabilization with Cement

Portland cement has been used for soil stabilization for a wide variety of soils, including granular soils, silts, and clays. Portland cement is an appropriate stabilizer for the soils, that the shear strength of the soil should be taken into consideration. It increases the shrinkage limit and shear strength of the soil and improves the resilient modulus of the soil (Chen, 1975; Petry & Little, 2002).

The stabilization process of cement for clays is similar to the stabilization process of lime. Also, the mixing procedure of the cement is similar to a lime. When the lime is not reactive with the soil, generally cement is used as a stabilizer (Mitchell & Raad, 1973).

The important procedure of the cement treatment is the addition of cement and final mixing should be shorter than the lime, due to the early hydration and setting of cement. The other advantage of that is an increase in the strength of the soil (Nelson et al., 2015).

Generally, from 2% to 6% by weight cement is mixed with the top layer of the expansive soil (Chen, 1975).

Treatment of expansive soil with cement provides that the underlying soil of the structures behaves like a rigid slab and that minimizes the cracks on the structures caused by differential heave (Nelson et al., 2015).

The mixing methods, operations, procedures and the total cost of the application are almost the same for lime and cement. The only difference is the cost of the cement and the cost of the lime (Portland Cement Association, 1970).

2.3.1. Chemical Composition of Cement

The clinker of portland cement typically contains 67% CaO, 22% SiO_2, 5% Al_2O_3, 3% Fe_2O_3 and 3% other components, and normally contains alite, belite, aluminate and ferrite as major components. The hardening of the cement paste generally controlled by the reactions between these major components and water (Taylor, 1948).

2.3.2. Chemical Reactions

The chemical reactions in the cement-treated soils are the same as in the lime treated soils. However, the lime treatment is effective on clays; some clayey soils have a high affinity of water and the cement may not hydrate to complete the pozzolanic reactions. The lack of completing the pozzolanic reactions decreases the effectiveness of the stabilization (Mitchell & Raad, 1973).

The hydration of portland cement in expansive clays stimulates the pozzolanic reactions that are resulted in a variety of different compounds and gels (Chen, 1988)

By considering all the effects of the cement-soil reactions, the following benefits can be provided by cement stabilization:

- The decrease in the liquid limit and plasticity of the soil
- Decrease in the swelling potential of the soil
- Increase in the shrinkage limit of the soil
- Increase in workability
- Rapid improvements in the soil strength, and deformation properties of the soil.

2.4. Stabilization with Fly Ash

Fly ash is generally used as an additive for the treatment of soil with lime to increase the pozzolanic reactions. The pozzolanic activity of the silty soil is improved by 50% by using lime-fly ash treatment (Woods, Berry, & Goetz, 1960).

2.4.1. Utilization of Fly Ash

As the fly ash is a waste material, the utilization of it is important for environmental reasons. For the years between 2000 and 2017, the amount of the fly ash that has been produced and has been utilized in the USA are shown in Figure 2-1. While the used amounts of fly ash have not changed at all, the decrease in the produced amount of fly ash increases the percentage of the used amount of it in the produced amount (American Coal Ash Association, 2017).

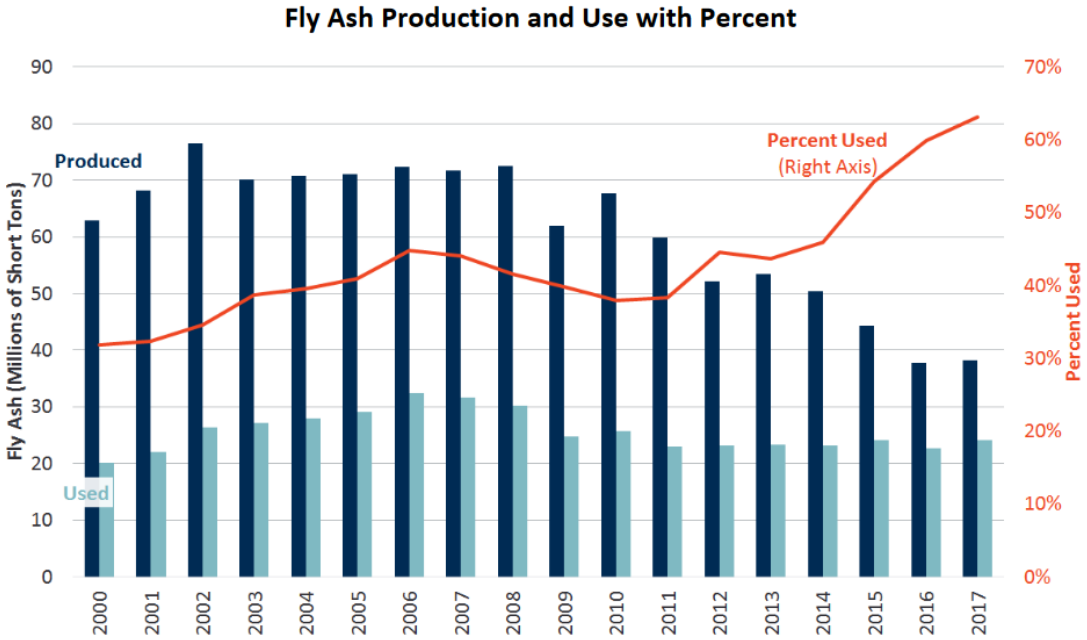

Figure 2-1. Annual fly ash production and utilization amounts in the USA (ACAA, 2017)

In EU countries, approximately 43% of the total production of fly ash is utilized. The utilization applications of the fly ash are an addition in concrete for replacing cement or aggregate or binder material for the road constructions. Also, they can be used as mineral fillers and fertilizers (ECOBA, 2016). The percentages of the utilized fly ash in the construction industry and underground mining can be shown in Figure 2-2.

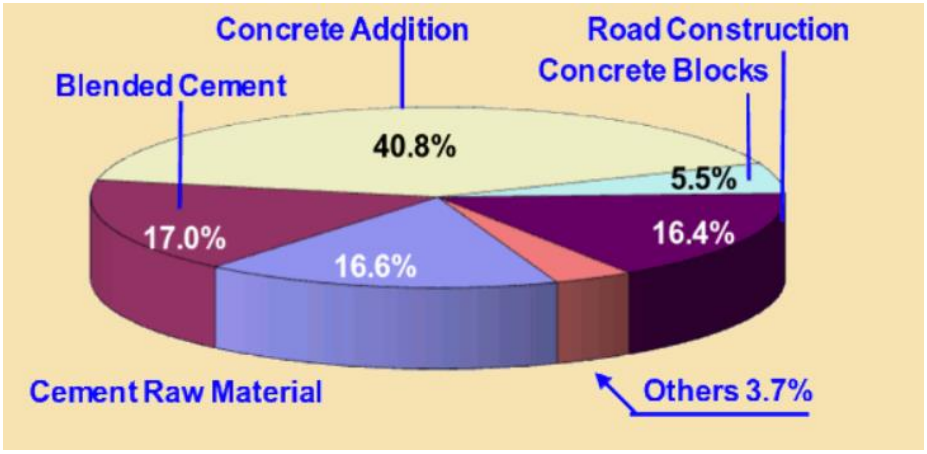

Figure 2-2. Utilization of fly ash in the construction industry and underground mining in Europe (ECOBA, 2016)

2.4.2. Chemical Composition of Fly Ash

Fly ash mainly consists of the silicon and aluminum compounds, and it is a by-product of combustion of coal. There are many types of fly ashes, directly linked with the type of coal that is combusted.

The XRF analysis data of fly ash are summarized in Table 2.2 (Nordin, Abdullah, Tahir, Sandu, & Hussin, 2016).

Table 2.2. *XRF analysis data of fly ash composition (Nordin et al., 2016)*

Composition	**Percentage**
SiO_2	52.11 %
Al_2O_3	23.59 %
Fe_2O_3	7.39 %
TiO_2	0.88 %
CaO	2.61 %
MgO	0.78 %
Na_2O	0.42 %
K_2O	0.80 %
P_2O_5	1.31 %
SiO_3	0.49 %
MnO	0.03 %

There are two major classes of fly ash and both classes can be regarded as pozzolans (Çokça, 2001):

- Class F fly ash: produced from burning anthracite or bituminous coal
- Class C fly ash: produced from burning lignite or sub-bituminous coal

The advantages of using fly ash with lime or cement or both as a stabilizer are (Nelson et al., 2015):

- Reduces the plasticity index, permeability and expansion potential of the soil
- Increases stiffness, strength and freeze-thaw resistance.

2.5. Stabilization with Red Mud

There is limited number of application and research about using the red mud as stabilization additive in literature. In this study, mainly the possibility of using the red mud as stabilizer has been examined.

Since the red mud is waste material, the solution of stabilization of soil with red mud can be inexpensively performed. Also, using this waste material gives an advantage of decreasing the effort of storage of red mud.

2.5.1. Red Mud Production and Environmental Effects

Red mud is the main waste material of the aluminum production industry. The aluminum is obtained from bauxite through the Bayer Process. In the Bayer process of extraction of alumina from bauxite, the insoluble product generated after bauxite digestion with sodium hydroxide at elevated temperature and pressure is known as red mud or bauxite residue (See Appendix for Bayer's process flow chart, chemical process, chemical reactions, and schematic illustration). The red mud, which is the residue of the bauxite, causes serious environmental problems. Approximately, 55-65% of the bauxite is disposed as a red mud through the Bayer Process. The red mud is generally disposed on land or in the isolated dams or disposed in nearby sea or oceans. Due to the high alkalinity caused by ions in it, it has harmful effects on the land, air, and water of the surrounding area (Mahadevan & Ramachandran, 1996).

In recent years; two major accidents occurred in different areas of the World. In 24th February 2018, the storage of the red mud is spilled due to the heavy rainfall in Brazil in Norwegian Hydro Aluminum Factory. The contamination has threatened the ecological life in and around the Amazon River (Figure 2-3). In 4th October 2010, the corner of the reservoir 10 at the Ajka Alumina Plant has collapsed in Hungary (Figure 2-4) and one million m^3 of liquid waste is leaked. Approximately, 40 km^2 area is initially affected by the contamination and the long-term effects are being currently researched.

According to the Mineral Commodity Summaries; each approximately 300,000 tons of bauxite is mined, while approximately 130,000 tons of alumina is produced of that bauxite (US Geological Survey, 2019). The harmful effects of the red mud make utilization of the red mud is an important case by considering the environmental issues.

Each year, ETİ Seydişehir Aluminium plant processes 400,000 tons of bauxite and approximately half of this amount (approximately 200,000 tons) is red mud.

Figure 2-3. Spilled red mud dam in Brazil (Instituto Evandro Chagas, 2018)

Figure 2-4. Collapsed red mud dam in Hungary (Gyoergy Varga /AP)

2.5.2. Utilization of Red Mud

By considering the environmental and cost issues, the utilization of the red mud is important for decreasing the harmful effects of it to the environment and decreasing the cost as substituting the expensive materials.

The possible areas of the utilization of the red mud are as follows (Agrawal, Sahu, & Pandey, 2004):

- Construction materials: bricks, blocks, lightweight aggregates…
- Cement: cement, special cement, additive for cement, mortars, concrete…
- Paint industry: coloring agent
- Paper industry
- Polymer products, ceramics
- The raw material for the steel and iron industry
- And other specific uses.

2.5.3. Chemical Composition of Red Mud

The chemical and mineralogical composition of the red mud can be shown in Table 2.3 and Table 2.4 (Evans, Nordheim, & Tsesmelis, 2016).

Table 2.3. *Chemical composition of red mud*

Component	Typical range (%)
Fe_2O_3	20 - 45
Al_2O_3	10 - 22
TiO_2	4 - 20
CaO	0 - 14
SiO_2	5 - 30
Na_2O	2 - 8

Table 2.4. *Mineralogical composition of red mud*

Component	Typical range (%)
Sodalite ($3Na_2O.3Al_2O_3.6SiO_2.Na_2SO_4$)	4 - 40
Goethite (FeOOH)	10 - 30
Hematite (Fe_2O_3)	10 - 30
Magnetite (Fe_3O_4)	0 - 8
Silica (SiO_2) crystalline and amorphous	3 - 20
Calcium aluminate ($3CaO.Al_2O_3.6H_2O$)	2 - 20
Boehmite (AlOOH)	0 - 20
Titanium Dioxide (TiO_2) anatase and rutile	2 - 15
Muscovite ($K_2O.3Al_2O_3.6SiO_2.2H_2O$)	0 - 15
Calcite ($CaCO_3$)	2 - 20
Kaolinite ($Al_2O_3.2SiO_2.2H_2O$)	0 - 5
Gibbsite ($Al(OH)_3$)	0 - 5
Perovskite ($CaTiO_3$)	0 - 12
Cancrinite ($Na_6[Al_6Si_6O_{24}].2CaCO_3$)	0 - 50
Diaspore (AlOOH)	0 - 5

2.5.4. Chemical Reactions

The chemical reactions between clay soils and red mud are not researched before, so the chemical reactions between the clays and red mud cannot be interpreted exactly. The experimental works of this study examined the effectiveness of the red mud for improvement of the soil through proper chemical reactions.

Although, no research about the clay-red mud interaction, the utilization applications of the red mud in the related areas gives an idea about the possible reactions of the red mud in the soil.

The first possible reaction is changing the adsorbed monovalent cations in the structure of the clay with the multivalent cations in the structure of the red mud. The multivalent cations are decreasing the swelling potential of the soil similar to lime reactions.

The other possible reactions are pozzolanic reactions. The idea of the pozzolanic reactions to occur comes from that the red mud is used for increasing the pozzolanic activity in the concrete as stated above.

This type of reactions can give the soil the advantages of:

- reducing the plasticity index, permeability and expansion potential,
- increasing the stiffness and strength

of the soil as in fly ash.

CHAPTER 3

EXPERIMENTAL WORK

3.1. Purpose

The purpose of doing this experimental work is to improve the swelling and strength properties of an expansive soil by adding red mud, fly ash, lime, and cement. The tests have been performed for this purpose, will be explained in the following sections in details.

3.2. Materials

The information will be given separately in following sections about the kaolinite and bentonite, which forms the swelling soil, and Red Mud, Fly Ash, Lime and Cement, which improve the swelling soil (i.e. which were added to the expansive soil for reducing swell potential and increasing strength).

3.2.1. Kaolinite

The kaolinite is the main material for the swelling soil. 85% of the swelling soil is kaolinite. It was taken from Kale Mining Industrial Raw Materials Industry and Trade Co. from Çanakkale, Turkey. Kaolinite has been crushed and passed through the No. 40 and oven-dried before preparing specimens (Figure 3-1).

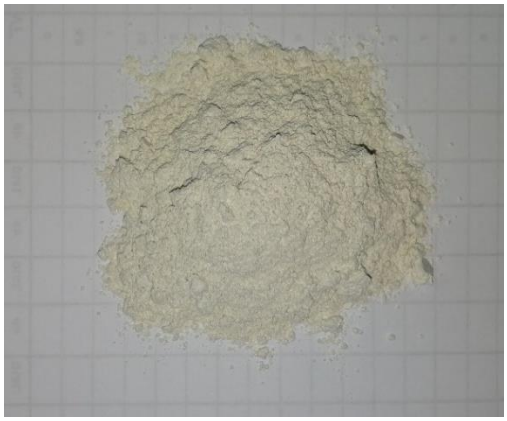

Figure 3-1. Kaolinite

3.2.2. Bentonite

The bentonite is the other material of the swelling soil. 15% of the swelling soil is bentonite. It was taken from Karakaya Bentonite Factory. Bentonite has been passed through the No. 40 sieve and oven-dried before preparing specimens (Figure 3-2).

Figure 3-2. Bentonite

3.2.3. Red Mud

The red mud is one of the major additives that has been used in experiments. It was taken from ETI Mining Seydişehir Aluminum Factory. Red mud has been crushed and passed through the No. 40 sieve and oven-dried before preparing the specimens (Figure 3-3).

Figure 3-3. Red Mud

3.2.4. Fly Ash

The fly ash is the other major additive that has been used in experiments. It was taken from Soma Thermal Power Plant. Fly ash has been passed through the No. 40 sieve and oven-dried before preparing specimens (Figure 3-4).

Figure 3-4. Fly Ash

3.2.5. Lime

The lime is one of the minor additives that has been used in experiments. It was TS EN 459-1 CL 70 S type lime. It was taken from Baştaş Lime Factory. Lime has been passed through the No. 40 sieve and oven-dried before preparing specimens (Figure 3-5).

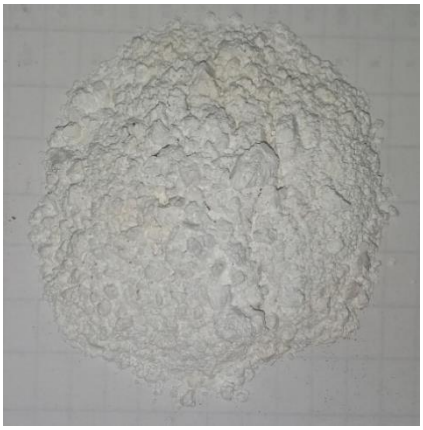

Figure 3-5. Lime

3.2.6. Cement

The cement is the other minor additive that has been used in experiments. It was “CEM II/A-M (P-LL) 42.5 R” type cement. It was taken from Aşkale Cement Industry Co. Inc.’s Aşkale Cement Factory. Cement has been passed through the No. 40 sieve and oven-dried before preparing specimens (Figure 3-6).

Figure 3-6. Cement

3.2.7. Chemical Compositions of the Materials

The Chemical compositions of the kaolinite, bentonite, red mud and fly ash that have been used in experiments are tabulated in Table 3-1. Industrial materials are specified by their standards.

The chemical composition of kaolinite is taken from General Directorate of Mineral Research and Exploration (MTA, 2019b).

The chemical composition of bentonite is taken from General Directorate of Mineral Research and Exploration (MTA, 2019a).

The chemical composition of Seydişehir ETİ Mining's Red Mud is taken from the research of (Tınkılıç & Erdem, 1996).

The chemical composition of the Fly ash is taken from the Fly Ash research of (Türker, Erdoğan, Katnaş, & Yeğinobalı, 2009).

Table 3-1. *Chemical compositions of kaolinite, bentonite, red mud and fly ash*

Chemical Composition (%)	**Materials**			
	Kaolinite	**Bentonite**	**Red Mud**	**Fly Ash**
MgO	0.1	2.2	-	1.7
Al_2O_3	22.0-29.0	19.3	17.0	20.8
SiO_2	51.0-67.5	57.6	6.9	42.8
CaO	0.1	4.2	2.2	23.5
Fe_2O_3	0.4	3.3	38.6	4.6
K_2O	0.5-2.0	2.6	-	1.3
Na_2O	0.3-0.4	2.41	10.3	0.3
TiO_2	0.4-0.5	0.3	5.1	-
V_2O_5	-	-	0.1	-
P_2O_5	-	-	0.2	-
S	-	-	0.1	-
Loss of Ignition	9.0-20.0	7.4	-	2.8

The chemical compositions of lime and cement have been given in sections 2.2.1 and 2.3.1, respectively. The lime and cement types, which have been used in the experiments have given in sections 3.2.5 and 3.2.6, respectively.

3.3. Preparation of Samples

Kaolinite is not showing the swelling property in its nature, while bentonite is swelling excessively. In order to model the soil, which has high swelling potential, kaolinite and bentonite are mixed by the ratio of 85% to 15%. The resultant soil model is 85% kaolinite and 15% bentonite by mass. In this research, this soil was named as “Sample A”. In order to compare the effect of additives on the Sample A, they have been added to the Sample A. The ratio of the kaolinite and bentonite have not changed during these operations. The Samples and its ingredients are shown in Table 3-2. The percentages of the materials in each sample were determined by the pilot experiments had been performed before.

All the materials, soil materials or additives, were ground for passing through the No. 40 sieve. After sieving, the materials were dried in an oven for 24 hours at 50 ℃. From these oven-dried materials, the necessary amounts, the materials have been weighed and added to the mixture of the sample, that will be tested. The resultant sample mix is blended homogenously. While blending the mix, the water is added to it as the amount of 10% of its weight.

For the experiments, which the samples were cured, the same technique was used for preparing the specimens. After mixing operations, the samples were set for curing at 22 ℃ and 70% moisture for 7 days and 28 days.

Firstly, the pilot experiments had been handled, in order to define which mineral is effective for decreasing the swelling potential of the soil. After pilot experiments, 7 different kinds of samples have been chosen and the experiments have been handled for these samples.

All the samples include red mud. The samples can be grouped as to whether it includes fly ash, or it does not. In order to observe the effect of the lime or cement, they have been added to both groups separately. As a result, there are seven different samples.

Table 3-2. *Ingredients of the samples*

No	Sample Name	Amount of Material (By Mass) %					
		Kaolinite	**Bentonite**	**Red Mud (RM)**	**Fly Ash (FA)**	**Lime (L)**	**Cement (C)**
#1	Sample A	85	15	-	-	-	-
#2	85%Sample A + 15%RM	72.25	12.75	15	-	-	-
#3	80%Sample A + 15%RM + 5%L	68	12	15	-	5	-
#4	80%Sample A + 15%RM + 5%C	68	12	15	-	-	5
#5	70%Sample A + 15%RM + 15%FA	59.50	10.50	15	15	-	-
#6	65%Sample A + 15%RM + 15%FA + 5%L	55.25	9.75	15	15	5	-
#7	65%Sample A + 15%RM + 15%FA + 5%C	55.25	9.75	15	15	-	5

3.4. Sample Properties

For Sample #1; hydrometer test, Atterberg limit test, specific gravity test, shrinkage limit test, and mechanical cone penetration test were performed according to the related ASTM standards.

The swelling potentials of the Sample #1 was estimated by its activity values before the experiments (Seed, Woodward, & Lundgren, 1962).

The activity of the clay (Seed et al.,1962):

$$A_c = \frac{PI}{C-5} \qquad (3.1)$$

where

A_c : Activity

PI : Plasticity Index (%)

C : percentage of particles finer than 2 μm (%)

The results of the performed tests have given information about the Sample #1's silt and clay size fraction and consistency limits.

By using the Equation 3.1, the Activity Value of the Sample #1 is 1.43 and it has clay fraction of 50 %. The swelling potential of the sample #1 can be regarded as "Very High" by using the chart in Figure 3-7.

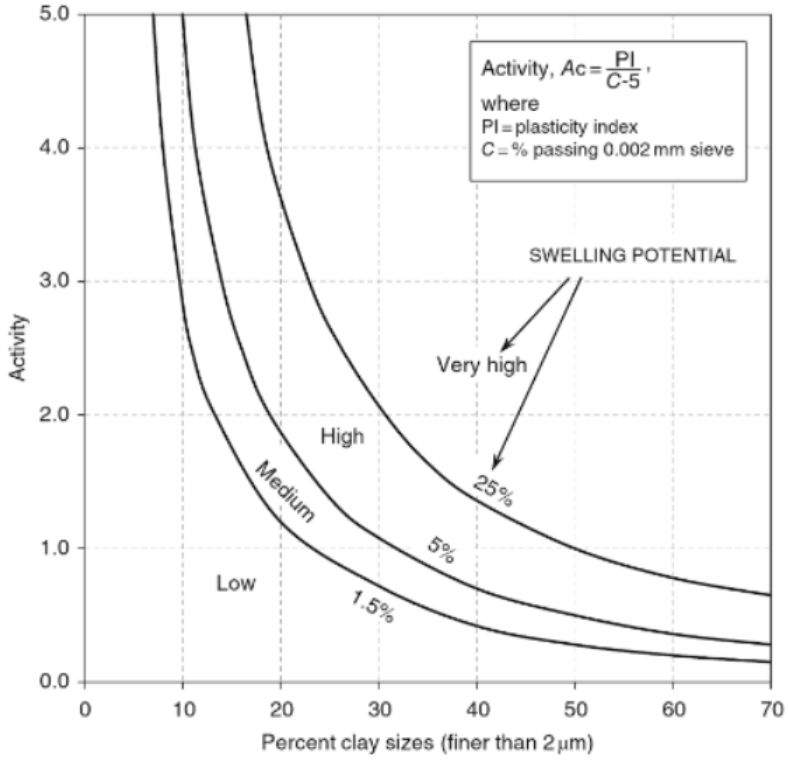

Figure 3-7. Classification chart for swelling potential (Seed et al., 1962)

The soil classification, which is the result of the grain size distribution curves, has been done according to the Unified Soil Classification System (USCS). The grain size distributions of all samples have been shown in Figure 3-8.

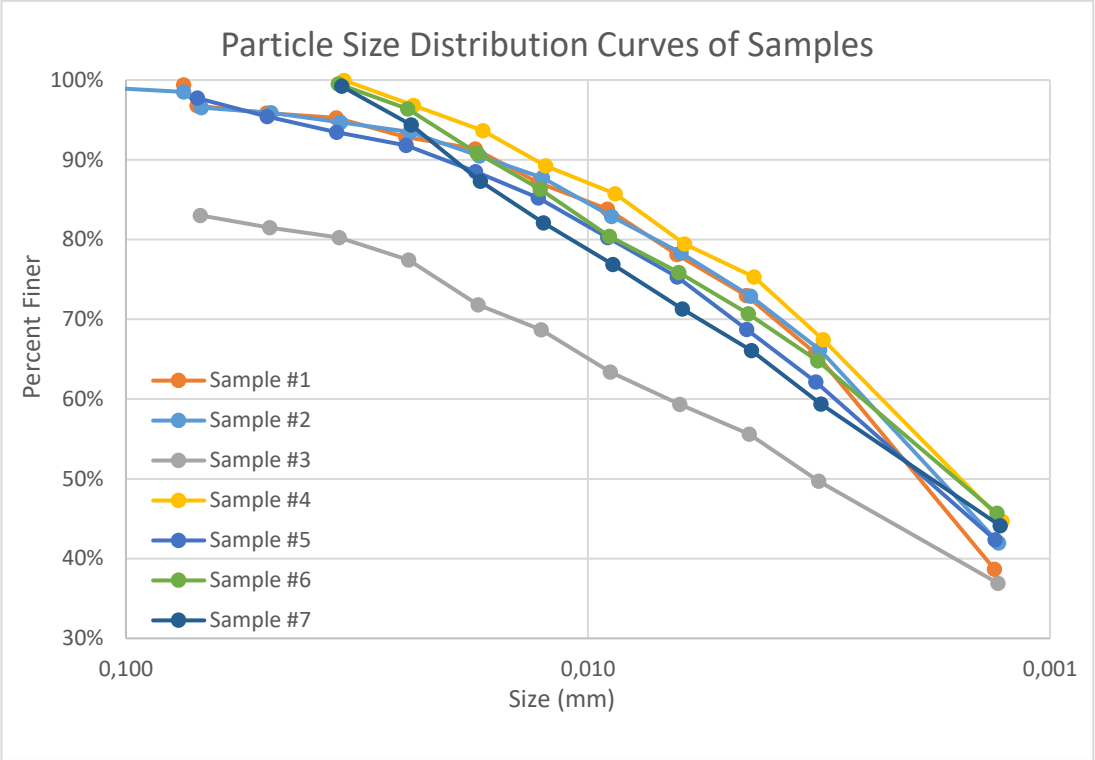

Figure 3-8. Particle size distribution curves of samples

For each sample; the unconfined compression tests, direct tensile strength tests, split tensile strength tests were performed according to the related ASTM standards.

The result of the performed tests has given information about the samples' strength characteristics.

The Proctor tests of each sample were performed with Mini Compaction Test Apparatus, which is modified for the fine-grained soils (Sridharan & Sivapullaiah, 2005).

The test methods and their related standards were tabulated in Table 3-3.

Table 3-3. *Test methods and related standards*

Test Method	Related Standard
Hydrometer and Sieve analysis	ASTM D422-63
Atterberg Limits Tests	ASTM D4318-17^{E1}
Shrinkage Limit Tests	ASTM D427-04
Mechanical Cone Penetration Tests	ASTM D3441-16
Unconfined Compression Tests	ASTM D2166/D2166M-16
Direct Tensile Strength Tests	ASTM C307-03
Split Tensile Strength Tests	ASTM C496/C496M-17

3.5. Testing Procedure

In this study, the effectiveness of the additives for stabilization of soil against swelling are tested by Free Swell Method. The preparation of the samples is described in detail in Section 3.3.

For testing the strength values of the samples; Unconfined Compression Tests, Direct Tensile Strength Tests and Split Tensile Strength Tests were performed according to the standards, which is given in Section 3.4.

The dry densities of the samples are tabulated and can be shown in Table 3-4, Table 3-5 and Table 3-6.

Table 3-4. *Dry density values of the swell test specimens*

Dry Densities of Swell Test Specimens (g/cm^3)			
Swell Test Specimen	**No cure**	**7-day cured**	**28-day cured**
Sample #1	1.59	1.52	1.72
Sample #2	1.51	1.47	1.56
Sample #3	1.47	1.56	1.56
Sample #4	1.49	1.56	1.56
Sample #5	1.46	1.56	1.56
Sample #6	1.46	1.56	1.56
Sample #7	1.48	1.56	1.56

Table 3-5. *Dry density values of the unconfined compression test specimens*

Dry Densities of Unconfined Compression Test Specimens (g/cm^3)			
Unconfined Compression Test Specimen	**No cure**	**7-day cured**	**28-day cured**
Sample #1	1.49	1.50	1.50
Sample #2	1.49	1.50	1.50
Sample #3	1.49	1.50	1.50
Sample #4	1.49	1.49	1.49
Sample #5	1.50	1.49	1.50
Sample #6	1.50	1.49	1.50
Sample #7	1.50	1.49	1.50

Table 3-6. *Dry density values of the split tensile strength test specimens*

Dry Densities of Split Tensile Strength Test Specimens (g/cm^3)			
Split Tensile Strength Test Specimen	**No cure**	**7-day cured**	**28-day cured**
Sample #1	1.48	1.50	1.50
Sample #2	1.48	1.50	1.50
Sample #3	1.48	1.49	1.50
Sample #4	1.48	1.49	1.49
Sample #5	1.49	1.49	1.50
Sample #6	1.49	1.49	1.50
Sample #7	1.48	1.49	1.49

3.5.1. Free Swell Method

The free swell method has been used for measuring the one-dimensional swell percentage of the samples. Before placing the samples in the consolidation ring, 10 % water of the dry sample weight was added to the mixture. The specimens have been placed in the consolidation ring with the densities given in Table 3-4. A small surcharge was applied to the specimens. When the water was added on the specimens, the specimens are swelling freely. The deflection of the dial gauge was recorded at

specified times. The recordings of the dial gauge are remaining the same after some time. Generally, the experiment is finished if the last three or four records are the same.

The recorded data have been used for determining the free swell of the specimen. The percentage of free swell is:

$$Free\ swell = \frac{\Delta H}{H} * 100$$

where,

ΔH: Change in height of the specimen (from dial gauge records)

H: Initial height of the specimen

The swelling test procedure:

- All the samples are sieved through the No.200 sieve and added 10 % water of the sample by weight.
- The sample is placed in the consolidation ring.
- Dry filter papers are placed below the top and on top of the specimen and it is placed in the oedometer test apparatus (Figure 3-9).
- After the specimen is ready, air-dried porous stone is placed on top of the specimen.
- The loading device is mounted with a cap, in order to distribute the load on specimen homogenously. A small surcharge (7 kPa) is applied on the specimen with loading device.
- The water is applied to the specimen from the top and water is added until the specimen is fully submerged.
- Periodically water in the apparatus is controlled and water is added if necessary.
- Periodical readings are taken, when the last three or four reading is the same, the experiment is finished.

- Two tests for each sample have been performed and the average of them has been taken as result

Figure 3-9. Free swell test apparatus (Oedometer)

3.5.2. Unconfined Compression Test

Unconfined compression tests have been performed to determine the undrained shear strength of the samples. Uniaxial test apparatus was used to determine the undrained shear strength of the specimen. The undrained shear strength of the specimen is:

$$c_u = \frac{q_u}{2}$$

where,

c_u: undrained shear strength

q_u: the maximum axial compressive stress that the specimen carry

The procedure of the test as follows:

- The specimens are prepared in 36 mm diameter and 72 cm length in cylindrical shape.
- The specimen is placed in uniaxial test apparatus (Figure 3-10).
- When initial Load is applied the experiment is started.
- Load and strain values are recorded while the experiment continues.
- When the specimen is failed, the experiment is finished.
- Stress and strain diagrams of the specimens are plotted, according to the related standards.
- Two tests for each sample have been performed and the average of them has been taken as result.

Figure 3-10. Uniaxial test apparatus

3.5.3. Direct Tensile Test

The direct tensile test was used to determine the tensile strength of the samples. The direct tensile test apparatus (Figure 3-12) was used in the experiments. The test procedure is :

- The three specimens are prepared in the special 8-shaped mold (Figure 3-11).
- Molded specimens are placed into Direct Tensile Test Apparatus separately.

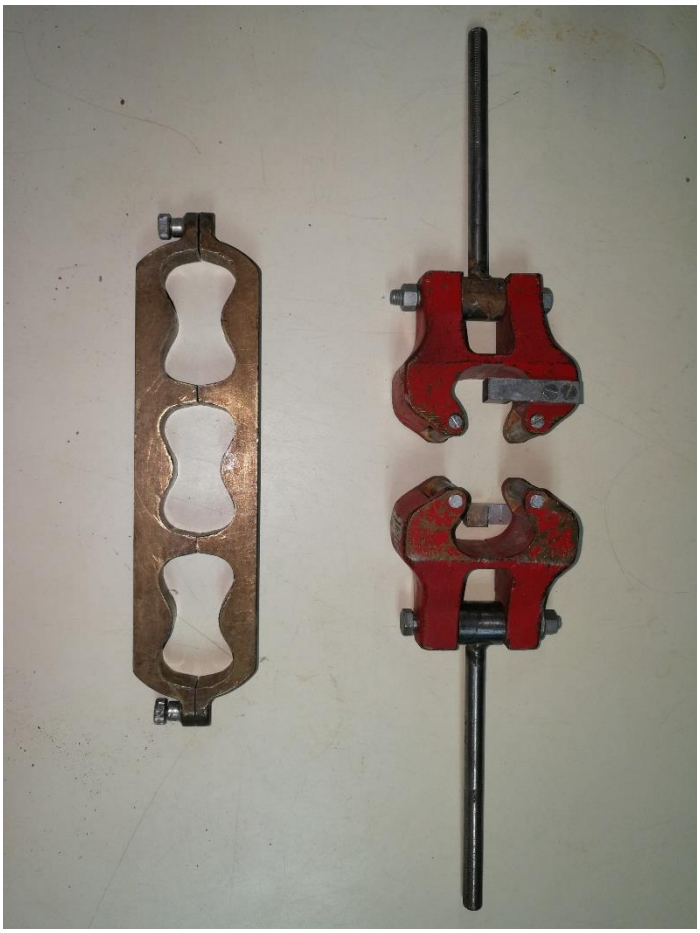

Figure 3-11. Special 8-shaped mold and direct tensile test apparatus

- The bucket, which is connected to the lower half portion of the apparatus filled with sand carefully.
- When the specimen is failed from its neck, that has 25.4 mm x 25.4 mm cross section dimensions, the experiment is over.

- The maximum load that the specimens can carry is recorded.
- The loads are divided into the planar area of the neck of the specimen.
- The average of the three samples is regarded as the tensile strength of the sample.
- Two tests for each sample have been performed and the average of them has been taken as result.

Figure 3-12. Direct tensile test apparatus during the experiment

The calculation of the stress has been done according to the following formula:

$$\sigma_{max,dt} = \frac{F_{max,dt}}{A_{neck}}$$

where,

$F_{max,dt}$: The maximum load that the specimen can carry

A_{neck} : Cross sectional area of the neck of the specimen

3.5.4. Split Tensile Test

The uniaxial test apparatus was used for the split tensile test experiments. Some extra pieces of the equipment, that specialized for split tensile test, were used for these experiments. The testing procedure is:

- The specimen is prepared as in for the unconfined compression test.
- The specimen is placed in the Uniaxial Test Apparatus horizontally (Figure 3-13 and Figure 3-14).
- The recordings of the experiments are the same as the unconfined compression test.
- The tensile stresses were calculated by dividing the applied load to the fracture area.
- The fracture area is calculated as Area = Diameter x Length.
- Two tests for each sample have been performed and the average of them has been taken as result.

Figure 3-13. Uniaxial test apparatus for split tensile test

Figure 3-14. Specimen placement in direct tensile test

The tensile strength can be calculated for the disk, which is subjected to compression (Timoshenko, 1934). The stress field in the axial direction of a cylinder can be easily determined by using the formula:

$$\sigma_x = \frac{2F}{\pi db}\left(\frac{d^2 - 4x^2}{d^2 + 4x^2}\right)^2$$

where,

F : compression load

d : diameter

b : length

x : radial distance from the center

The maximum tensile stress in the specimen is at x=0, and the formula turns out:

$$\sigma_{max} = \frac{2F}{\pi db}$$

3.5.5. Permeability Test

The permeability test was performed by using the triaxial test apparatus (Figure 3-15) in this study. The procedure of the test is:

- The specimens are prepared as the same in the unconfined compression test.
- The specimen is placed into the apparatus with a cell pressure of 200 kPa and backpressure of 100 kPa.
- The water is allowed to drain through the soil.
- When the change in the height of the water in the standpipes are equal to the recordings are started to be noticed.
- The change in water level in standpipes in unit time helps us to determine the permeability of the sample.

Figure 3-15. Triaxial test apparatus

3.6. Experimental Program

With the help of the pilot experiments, 7 samples have been selected in order to determine the effects of the additives on the swelling and strength characteristics of the soil.

Experimental studies were performed in 9 phases:

1- Index properties of the samples: hydrometer tests, Atterberg limit tests, specific gravity tests, shrinkage limit tests, mechanical cone penetration tests (fall cone test).
2- Optimum moisture content determination of the soil with Mini Compaction Test Apparatus
3- Permeability determination of the soil with Triaxial Test Apparatus

4- Swelling percentage determination of the samples without curing
5- Swelling percentage determination of the samples after 7-day curing
6- Swelling percentage determination of the samples after 28-day curing
7- Strength property determination of the samples without curing
8- Strength property determination of the samples after 7-day curing
9- Strength property determination of the samples after 28-day curing

3.7. Test Results

3.7.1. Consistency Limit Tests

The Fall Cone Test, Atterberg Limit test and Shrinkage limit test results of the samples are shown in Table 3-7.

Table 3-7. Fall cone test, atterberg l*imit test and shrinkage limit test results of the samples*

ATTERBERG LIMIT TEST RESULTS OF THE SAMPLES					
SAMPLE	**LL (%) (MCPT)**	**LL* (%)**	**PL* (%)**	**PI** (%)**	**SL (%)**
Sample #1	94	91	27	64	20
Sample #2	93	91	31	61	28
Sample #3	130	100	31	69	63
Sample #4	130	107	37	70	77
Sample #5	104	86	29	57	37
Sample #6	123	100	32	68	57
Sample #7	128	104	35	69	61
*by Casagrande Apparatus ** PI=LL-PL. LL and PL values from Atterberg Limits Test has used.					

The effects of the additive materials on swelling soil's Liquid Limit (Mechanical Cone Penetration Test), Liquid Limit, Plastic Limit, Plasticity Index and Shrinkage Limit are visualized by bar charts in Figure 3-16, Figure 3-17, Figure 3-18, Figure 3-19 and Figure 3-20, respectively.

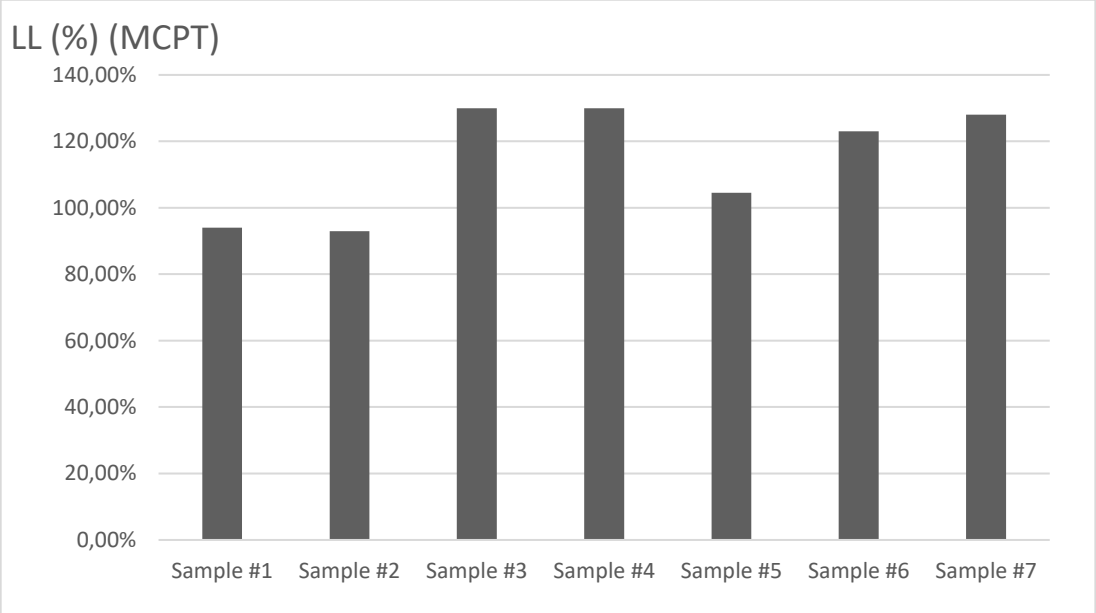

Figure 3-16. Liquid limit test results from mechanical cone penetration test

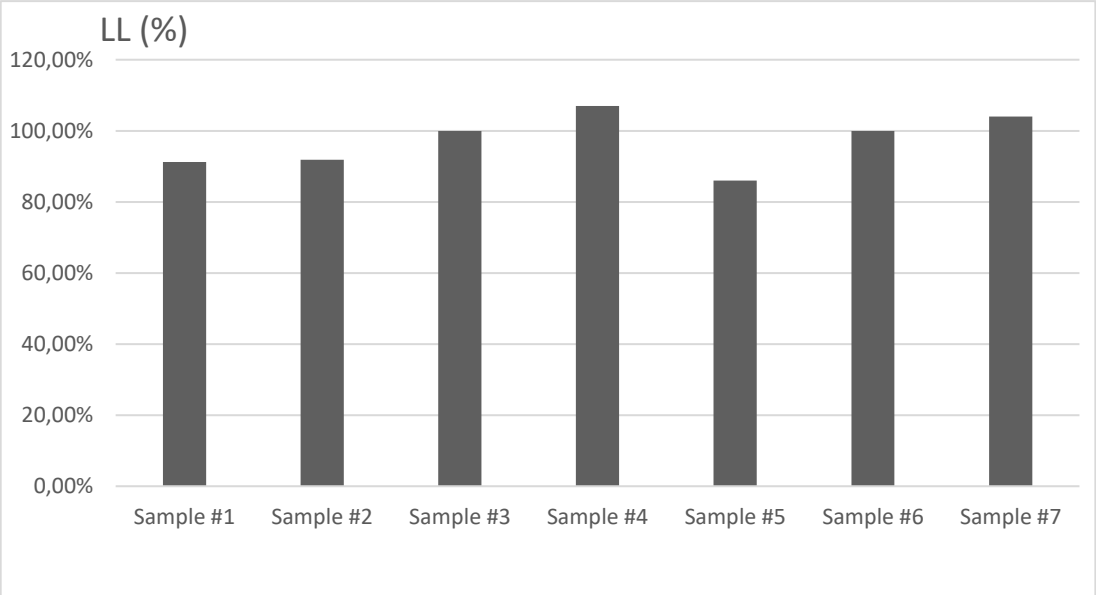

Figure 3-17. Liquid limit test results (by Casagrande apparatus)

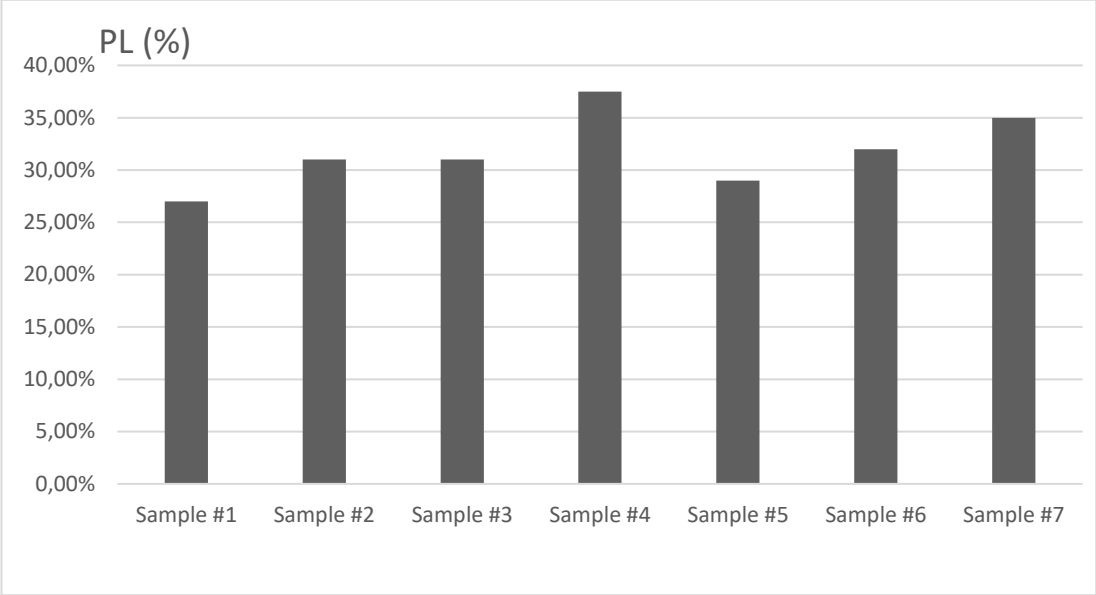

Figure 3-18. Plastic limit test results

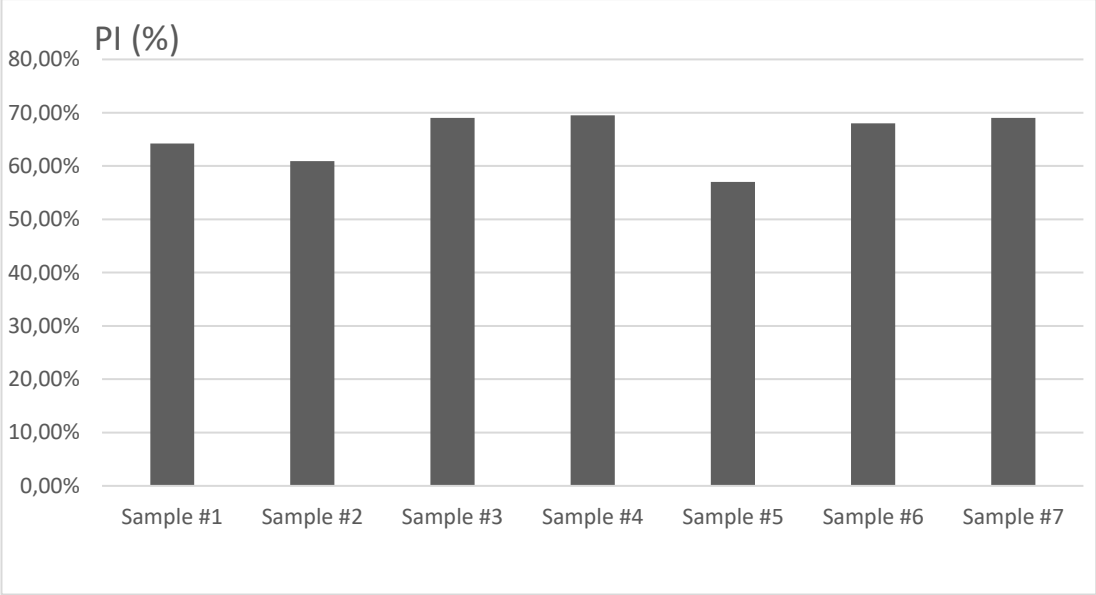

Figure 3-19. Plasticity index values from atterberg limits test

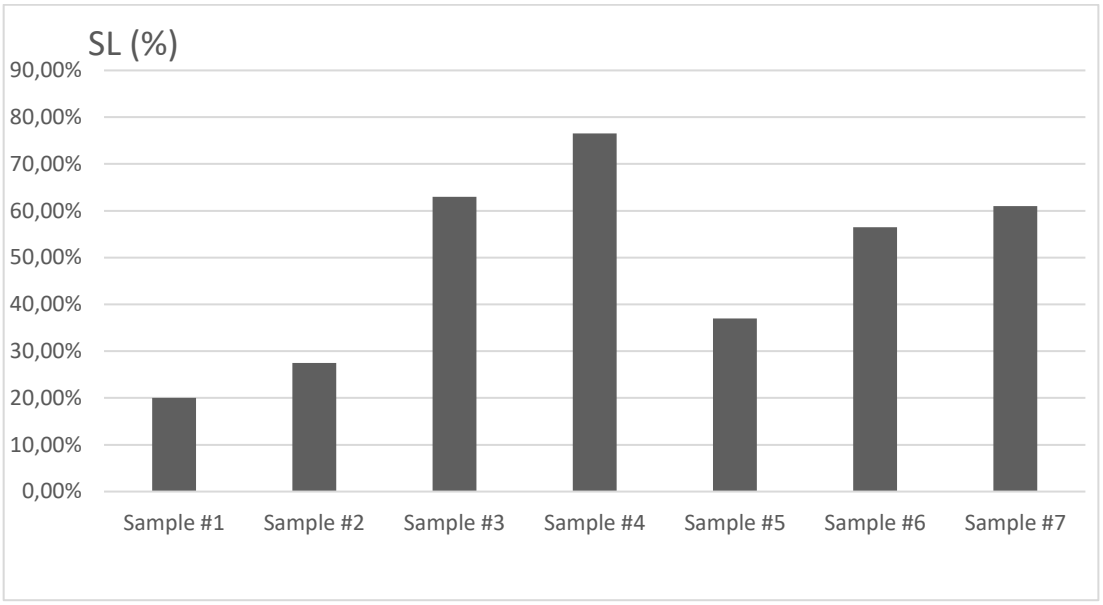

Figure 3-20. Shrinkage limit test results

3.7.2. Compression Characteristics Tests

The compression characteristics like OMCs (optimum moisture contents), MDDs (maximum dry densities) were tested for all the samples. The OMCs and MDDs of the samples are tabulated in Table 3-8 and they are also shown in bar graph in Figure 3-21 and Figure 3-22, respectively.

Table 3-8. *Optimum moisture content and maximum dry densities of the samples*

SAMPLE	**OMC (%)**	**MDD (g/cm^3)**
Sample #1	26	1.39
Sample #2	33	1.93
Sample #3	27	1.36
Sample #4	29	1.37
Sample #5	32	1.30
Sample #6	33	1.21
Sample #7	37	1.37

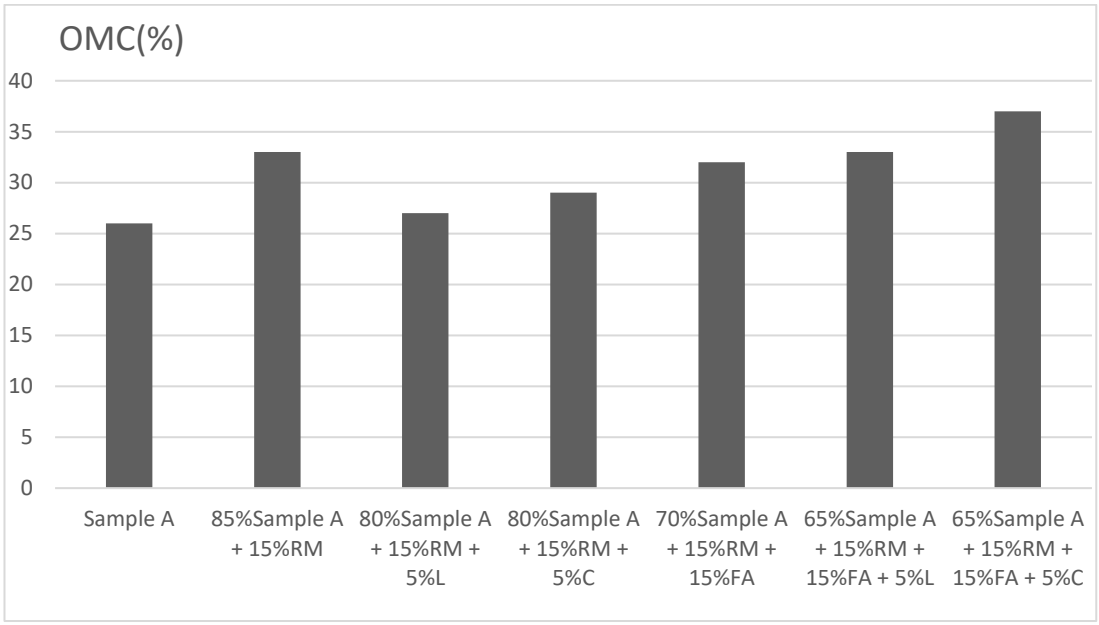

Figure 3-21. Optimum moisture contents of the samples

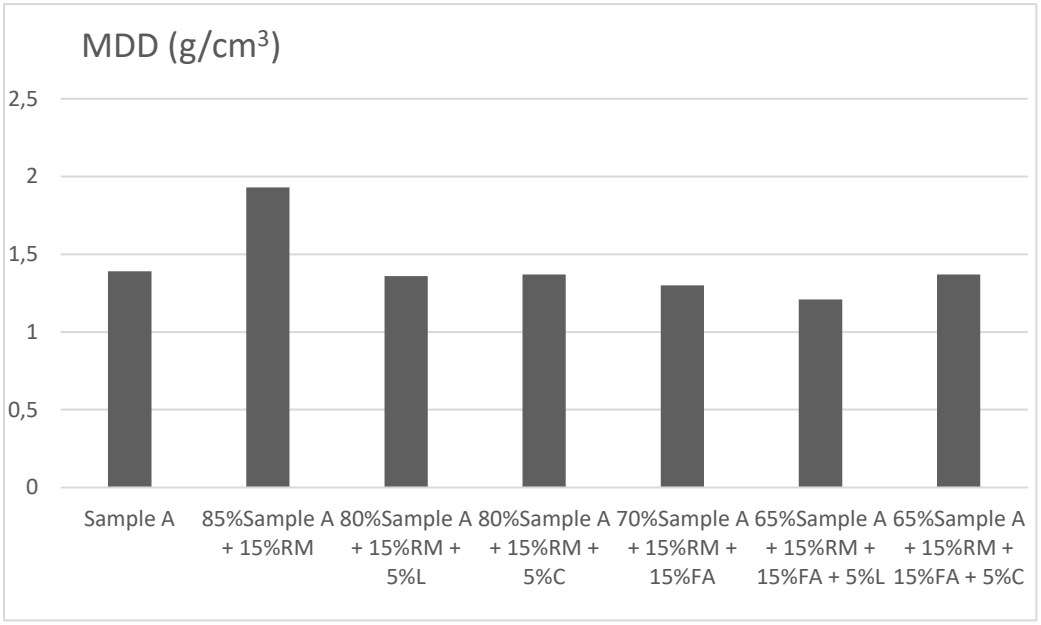

Figure 3-22. Maximum dry densities of the samples

3.7.3. Permeability Tests

The permeability of the specimens are determined and tabulated in Table 3-9 and they also shown in bar graph in Figure 3-23.

Table 3-9. *Permeability of the specimens*

SPECIMEN	Permeability (mm/sec)
Sample #1	2.5 x 10-4
Sample #2	2.5 x 10-4
Sample #3	7 x 10-4
Sample #4	5 x 10-4
Sample #5	6 x 10-4
Sample #6	1.1 x 10-3
Sample #7	Impermeable

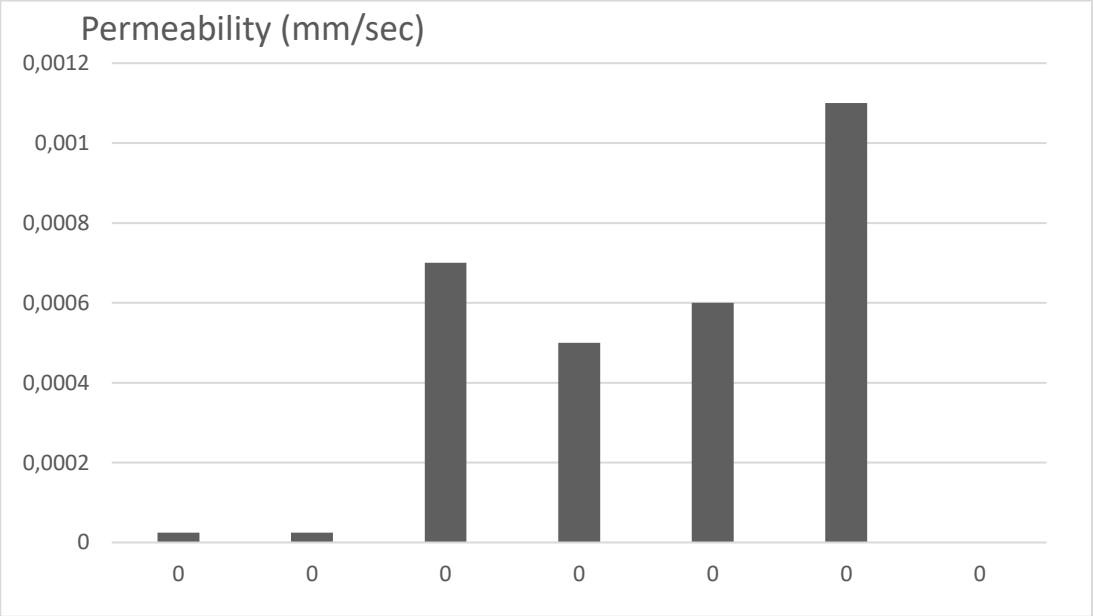

Figure 3-23. Permeability of the specimens

The permeabilities of stabilized specimens are generally in the order of 10^{-5} cm/sec. This magnitude would provide reasonably low permeability as in clayey silt or dense silt soils.

3.7.4. Swelling Tests

The swelling vs square root of time graphs of the non-cured Sample #1, which are obtained from the free swell tests, are shown in Figure 3-24. The other specimens' graphs are in Appendix A.

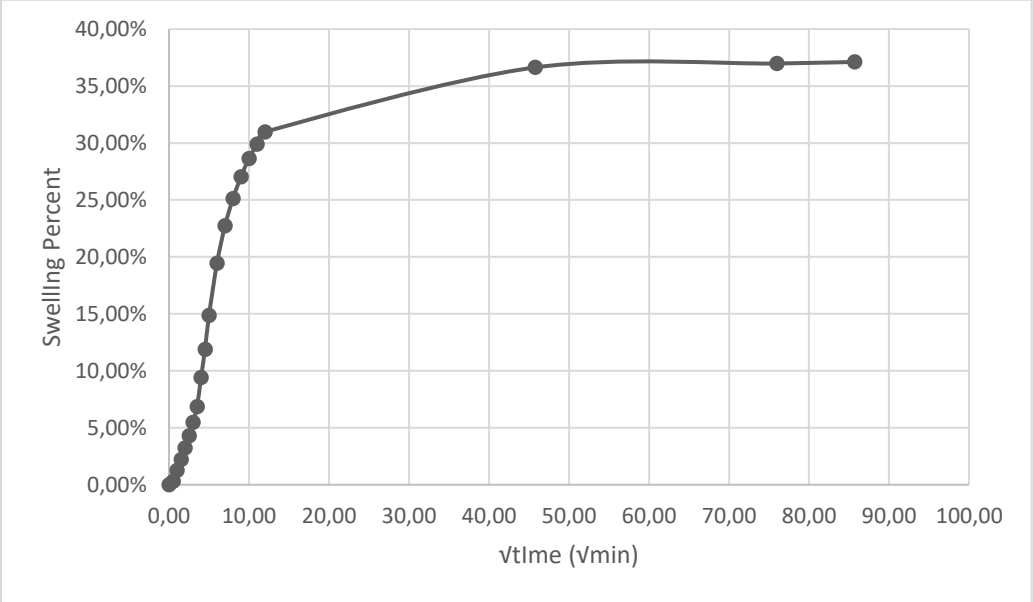

Figure 3-24. Swell percentage versus square root of time graph of non-cured Sample #1

The maximum swell percentage at the end of the test of the specimens are tabulated in Table 3-10. Also, the swelling rates of the specimens, which is the time required to reach the half of the maximum swell percent, are tabulated in Table 3-11.

Table 3-10. *The maximum swelling percent of the specimens*

Sample	**Swell Percentage**		
	Non-cured	**7-day Cured**	**28-day Cured**
Sample #1	37.11 %	35.78 %	24.34 %
Sample #2	23.57 %	28.70 %	21.04 %
Sample #3	15.89 %	12.46 %	16.61 %
Sample #4	16.05 %	17.06 %	12.27 %
Sample #5	6.00 %	13.34 %	7.23 %
Sample #6	11.58 %	14.72 %	12.96 %
Sample #7	13.84 %	12.65 %	13.18 %

Table 3-11. *The swelling rate of the specimens*

Sample	Swelling Rate (minutes)		
	Non-cured	**7-day Cured**	**28-day Cured**
Sample #1	36	42	56
Sample #2	30	36	42
Sample #3	15	12	7.5
Sample #4	12	10	9
Sample #5	6	14	15
Sample #6	6	6	9
Sample #7	9	6	4

With the help of Table 3-10, the change in the swell percentage of the soil with respect to materials have added for non-cured, 7-day cured and 28-day cured specimens are shown in bar charts in Appendix C.

The effect of the curing on the swell percentage of the specimens are shown in Figure 3-25.

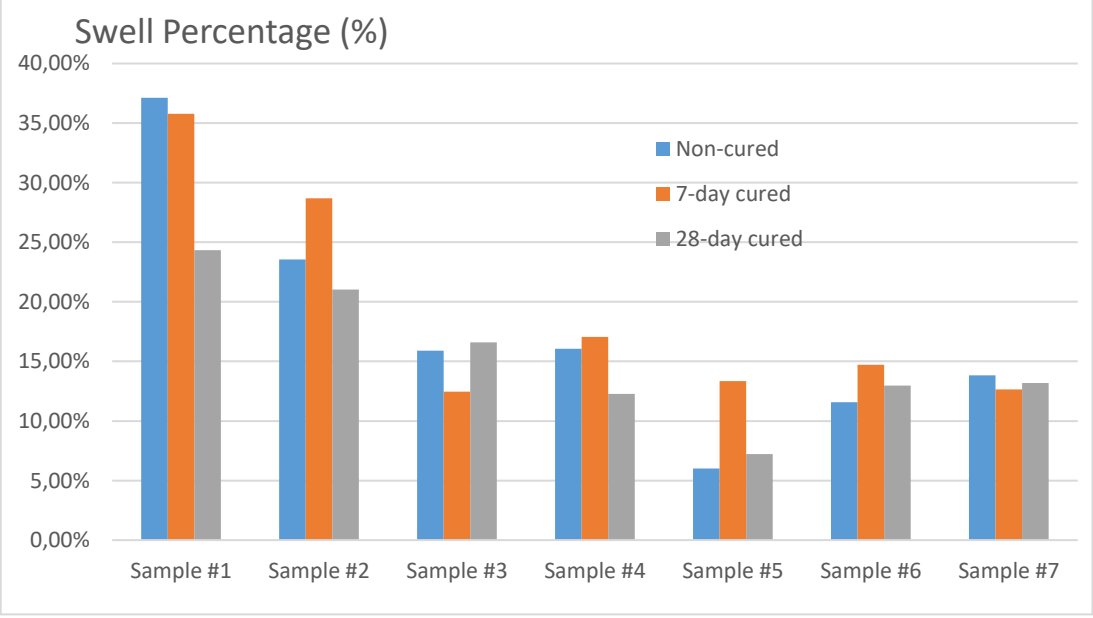

Figure 3-25. Effect of curing on swell percentage of the specimens

The change in the swelling rate of the soil with respect to materials that have been added for non-cured, 7-day cured, and 28-day cured specimens are shown in bar charts in Appendix C.

The effect of the curing on the swelling rates of the specimens are shown in Figure 3-26.

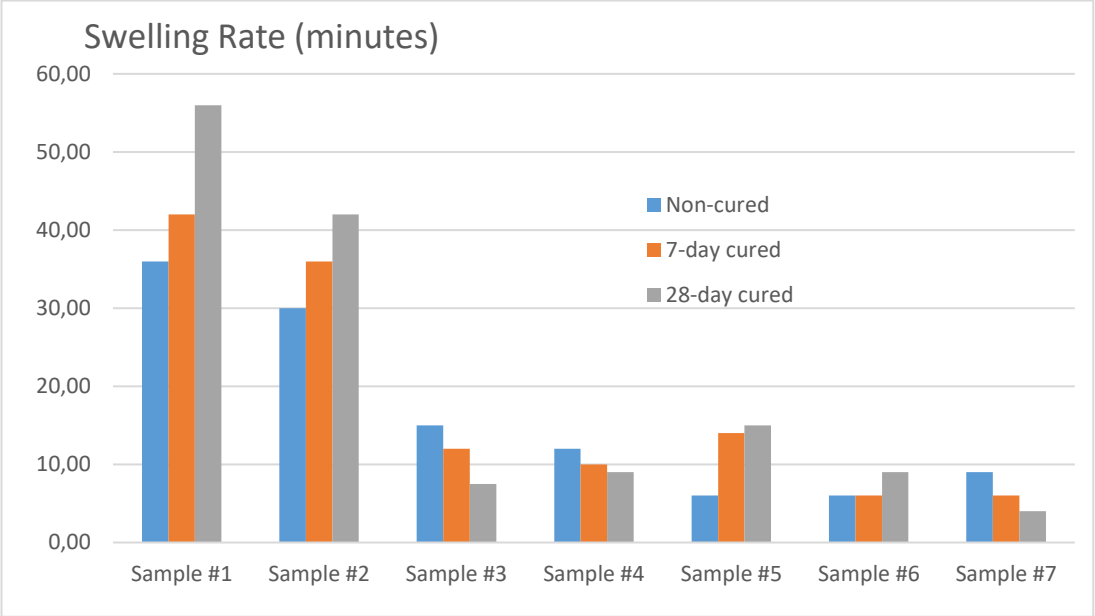

Figure 3-26. Effect of curing on swelling rate of the specimens

The change of the swelling percent and the swelling rate of the specimens, Sample #2 to Sample #7, with respect to Sample #1 are shown in Table 3-12 and Table 3-13. respectively. The changes are the differences between the considered specimen and Sample #1 of that curing group.

Table 3-12. *Swelling percent change of Sample #2 to Sample #7*

Sample	Swelling Percent Change		
	Non-cured	**7-day Cured**	**28-day Cured**
Sample #1	37.11 %	35.78 %	24.34 %
Sample #2	-13.54 %	-7.08 %	-3.30 %
Sample #3	-21.22 %	-23.32 %	-7.73 %
Sample #4	-21.06 %	-18.72 %	-7.07 %
Sample #5	-31.11 %	-22.44 %	-17.11 %
Sample #6	-25.53 %	-21.06 %	-11.38 %
Sample #7	-13.27 %	-23.13 %	-11.16 %

Table 3-13. *Swelling rate change of Sample #2 to Sample #7*

Sample	Swelling Rate Change		
	Non-cured	**7-day Cured**	**28-day Cured**
Sample #1	36	42	56
Sample #2	-6	-6	-14
Sample #3	-21	-30	-48.5
Sample #4	-24	-32	-47
Sample #5	-30	-28	-41
Sample #6	-30	-36	-47
Sample #7	-27	-36	-52

3.7.5. Unconfined Compression Tests

The samples of sizes 36 mm diameter and height of 72 mm were prepared by compaction method to achieve maximum dry density at their optimum moisture contents. All the prepared samples were cured for 7 days and 28 days. Unconfined compressive strength tests were conducted after completion of their curing periods at a strain rate of 1.25 mm/min. The test results are tabulated in Table 3-14.

Table 3-14. *The undrained shear strength of the specimens*

Sample	Undrained Shear Strength (kPa)		
	Non-cured	7-day Cured	28-day Cured
Sample #1	15.95	16.85	16.22
Sample #2	10.50	11.11	11.49
Sample #3	25.82	23.90	29.26
Sample #4	27.08	44.41	70.88
Sample #5	9.81	14.45	18.60
Sample #6	17.55	20.63	27.28
Sample #7	19.32	60.01	64.41

The undrained shear strength values of the non-cured, 7-day cured, and 28-day cured samples are shown in bar charts in Appendix D.

The effect of curing on the undrained shear strength of the specimens is shown in a bar chart in Figure 3-27.

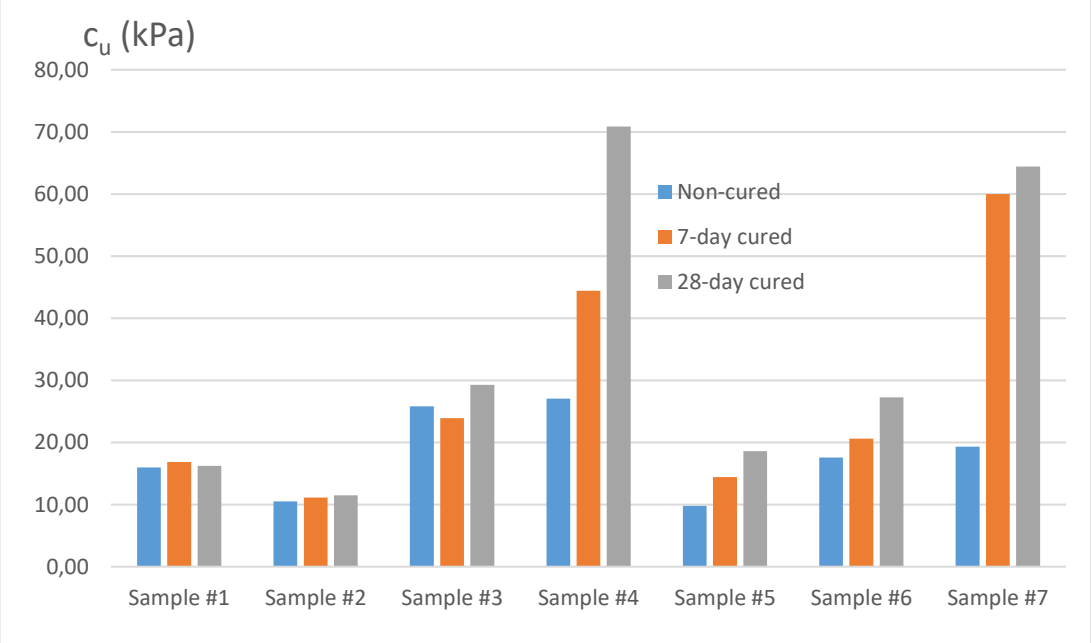

Figure 3-27. Effect of curing on undrained shear strength of the specimens

3.7.6. Direct Tensile Strength Tests

The direct tensile strength tests have been performed for determining the effect of the additive materials on Tensile strength of the non-cured, 7-day cured, and 28-day cured specimens. The test results are tabulated in Table 3-15.

Table 3-15. *The tensile strength of the specimens from direct tensile strength test*

Sample	**Tensile Strength (kPa)**		
	Non-cured	**7-day Cured**	**28-day Cured**
Sample #1	5.26	5.41	5.32
Sample #2	6.06	7.37	7.23
Sample #3	2.43	3.34	2.48
Sample #4	2.63	7.79	27.44
Sample #5	4.41	9.45	14.87
Sample #6	4.41	13.03	15.82
Sample #7	2.48	13.19	30.54

Tensile strength values of the non-cured, 7-day cured, and 28-day cured specimens from direct tensile strength test are shown in bar chart in Appendix E.

The effect of curing on the tensile strength of the specimens from direct tensile tests is shown in a bar chart in Figure 3-28.

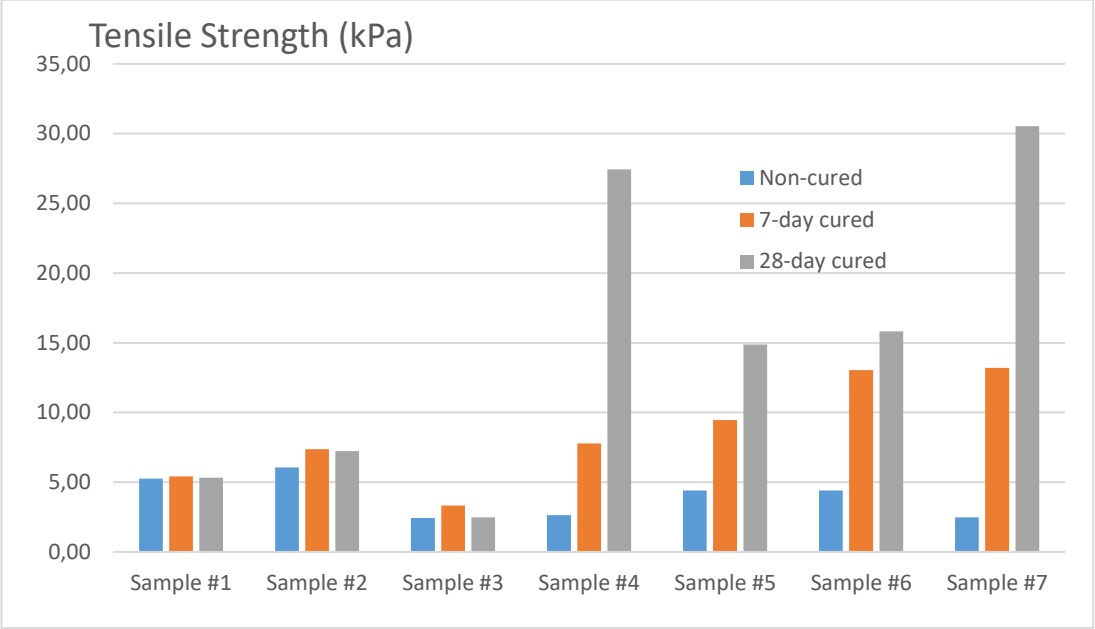

Figure 3-28. Effect of curing on tensile strength from direct tensile strength test of the specimens

3.7.7. Split Tensile Strength Tests

The split tensile strength tests have been performed for determining the effect of the additive materials on tensile strength of the non-cured, 7-day cured, and 28-day cured specimens. The test results are tabulated in Table 3-16.

Table 3-16. *The tensile strength of the specimens from split tensile strength test*

Sample	**Tensile Strength (kPa)**		
	Non-cured	**7-day Cured**	**28-day Cured**
Sample #1	7.87	8.80	8.08
Sample #2	8.65	8.59	9.22
Sample #3	15.98	10.01	11.26
Sample #4	29.06	21.09	26.39
Sample #5	9.04	7.45	12.13
Sample #6	24.04	13.51	16.71
Sample #7	43.00	47.70	38.56

Tensile strength values of the non-cured, 7-day cured, and 28-day cured specimens from split tensile strength test are shown in bar chart in Appendix E.

The effect of curing on the tensile strength of the specimens from direct tensile tests is shown in a bar chart in Figure 3-29.

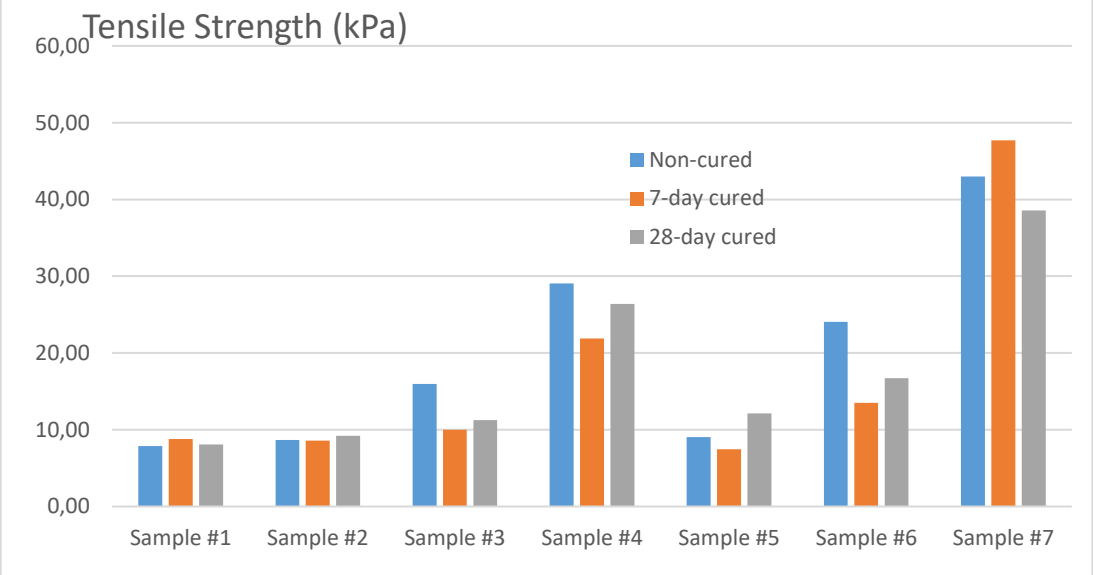

Figure 3-29. Effect of curing on tensile strength from split tensile strength test of the specimens

CHAPTER 4

DISCUSSION OF RESULTS

4.1. Effect of Stabilizers on Liquid Limit

To determine the Liquid Limits of the samples, Atterberg Limit tests and Mechanical Cone Penetration Tests have been performed. The effect of the stabilizers is shown in Table 3-7 and visually represented in Figure 3-16 and Figure 3-17.

The mechanical cone penetration test results show that the Sample #1 has LL = 94.00 %. This value is decreased by 1.00 % when only red mud is added (Sample #2). The LL of the red mud and cement or lime added sample (Sample #3 and Sample #4) is 34.00 % higher than the Sample #1. Adding fly ash and red mud to the Sample #1 increases its (Sample #5) LL by 10.50 %. Adding lime (Sample #6) or cement (Sample #7) to the red mud and fly ash added sample increases their LL value to 123.00 % and 128.00 % respectively.

The Liquid limit test results from the Atterberg Limits Tests show that the Sample #1 has LL = 91.20 %. This value is increased by 0.70 % when only red mud is added (Sample #2). The LL of the red mud and cement or lime added sample (Sample #3 and Sample #4) is 8.80 % and 15.80 % higher than the Sample #1 respectively. Adding fly ash and red mud to the Sample #1 decreases its (Sample #5) LL by 5.20 %. Adding lime (Sample #6) or cement (Sample #7) to the red mud and fly ash added sample increases their LL value to 100.00 % and 104.00 % respectively.

However, the LL values of the stabilized samples are expected to be smaller than the Sample #1, the LL of the sample is increased with the amount of the stabilizers added to it. The results of the Atterberg Limit Tests are more realistic. The maximum change in the LL is the difference between Sample #1 and Sample #4, which is 15.80 %.

4.2. Effect of Stabilizers on Plastic Limit

To determine the Plastic Limits of the samples, Atterberg Limit tests have been performed. The effect of the stabilizers is shown in Table 3-7 and visually represented in Figure 3-18.

The Plastic Limit test results from the Atterberg Limits Tests show that the Sample #1 has PL = 27.00 %. This value is increased by 4.00 % when only red mud (Sample #2) or red mud and lime together (Sample #2), is added. The PL of the red mud and cement added sample (Sample #4) is 10.50 % higher than the Sample #1. Adding fly ash and red mud to the Sample #1 increases its (Sample #5) PL by 2.00 %. Adding lime (Sample #6) or cement (Sample #7) to the red mud and fly ash added sample increases their PL value to 32.00 % and 35.00 %, respectively.

As a result, the PL values of the soil is increasing with the increasing amount of added stabilizer. The cement or lime addition is increasing the shrinkage limit of the Sample #1 much more. The cement and lime added samples has much greater value than the only fly ash and red mud added samples.

4.3. Effect of Stabilizers on Shrinkage Limit

The Shrinkage Limits of the samples are obtained from Shrinkage Limit Tests. The effect of stabilizers is shown in Table 3-7 and visually represented in Figure 3-20.

The Shrinkage Limit of the Sample #1 is SL = 20.00 %. This value is increased by 7.50 % when only red mud (Sample #2) is added. Sample #3 has SL value of 63.00 %, which is 43.00 % greater than Sample #1. The SL of the red mud and cement added sample (Sample #4) is 56.50 % higher than the Sample #1. Adding fly ash and red mud to the Sample #1 increases its (Sample #5) SL by 17.00 %. Adding lime (Sample #6) or cement (Sample #7) to the red mud and fly ash added sample increases their SL value to 56.50 % and 61.00 %, respectively.

The shrinkage limits are increasing with the amount of the added stabilizers. The cement addition is increasing the shrinkage limit of the Sample #1 much more. Cement added samples has much greater SL value than the others.

4.4. Effect of Stabilizers on Plasticity Index

The plasticity index values of the samples are calculated from the PL and LL values obtained from the Atterberg Limit Tests. The effect of stabilizers is shown in Table 3-7 and visually represented in Figure 3-19.

The Plasticity Index of the Sample #1 is PI = 64.20 %. This value is decreased by 3.30 % when only red mud (Sample #2) is added. Sample #3 has PI value of 69.00 %, which is 4.80 % greater than Sample #1. The PL of the red mud and cement added sample (Sample #4) is 5.30 % higher than the Sample #1. Adding fly ash and red mud to the Sample #1 decreases its (Sample #5) PI by 7.20 %. Adding lime (Sample #6) or cement (Sample #7) to the red mud and fly ash added sample increases their PI value to 68.00 % and 69.00 %, respectively.

The plasticity index values are not changing considerably with the addition of the stabilizers.

4.5. Effect of Stabilizers on Activity

The activity (A_c) value of the Sample #1 is calculated from the results of the Atterberg limits tests. The Activity value is the helpful theoretical prediction of the swelling potential of the sample. By using the activity value and clay percentage of the Sample #1, it can be regarded as a “Very High” swelling potential (Seed et al.,1962). With the stabilization, decrease of the activity values of the other samples are expected.

4.6. Effect of Stabilizers on Permeability

The permeability tests have been performed on the non-cured specimens by using the triaxial test apparatus and permeability values are generally increasing with the amount of the stabilizers (i.e. from 2.5 $x10^{-4}$ mm/sec to from 1.1 $x10^{-3}$ mm/sec). Only the Sample #7 is different from the other specimens. The permeability value of the

Sample #7 cannot be measured. It is probably the result of the cement inclusion of the specimen.

4.7. Effect of Stabilizers on Swelling Percentage

To determine the swelling percentage of the samples, oedometer tests have been performed on the samples. Free swell method has been used for the calculation of the swelling percentage. The maximum swelling percentage values of the samples are shown in Table 3-10. The graphical representation of the swelling of the samples is shown in Appendix A. The comparison of the maximum swelling percentage of the samples is also shown in bar graph in Figure 3-25. The values of the percent improvement of the stabilizers can also be shown in Table 3-12.

The maximum swell percentage of the non-cured Sample #1 is 37.11 %. This value is decreased by 13.54 % when only red mud (non-cured Sample #2) is added. Non-cured Sample #3 has maximum swell percentage value of 15.89 %, which is 21.22 % less than Sample #1. The maximum swell percentage of the red mud and cement added non-cured sample (Sample #4) is 21.06 % less than the Sample #1. Adding fly ash and red mud to the non-cured Sample #1 decreases its (non-cured Sample #5) maximum swell percentage by 31.11 %. Adding lime (non-cured Sample #6) or cement (non-cured Sample #7) to the red mud and fly ash added sample decreases their maximum swell percentage value to 11.58 % and 13.84 % respectively.

The maximum swell percentage of the 7-day cured Sample #1 is 35.78 %. This value is decreased by 7.08 % when only red mud (7-day cured Sample #2) is added. 7-day cured Sample #3 has maximum swell percentage value of 12.46 %, which is 23.32 % less than Sample #1. The maximum swell percentage of the red mud and cement added 7-day cured sample (Sample #4) is 18.72 % less than the Sample #1. Adding fly ash and red mud to the 7-day cured Sample #1 decreases its (7-day cured Sample #5) maximum swell percentage by 23.44 %. Adding lime (7-day cured Sample #6) or cement (7-day cured Sample #7) to the red mud and fly ash added sample decreases their maximum swell percentage value to 14.72 % and 12.65 %, respectively.

The maximum swell percentage of the 28-day cured Sample #1 is 24.34 %. This value is decreased by 3.30 % when only red mud (28-day cured Sample #2) is added. 28-day cured Sample #3 has maximum swell percentage value of 16.61 %, which is 7.73 % less than Sample #1. The maximum swell percentage of the red mud and cement added 28-day cured sample (Sample #4) is 12.07 % less than the Sample #1. Adding fly ash and red mud to the 28-day cured Sample #1 decreases its (28-day cured Sample #5) maximum swell percentage by 17.11 %. Adding lime (28-day cured Sample #6) or cement (28-day cured Sample #7) to the red mud and fly ash added sample decreases their maximum swell percentage value to 12.96 % and 13.18 %, respectively.

The effect of the stabilizers is evaluated in three different groups for non-cured, 7-day cured, and 28-day cured samples. For non-cured and 28-day cured groups Sample #5 is provided the most effective stabilization for swelling, while Sample #3 for the 7-day cured sample group. By regarding all the groups, non-cured Sample #5 is providing the most effective improvement.

Swell percentage of Sample #1 (37%) is greater than 25%, so Sample #1 has very high swell potential. Swell percentages of all the stabilized specimens are in between 5% and 25%, so they have high swell potential. Swell potential of Sample #4 and Sample #7 drops to approximately one third of Sample #1 (Figure 3-25).

4.8. Effect of Stabilizers on Rate of Swell

To determine the swelling rate, t_{50} values of the swelling graphs have been used. The swelling rate values of the samples are shown in Table 3-11. The comparison of the swelling rate of the samples is also shown in bar graph in Figure 3-26. The values of the improvement of the stabilizers can also be shown in Table 3-13.

The swelling rate of the non-cured Sample #1 is 36 minutes. This value is decreased by 6 minutes when only red mud (non-cured Sample #2) is added. Non-cured Sample #3 has a swelling rate value of 15 minutes, which is 21 minutes less than Sample #1. The swelling rate of the red mud and cement added non-cured sample (Sample #4) is

24 minutes less than the Sample #1. Adding fly ash and red mud to the non-cured Sample #1 decreases its (non-cured Sample #5) swelling rate by 30 minutes. Adding lime (non-cured Sample #6) or cement (non-cured Sample #7) to the red mud and fly ash added sample decreases their swelling rate value to 6 and 9 minutes, respectively.

The swelling rate of the 7-day cured Sample #1 is 42 minutes. This value is decreased by 6 minutes when only red mud (7-day cured Sample #2) is added. 7-day cured Sample #3 has swelling rate value of 12 minutes, which is 40 minutes less than Sample #1. The swelling rate of the red mud and cement added 7-day cured sample (Sample #4) is 32 minutes less than the Sample #1. Adding fly ash and red mud to the 7-day cured Sample #1 decreases its (7-day cured Sample #5) swelling rate by 28 minutes. Adding lime (7-day cured Sample #6) or cement (7-day cured Sample #7) to the red mud and fly ash added sample decreases their swelling rate value to 6 minutes.

The swelling rate of the 28-day cured Sample #1 is 56 minutes. This value is decreased by 14 minutes when only red mud (28-day cured Sample #2) is added. 28-day cured Sample #3 has swelling rate value of 7.5 minutes, which is 48.5 minutes less than Sample #1. The swelling rate of the red mud and cement added 28-day cured sample (Sample #4) is 47 minutes less than the Sample #1. Adding fly ash and red mud to the 28-day cured Sample #1 decreases its (28-day cured Sample #5) swelling rate by 41 minutes. Adding lime (28-day cured Sample #6) or cement (28-day cured Sample #7) to the red mud and fly ash added sample increases their swelling rate value to 9 minutes and 4 minutes, respectively.

The effect of the stabilizers is evaluated in three different groups for non-cured, 7-day cured, and 28-day cured samples. For non-cured group Sample #5 and Sample #6 are provided the most effective stabilization for swelling rate, while Sample #6 and Sample #7 for the 7-day cured sample group and Sample #7 for the 28-day cured group. By regarding all the groups, 28-day cured Sample #7 is providing the most effective improvement, as it is decreasing 56 minutes to the 4 minutes for swelling

rate. Swelling rates of Sample #4 and Sample #7 drop to approximately one fourth of Sample #1 (Figure 3-26).

4.9. Effect of Stabilizers on Undrained Shear Strength

The unconfined compression tests have been performed for determining the undrained shear strengths of the samples. The undrained shear strengths of the samples are shown in Table 3-14 and they are also visually represented for non-cured, 7-day cured and 28-day cured samples in bar chart in Figure 3-27.

The undrained shear strength of the non-cured Sample #1 is 15.95 kPa. This value is decreased by 5.45 kPa when only red mud (non-cured Sample #2) is added. Non-cured Sample #3 has undrained shear strength value of 25.82 kPa, which is 9.87 kPa greater than Sample #1. The undrained shear strength of the red mud and cement added non-cured sample (Sample #4) is 11.13 kPa greater than the Sample #1. Adding fly ash and red mud to the non-cured Sample #1 decreases its (non-cured Sample #5) undrained shear strength by 6.14 kPa. Adding lime (non-cured Sample #6) or cement (non-cured Sample #7) to the red mud and fly ash added sample increases their undrained shear strength value to 17.55 and 19.32 kPa, respectively.

The undrained shear strength of the 7-day cured Sample #1 is 16.85 kPa. This value is decreased by 5.74 kPa when only red mud (7-day cured Sample #2) is added. 7-day cured Sample #3 has undrained shear strength value of 23.90 kPa, which is 7.05 kPa greater than Sample #1. The undrained shear strength of the red mud and cement added 7-day cured sample (Sample #4) is 27.56 kPa greater than the Sample #1. Adding fly ash and red mud to the 7-day cured Sample #1 decreases its (7-day cured Sample #5) undrained shear strength by 2.40 kPa. Adding lime (7-day cured Sample #6) or cement (7-day cured Sample #7) to the red mud and fly ash added sample increases their undrained shear strength value to 20.63 kPa and 60.01 kPa, respectively.

The undrained shear strength of the 28-day cured Sample #1 is 16.22 kPa. This value is decreased by 4.73 kPa when only red mud (28-day cured Sample #2) is added. 28-day cured Sample #3 has undrained shear strength value of 29.26 kPa, which is 13.04

kPa greater than Sample #1. The undrained shear strength of the red mud and cement added 28-day cured sample (Sample #4) is 54.66 kPa greater than the Sample #1. Adding fly ash and red mud to the 28-day cured Sample #1 increases its (28-day cured Sample #5) undrained shear strength by 2.38 kPa. Adding lime (28-day cured Sample #6) or cement (28-day cured Sample #7) to the red mud and fly ash added sample increases their undrained shear strength value to 27.28 kPa and 64.41 kPa respectively.

The undrained shear strengths of the cement and lime added samples are greater than the other samples without regarding the curing of the samples. Sample #5 has less undrained shear strengths from Sample #1 or it nearly remains the same. Undrained shear strengths of Sample #4 and Sample #7 increases to approximately four times of Sample #1 (Figure 3-27).

4.10. Effect of Stabilizers on Tensile Strength

The direct and split tensile tests have been performed for determining the tensile strengths of the samples. The direct and split tensile strength test results of the samples are shown in Table 3-15 and Table 3-16. Also, they are also visually represented for non-cured, 7-day cured and 28-day cured samples in bar chart in Figure 3-28 for direct tensile strengths; and Figure 3-29 for split tensile strengths.

Following paragraphs are the evaluation of the results of the direct tensile test.

The tensile strength of the non-cured Sample #1 is 5.26 kPa. This value is increased by 0.80 kPa when only red mud (non-cured Sample #2) is added. Non-cured Sample #3 has tensile strength value of 2.43 kPa, which is 2.83 kPa less than Sample #1. The tensile strength of the red mud and cement added non-cured sample (Sample #4) is 2.63 kPa less than the Sample #1. Adding fly ash and red mud to the non-cured Sample #1 decreases its (non-cured Sample #5) tensile strength by 0.85 kPa. Adding lime (non-cured Sample #6) or cement (non-cured Sample #7) to the red mud and fly ash added sample changes their tensile strength value to 4.41 and 2.48 kPa, respectively.

The tensile strength of the 7-day cured Sample #1 is 5.41 kPa. This value is increased by 1.96 kPa when only red mud (7-day cured Sample #2) is added. 7-day cured Sample #3 has tensile strength value of 3.34 kPa, which is 2.07 kPa less than Sample #1. The tensile strength of the red mud and cement added 7-day cured sample (Sample #4) is 2.38 kPa greater than the Sample #1. Adding fly ash and red mud to the 7-day cured Sample #1 increases its (7-day cured Sample #5) tensile strength by 4.04 kPa. Adding lime (7-day cured Sample #6) or cement (7-day cured Sample #7) to the red mud and fly ash added sample increases its tensile strength value to 13.03 kPa and 13.19 kPa, respectively.

The tensile strength of the 28-day cured Sample #1 is 5.22 kPa. This value is increased by 2.01 kPa when only red mud (28-day cured Sample #2) is added. 28-day cured Sample #3 has tensile strength value of 2.48 kPa, which is 2.84 kPa less than Sample #1. The tensile strength of the red mud and cement added 28-day cured sample (Sample #4) is 22.12 kPa greater than the Sample #1. Adding fly ash and red mud to the 28-day cured Sample #1 increases its (28-day cured Sample #5) tensile strength by 9.55 kPa. Adding lime (28-day cured Sample #6) or cement (28-day cured Sample #7) to the red mud and fly ash added sample increases its tensile strength value to 15.82 kPa and 30.54 kPa, respectively.

Direct tensile strength of Sample #4 and Sample #7 increases to approximately five times of Sample #1 (Figure 3-28).

Following paragraphs are the evaluation of the results of the split tensile test.

The tensile strength of the non-cured Sample #1 is 7.87 kPa. This value is increased by 0.78 kPa when only red mud (non-cured Sample #2) is added. Non-cured Sample #3 has tensile strength value of 15.98 kPa, which is 8.11 kPa greater than Sample #1. The tensile strength of the red mud and cement added non-cured sample (Sample #4) is 21.19 kPa greater than the Sample #1. Adding fly ash and red mud to the non-cured Sample #1 decreases its (non-cured Sample #5) tensile strength by 1.16 kPa. Adding lime (non-cured Sample #6) or cement (non-cured Sample #7) to the red mud and fly

ash added sample increases their tensile strength value to 24.04 and 43.00 kPa, respectively.

The tensile strength of the 7-day cured Sample #1 is 8.80 kPa. This value is decreased by 0.21 kPa when only red mud (7-day cured Sample #2) is added. 7-day cured Sample #3 has tensile strength value of 10.01 kPa, which is 2.21 kPa greater than Sample #1. The tensile strength of the red mud and cement added 7-day cured sample (Sample #4) is 14.29 kPa greater than the Sample #1. Adding fly ash and red mud to the 7-day cured Sample #1 decreases its (7-day cured Sample #5) tensile strength by 1.35 kPa. Adding lime (7-day cured Sample #6) or cement (7-day cured Sample #7) to the red mud and fly ash added sample increases its tensile strength value to 13.51 kPa and 47.70 kPa, respectively.

The tensile strength of the 28-day cured Sample #1 is 8.08 kPa. This value is increased by 1.14 kPa when only red mud (28-day cured Sample #2) is added. 28-day cured Sample #3 has tensile strength value of 11.26 kPa, which is 3.18 kPa greater than Sample #1. The tensile strength of the red mud and cement added 28-day cured sample (Sample #4) is 18.31 kPa greater than the Sample #1. Adding fly ash and red mud to the 28-day cured Sample #1 increases its (28-day cured Sample #5) tensile strength by 4.05 kPa. Adding lime (28-day cured Sample #6) or cement (28-day cured Sample #7) to the red mud and fly ash added sample increases its tensile strength value to 16.71 kPa and 38.56 kPa, respectively.

As a result, the tensile strength of the non-cured samples remains the same for direct tensile strength test, but it is increasing for lime or cement added samples in split tensile strength tests. For the samples, which do not include cement or lime, the tensile strength nearly same as Sample #1.

The tensile strength of the 7-day cured samples generally increases with the amount of added stabilizer for the direct tensile strength test. Only Sample #3 results in less tensile strength value than Sample #1. For split tensile strength test, as in the direct

tensile test results, the tensile strength test is increasing with the amount of the added stabilizer. Only Sample #5 has less tensile strength value than Sample #1.

Split tensile strengths of Sample #4 and Sample #7 increases to approximately three to four times of Sample #1 (Figure 3-29).

The tensile strength of the 28-day cured samples generally increases with the amount of added stabilizer for direct tensile strength test. Only Sample #3 results in less tensile strength value than Sample #1. For split tensile strength test, as in the direct tensile test results, the tensile strength test is increasing with the amount of the added stabilizer.

4.11. Effect of Curing on Swell Percentage

The results of the swelling percentage are given in Section 3.7 and analyzed in Section 4.7. The swelling percentage of the samples are generally decreasing with the curing time period increases. Only the Sample #5's swelling percentage is increasing with the time of curing period.

The decrease in the swell percent is the result of the replacement of the adsorbed cations in the clay and pozzolanic activities between the minerals in clay and minerals in the additives in the presence of water.

4.12. Effect of Curing on Rate of Swell

The results of the swelling percentage are given in the Section 3.7 and analyzed in the Section 4.8. The rate of the swell of the samples is generally increasing with the curing time period increases. Rate of swell of the Sample #3, Sample #4 and Sample #7 are decreasing with the time of curing period.

The time required for the swell in clay is decreasing with the stabilizers pozzolanic activities. The swell percent of the specimen is decreasing with the curing time and the swell occurs very rapidly due to the reactions between the soil and additives.

4.13. Effect of Curing on Undrained Shear Strength

The results of the undrained shear strength are given in the Section 3.7 and analyzed in the Section 4.9. The undrained shear strength values of the samples are generally increasing or nearly remains the same as the curing time period increases. The increase in the cement added samples are greater, because of the binding effect of the cement.

The increase in de undrained shear strength of the specimens with curing mostly caused by the hydration of the cementitious materials and pozzolanic activities in the presence of enough water.

4.14. Effect of Curing on Tensile Strength

The results of the undrained shear strength are given in Section 3.7 and analyzed in Section 4.10. The tensile strength values of the samples from the direct tensile test are generally increasing or nearly remains the same as the curing time period increases. The increase in the cement added samples are greater, because of the binding effect of the cement.

The tensile strength values of the samples from the split tensile test are generally decreasing or nearly remains the same as the curing time period increases. However, Sample #1, Sample #2, and Sample #5 is different from the other samples. Their tensile strengths are becoming greater than non-cured samples or nearly the same.

The increase in the tensile strength of the specimens with curing mostly caused by the hydration of the cementitious materials and pozzolanic activities in the presence of enough water.

4.15. Effect of Stabilizers and Curing to Soil Structure

When the swell and strength parameters and curing are considered Sample #4 and Sample #7give better results than other specimens. From the results, it is concluded that cement, fly ash and red mud mixture have changed the structure of expansive soil into flocculated structure thereby decreasing swelling potential, increasing the strength and permeability of the mixture

CHAPTER 5

CONCLUSIONS

In this study, the effect of addition of waste materials on the swelling and strength properties of expansive soils was investigated. Also, by comparing the non-cured, 7-day cured, and 28-day cured samples, the effect of curing on these properties are analyzed. According to the results of the experiments, the conclusions have been listed as follows:

1- The liquid limit and plastic limit values are increasing with the addition of the stabilizers. The liquid limit and plastic limit values of the Sample #4 is the greatest. This shows that the cement addition without fly ash increases the soil's liquid limit and plastic limit much more.
2- The shrinkage limits of the samples are increasing with the addition of the stabilizers. The shrinkage limit of the Sample #4 is the greatest. This shows that the cement addition without fly ash increases the soil's shrinkage limit much more.
3- The plasticity index values of the samples are not changing considerably with the addition of the stabilizers.
4- However, the consistency limits of the samples are increasing with the addition of stabilizer, the swelling properties and strength parameters of the Sample #1 is increased with the addition of stabilizers.
5- The activity values are helpful for determining the swelling potential of the soils. According to the calculated activity result, Sample #1 has very high activity. The activity calculations may not be suitable for the stabilized samples of soils. The activity of the stabilized samples should be lower than Sample #1.
6- The permeability values are not considerably changing with the addition of stabilizer. However, only the Sample #7 is showing different characteristics.

Probably the inclusion of the fly ash and cement together does not allow water passing through it.

7- For non-cured and 28-day cured samples, only red mud and fly ash added sample has the lowest swelling percentage. For 7-day cured sample, red mud and lime added sample has the lowest swelling percentage. This shows that the red mud is the effective material for decreasing the swelling percentage of the expansive soil, by regarding both the 7-day and 28-day curing period.

8- For non-cured samples; red mud, fly ash added sample and red mud, fly ash, lime added sample have lowest swelling rates. For the 7-day cured samples; these samples are, red mud, fly ash, lime and red mud, fly ash, cement added samples. For the 28-day cured samples, the sample is red mud, fly ash, cement added sample. This shows that the inclusion of the red mud and fly ash decreases its swelling rates and the soil expands more rapidly.

9- The undrained shear strengths of the samples are increasing with the addition of the stabilizers, except red mud, fly ash added sample. This shows that when the soil needs the improvement of the undrained shear strength only red mud and fly ash are not enough. Especially cement and lime inclusion in the soil increases its undrained shear strength effectively.

10- Direct tensile strengths of the non-cured samples have not been affected by the addition of the stabilizers. Split tensile strengths of the lime or cement added samples are much greater than the other samples. For the 7-day cured samples, the direct and split tensile strengths of the samples are generally increasing with the addition of stabilizers. Only; red mud, lime added sample's direct tensile strength and red mud, fly ash added sample's split tensile strength are lower than Sample #1. For the 28-day cured samples, the direct and split tensile strengths of the samples are generally increasing with the addition of stabilizers. Only; red mud, lime added sample's direct tensile strength is lower than Sample #1. This shows that the cement addition to the soil mixture is important when the tensile strength is considered.

11- The curing of the sample is generally decreasing the swelling percentage of the samples, except red mud and fly ash added sample. If the red mud and fly ash are added, the curing of the soil will decrease its effectiveness of soil improvement against swelling.
12- The rate of swell is showing different characteristics during curing period. Rate of cement added samples' and lime added sample without fly ash decreases with the curing time, while for the remaining samples the rates are increasing with time.
13- The undrained shear strengths of the samples are generally increasing with the curing time. The cement added samples have greater increase because of the binding effect of the cement.
14- The tensile strengths of the samples are generally increasing with the curing time. The cement added samples have greater increase because of the binding effect of the cement. There are some exceptions in split tensile strengths, but their strength values are nearly same as the non-cured samples.
15- When the swell and strength parameters and curing are considered, Sample #4 and Sample #7give better results than other specimens. From the results, it is concluded that cement, fly ash and red mud mixture have changed the structure of expansive soil into flocculated structure thereby decreasing swelling potential, increasing the strength and permeability of the mixture
16- Due to the high alkaline content of the red mud, the leachate analysis should be made for environmental issues. In this issue, the permeability test results show that the cement and fly ash added sample is more convenient for not allowing alkaline content to leach environment.

In this study, the effectiveness of the waste materials (red mud and fly ash) for improving the expansive soil against swelling and strength properties are examined. The results show that the waste materials can be used for the improvement of the expansive soil, with or without the inclusion of lime or cement. Reducing the number

and amount of fabricated products (i.e. lime and cement) and using waste materials (i.e. red mud and fly ash), may make expansive soil improvements more feasible.

The main goal of this study is presenting an environmentally acceptable alternative method for soil stabilization. The detailed economic analysis may be made before the usage of it, in order to determine the cost efficiency. The utilization of red mud generated in the process of industrial production of alumina is still a worldwide problem. Yet, there is no economically viable and environmentally acceptable solution for the utilization of large volumes of red mud. The utilization of red mud is insufficient. Stockpiling is not a fundamental way to resolve the problems of red mud. Only, through economical and viable comprehensive utilization, can people resolve the red mud problem effectively in the long term. The use of red mud for expansive soil stabilization can be an effective way to reduce the stockpiling of red mud. However, its high alkalinity is a potential pollution to threat water, and there is a risk of introducing new contamination, therefore, in-depth studies are needed for comprehensive assessment of chemical and biological effects in environment.

REFERENCES

Agrawal, A., Sahu, K. ., & Pandey, B. . (2004). Solid waste management in non-ferrous industries in India. *Resources, Conservation and Recycling*, *42*(2), 99–120.

American Coal Ash Association. (2017). Production & Use Charts. Retrieved August 1, 2019, from ACAA Publications website: https://www.acaa-usa.org/publications/productionusereports.aspx

Amu, O. O., Adeyeri, J. B., Oduma, E. W., & Fayokun, O. A. (2008). Stabilization Characteristics of Lime on Palm Kernel Blended Lateritic Soil. *Trends in Applied Sciences Research*, *3*(2), 182–188.

ASTM C307-18, Standard Test Method for Tensile Strength of Chemical-Resistant Mortar, Grouts, and Monolithic Surfacings, ASTM International, West Conshohocken, PA, 2018, www.astm.org

ASTM C496 / C496M-17, Standard Test Method for Splitting Tensile Strength of Cylindrical Concrete Specimens, ASTM International, West Conshohocken, PA, 2017, www.astm.org

ASTM D2166 / D2166M-16, Standard Test Method for Unconfined Compressive Strength of Cohesive Soil, ASTM International, West Conshohocken, PA, 2016, www.astm.org

ASTM D3441-16, Standard Test Method for Mechanical Cone Penetration Testing of Soils, ASTM International, West Conshohocken, PA, 2016, www.astm.org

ASTM D422-63(2007)e2, Standard Test Method for Particle-Size Analysis of Soils (Withdrawn 2016), ASTM International, West Conshohocken, PA, 2007, www.astm.org

ASTM D427-04, Test Method for Shrinkage Factors of Soils by the Mercury Method (Withdrawn 2008), ASTM International, West Conshohocken, PA, 2004, www.astm.org

ASTM D4318-17e1, Standard Test Methods for Liquid Limit, Plastic Limit, and Plasticity Index of Soils, ASTM International, West Conshohocken, PA, 2017, www.astm.org

ASTM D4546-14, Standard Test Methods for One-Dimensional Swell or Collapse of Soils, ASTM International, West Conshohocken, PA, 2014, www.astm.org

Basma, A. A., & Tuncer, E. R. (1991). Effect of lime on volume change and compressibility of expansive clays. *Transportation and Research Record*.

Bell, F. G. (1996). Lime stabilization of clay minerals and soils. *Engineering Geology*, *42*(4), 223–237.

Benson, C. H., & Meer, S. R. (2009). Relative Abundance of Monovalent and Divalent Cations and the Impact of Desiccation on Geosynthetic Clay Liners. *Journal of Geotechnical and Geoenvironmental Engineering*, *135*(3).

Brekke, T. L., & Selmer-Olsen, R. (1965). Stability problems in underground constructions caused by montmorillonite-carrying joints and faults. *Engineering Geology*, *1*(1), 3–19.

Charlie, W. A., Osman, M. A., & Ali, E. M. (1984). Construction on Expansive Soils in Sudan. *Journal of Construction Engineering and Management*, *110*(3).

Chen, F. H. (1975). *Foundation on Expansive Soils* (Vol. 1). Elsevier.

Craig, R. F. (2004). *Craig's Soil Mechanics, Seventh Edition*.

Craig, R. F., & Knappett, J. (2012). *Craig's soil mechanics*. Spon Press.

Çokça, E. (2001). Use of Class C Fly Ashes for the Stabilizationof an Expansive Soil. *Journal of Geotechnical and Geoenvironmental Engineering*, *127*(7), 568–573.

Dakshinamurthy, V., & Raman, V. (1977). Identification of expansive soils from classification tests. *1st National Symposium on Expansive Soils*, *1*, 8–1 to 8–8.

Dhowian, A. W. (1990). Field performance of expansive shale formation. In *King Abdulaziz University Scientific Publishing Center*.

ECOBA. (2016). European Coal Combusion Products Association Utilisation. Retrieved August 1, 2019, from http://www.ecoba.com/ecobaccputil.html

Evans, K., Nordheim, E., & Tsesmelis, K. (2016). Bauxite residue management. *Light Metals 2012*, (July), 63–66.

Grim, R. E. (1953). Clay mineralogy. McGraw-Hill.

Indraratna, A. S., Balasubramanian, A. K., & Khan, M. J. (1995). Effect of fly ash with lime and cement on the behavior of a soft clay. *Quarterly Journal of Engineering Geology and Hydrogeology*, *28*(2), 131–142.

Kamon, M., Katsumi, T., & Nontananandh, S. (1991). Utilization of Industrial Wastes by Solidification. *Zairyo/Journal of the Society of Materials Science, Japan*.

Lambe, T. W., & Whitman, R. V. (1969). Soil Mechanics. In *Soil Mechanics*. New York: John Wiley & Sons.

Mahadevan, H., & Ramachandran, T. R. (1996). Recent trends in alumina and aluminium production technology. *Bulletin of Materials Science*, *19*(6), 905–

920.

Marr, S. A., Gilbert, R. B., & Rauch, A. F. (2004). A practical method for predicting expansive soil behavior. *Geotechnical Special Publication*, *126*(I), 1144–1152.

Mitchell, James K.; Soga, K. (2006). Fundamentals of Soil Behavior. In *Soil Science*.

Mitchell, J. K., & Raad, L. (1973). Control of Volume Changes in Expansive Earth Materials. *Proceedings of the Workshop on Expansive Clay and Shales in Highway Design and Construction*, *2*, 200–219.

MTA. (2019a). Bentonit. from http://www.mta.gov.tr/v3.0/bilgi-merkezi/bentonit

MTA. (2019b). Kaolin. from http://www.mta.gov.tr/v3.0/bilgi-merkezi/kaolin

National Lime Association. (2004). Lime-Treated Soil Construction Manual: Lime Stabilization & Lime Modification. *Bulletin*.

Nelson, J. D., Chao, K. C., Overton, D. D., & Nelson, E. J. (2015). *Foundation Engineering for Expansive soils* (1st ed.). Wiley.

Nelson, J. D., & Miller, D. J. (1992). *Expansive soils : problems and practice in foundation and pavement engineering*. J. Wiley.

Nordin, N., Abdullah, M. M. A. B., Tahir, M. F. M., Sandu, A. V., & Hussin, K. (2016). Utilization of fly ash waste as construction material. *International Journal of Conservation Science*, *7*(1), 161–166.

Norrish, K. (1954). The swelling of montmorillonite. *Discussions of the Faraday Society*.

Petry, T. M., & Little, D. (2002). Review of Stabilization of Clays and Expansive Soils in Pavement and Lightly Loaded Structures-History, Practice and Future. *Journal of Materials in Civil Engineering*, *14*(6), 218–224.

Popescu, M. E. (1986). A comparison between the behaviour of swelling and of collapsing soils. *Engineering Geology*.

Portland Cement Association. (1970). *Recommended Practice for Construction of Residential Concrete Floors on Expansive Soil*. *2*.

Rogers, C. D. F., & Bruce, C. J. (1991). *Slope Stability Engineering*. London: Thomas Telford.

Rogers, C. D. F., & Glendinning, S. (1997). Improvement of clay soils in-situ using lime piles in the UK. *Engineering Geology*, *47*, 243–257.

Seed, H. B., Woodward, J., & Lundgren, R. (1962). Prediction of Swelling Potential for Compacted Clays. *Journal of the Soil Mechanics and Foundations Division*, *88*(3), 53–88.

Slade, P. G., Quirk, J. P., & Norrish, K. (1991). Crystalline swelling of smectite samples in concentrated NaCI solutions in relation to layer charge. *Clays and Clay Minerals*.

Sridharan, A. & Sivapullaiah, P. (2005). "Mini Compaction Test Apparatus for Fine Grained Soils," *Geotechnical Testing Journal* 28, no. 3 (2005): 240-246.

Taylor, D. W. (1948). *Fundamentals of Soil Mechanics*. New York: John Wiley.

Teng, T. C., Mattox, R. M., & Clisby, M. B. (1972). *A study of active clays as related to highway design*.

Thompson, M. R. (1966). Lime-reactivity of illinois soils. *Journal of the Soil Mechanics and Foundations Division*, *92*(5), 67–92.

Timoshenko, S. (1934). *Theory of elasticity*. McGraw-Hill.

Tınkılıç, N., & Erdem, E. (1996). Production of iron(II) sulphate(feso4.7H2 O) from red-mud. *Pamukkale Univ Muh Bilim Derg*, *2*(2), 135–137.

Tonoz, M. C., Gokceoglu, C., & Ulusay, R. (2006). Lime stabilization stabilization of expansive Ankara clay with lime. *Expansive Soils: Recent Advances in Characterization and Treatment*.

Türker, P., Erdoğan, B., Katnaş, F., & Yeğinobalı, A. (2009). *Türkiye'deki Uçucu Küllerin Sınıflandırılması ve Özellikleri* (4th ed.). Ankara: Turkish Cement Manufacturer's Association.

US Geological Survey. (2019). *Mineral Commodity Summaries 2019*. Retrieved from https://www.usgs.gov/centers/nmic/mineral-commodity-summaries

Woods, K. B., Berry, D. S., & Goetz, W. (1960). Highway Engineering Handbook. New York: McGraw Hill.

APPENDICES

A. Swelling Percent vs. √time Graphs

The swelling vs square root of time graphs of the non-cured samples, which are obtained from the free swell tests, are shown below.

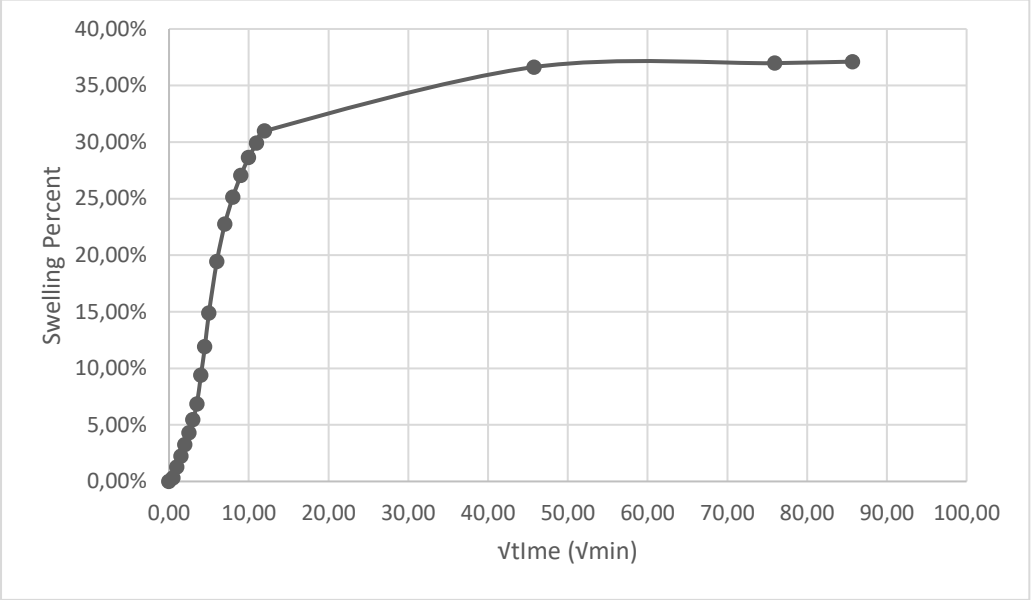

Figure A - 1. Swelling percent versus square root of time graph of non-cured Sample #1

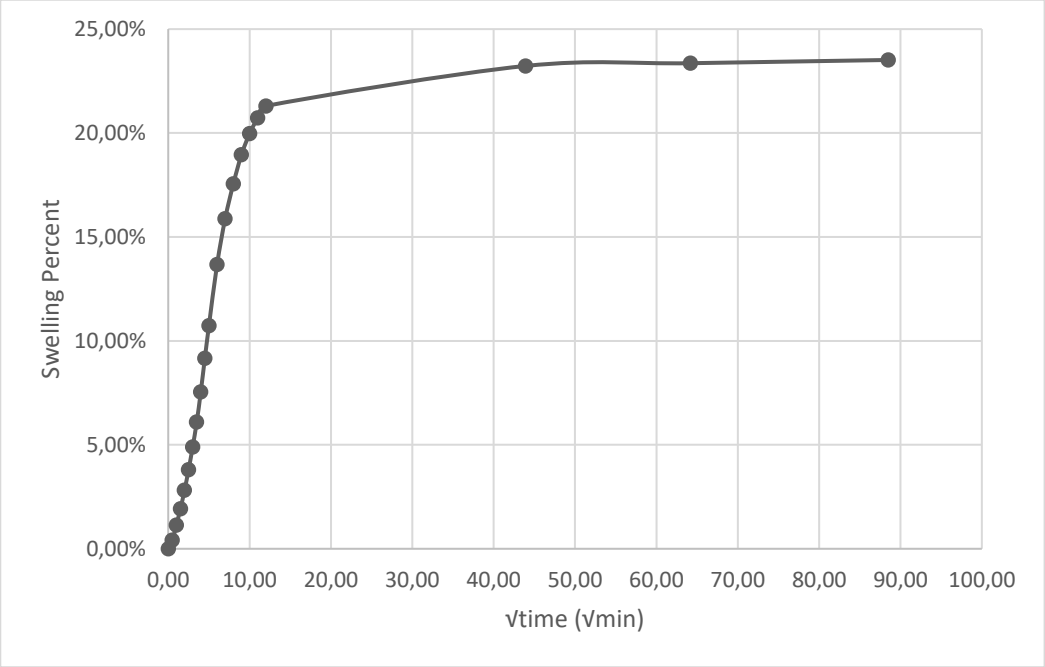

Figure A - 2. Swelling percent versus square root of time graph of non-cured Sample #2

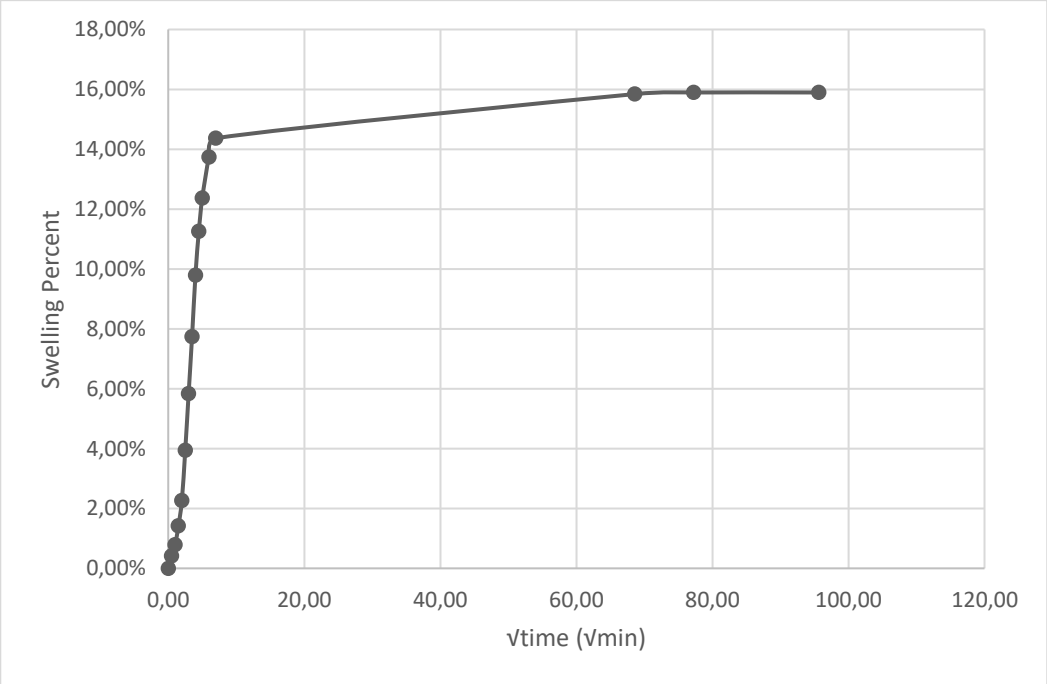

Figure A - 3. Swelling percent versus square root of time graph of non-cured Sample #3

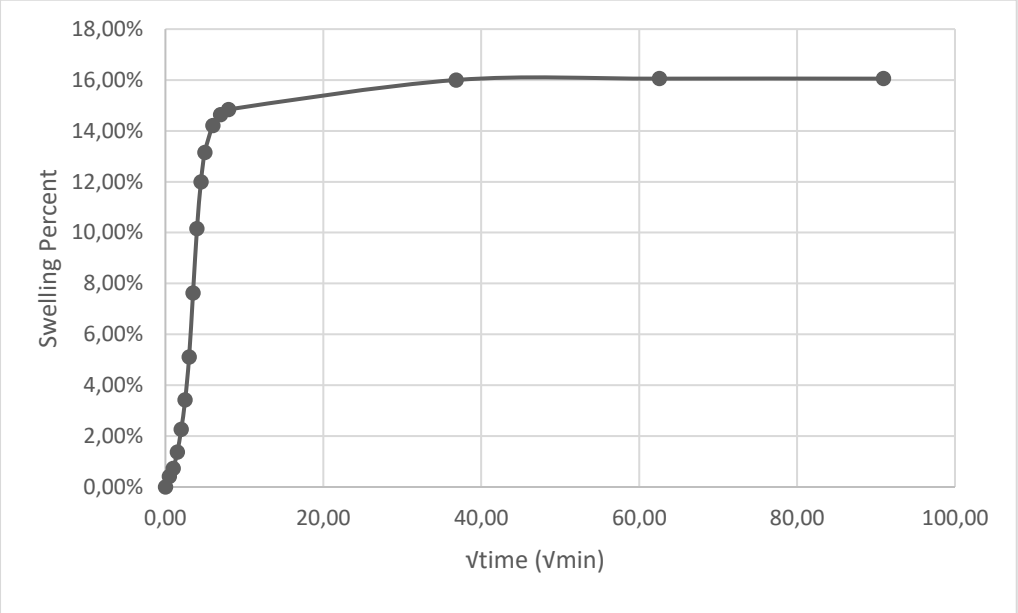

Figure A - 4. Swelling percent versus square root of time graph of non-cured Sample #4

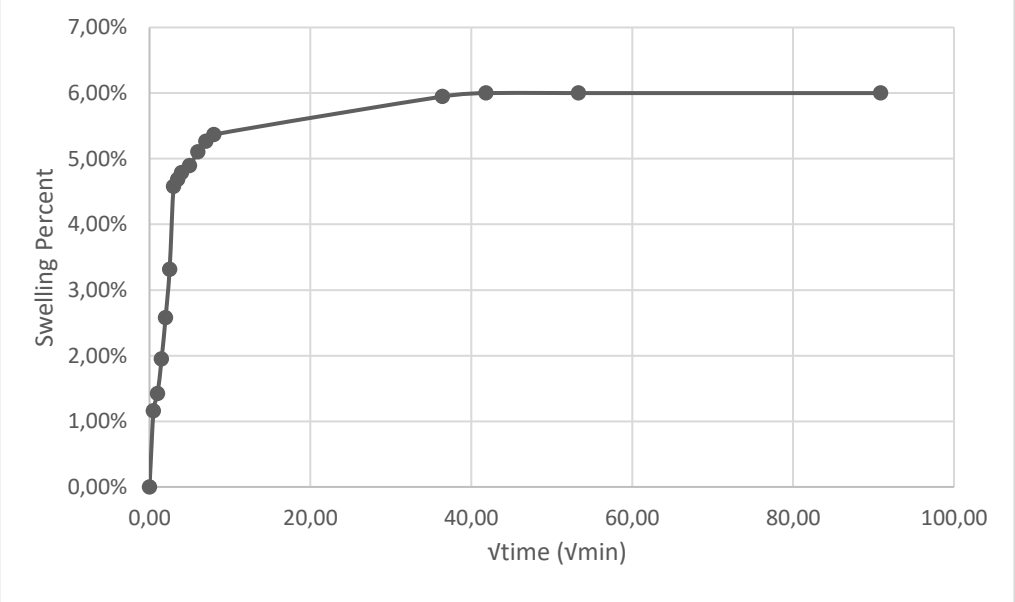

Figure A - 5. Swelling percent versus square root of time graph of non-cured Sample #5

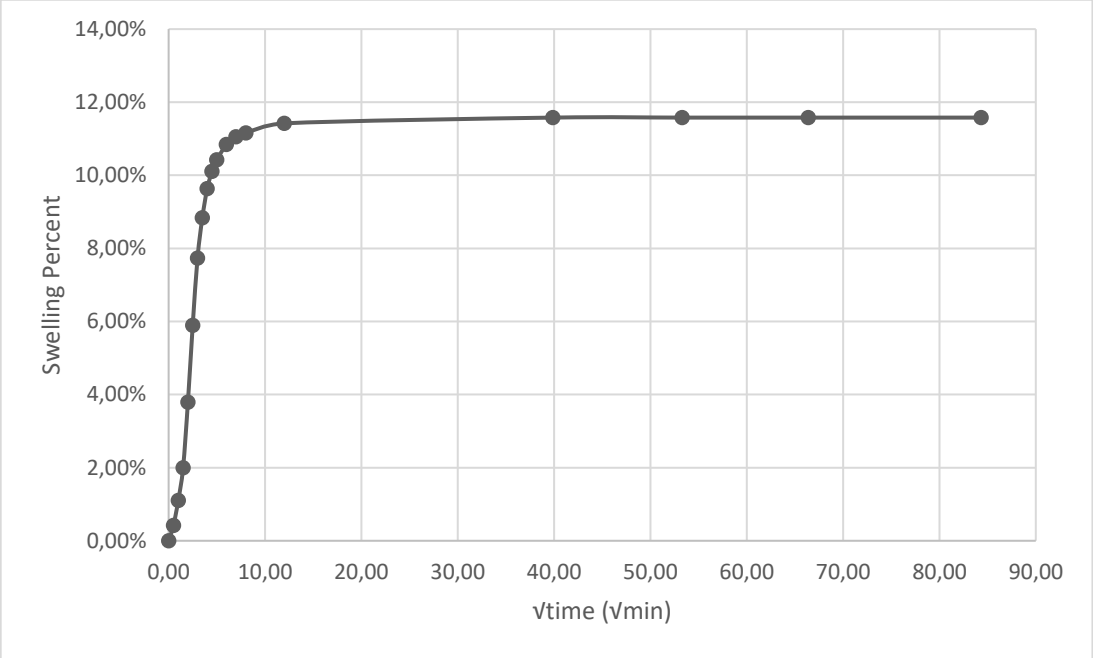

Figure A - 6. Swelling percent versus square root of time graph of non-cured Sample #6

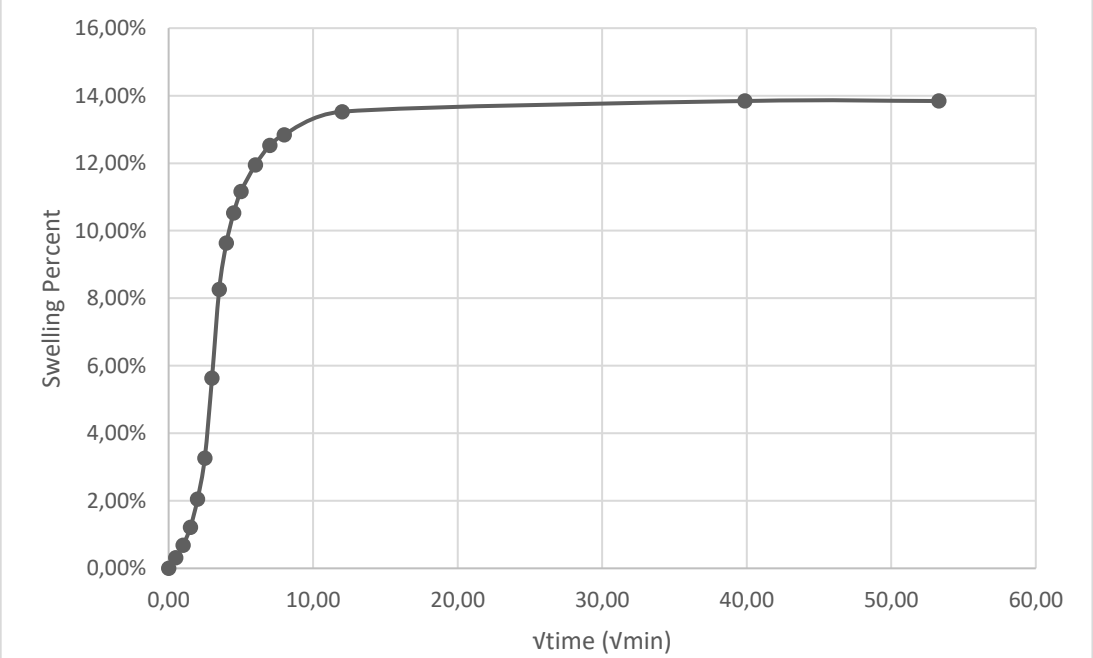

Figure A - 7. Swelling percent versus square root of time graph of non-cured Sample #7

The swelling vs square root of time graphs of the 7-day cured samples, which are obtained from the free swell tests, are shown below.

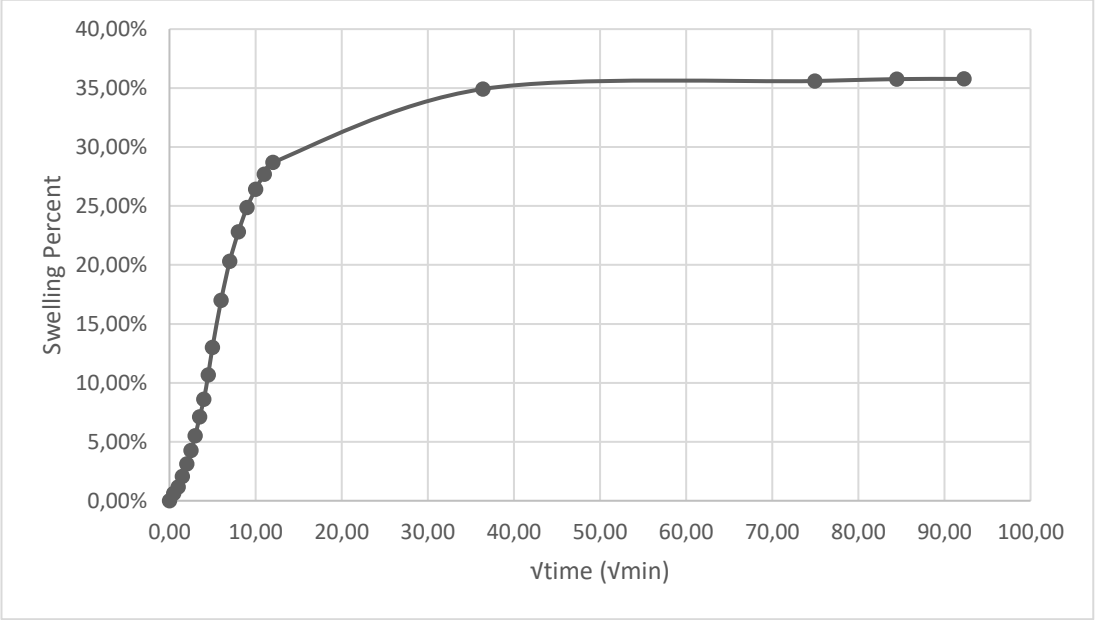

Figure A - 8. Swelling percent versus square root of time graph of 7-day cured Sample #1

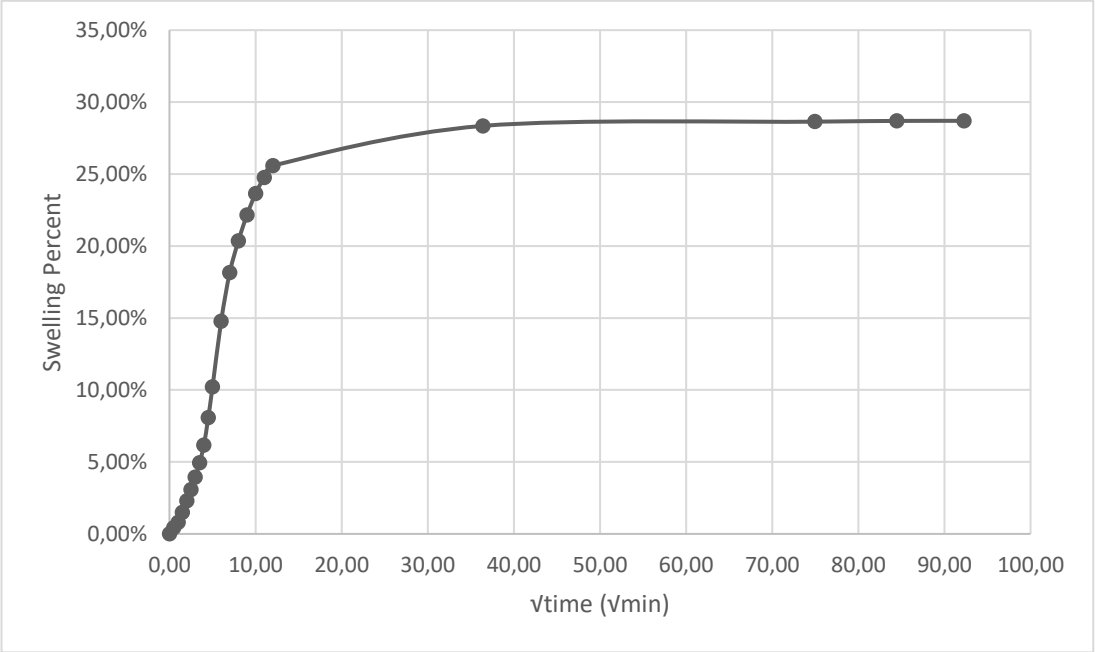

Figure A - 9. Swelling percent versus square root of time graph of 7-day cured Sample #2

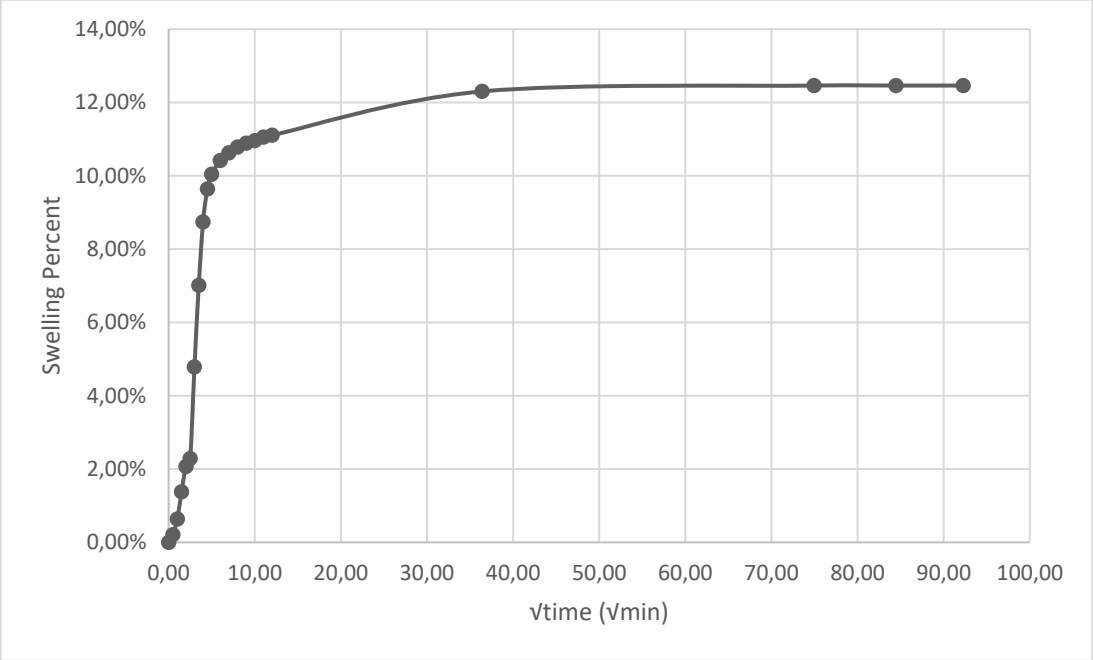

Figure A - 10. Swelling percent versus square root of time graph of 7-day cured Sample #3

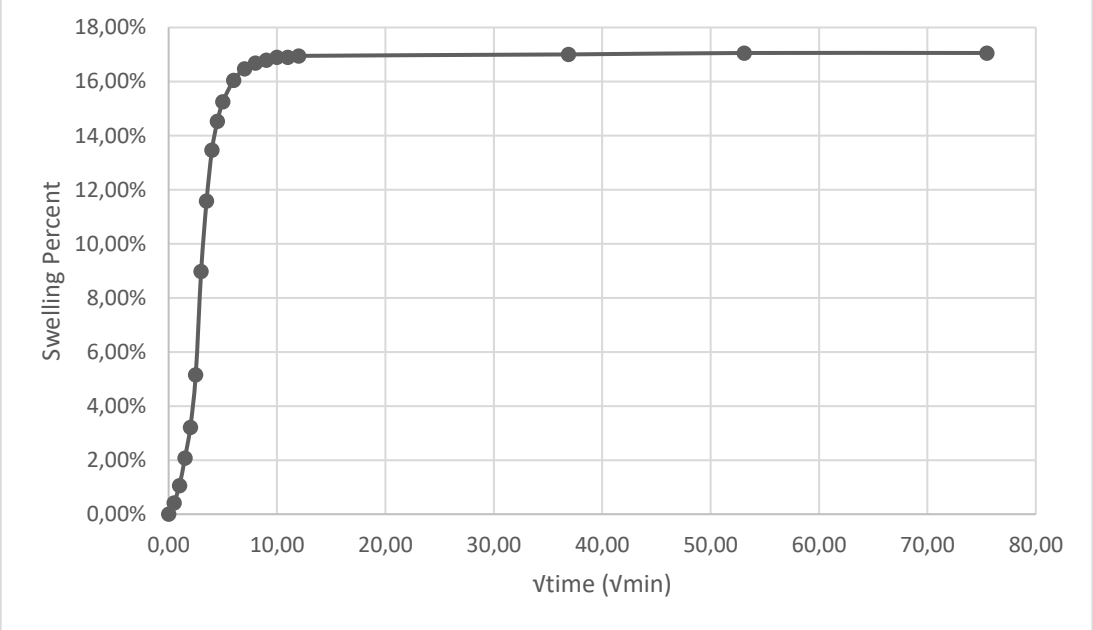

Figure A - 11. Swelling percent versus square root of time graph of 7-day cured Sample #4

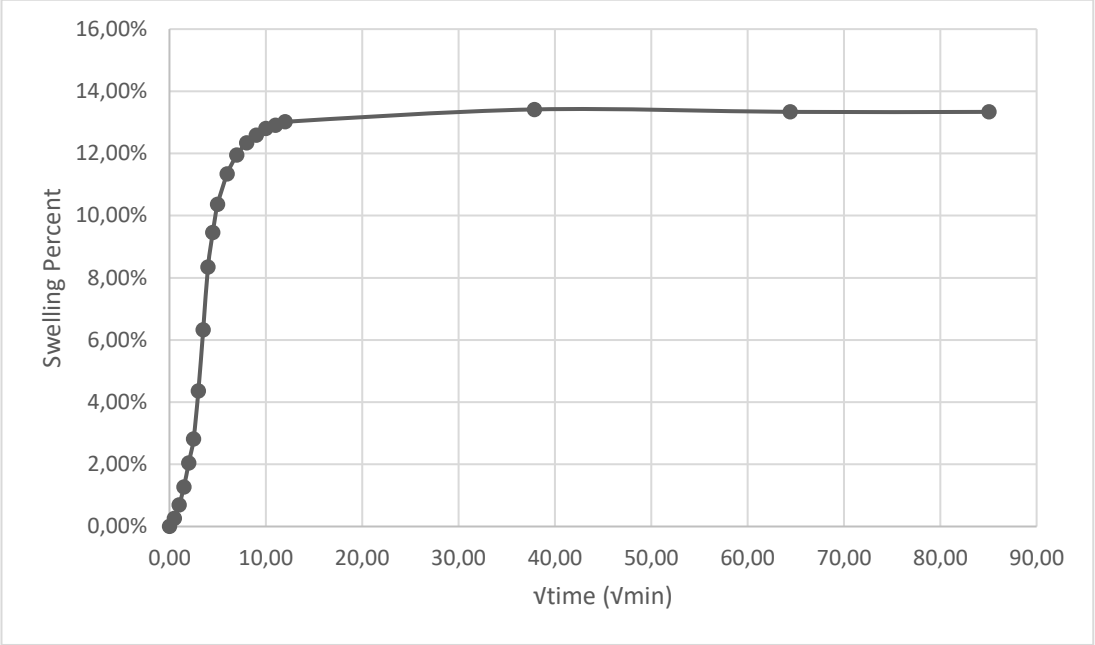

Figure A - 12. Swelling percent versus square root of time graph of 7-day cured Sample #5

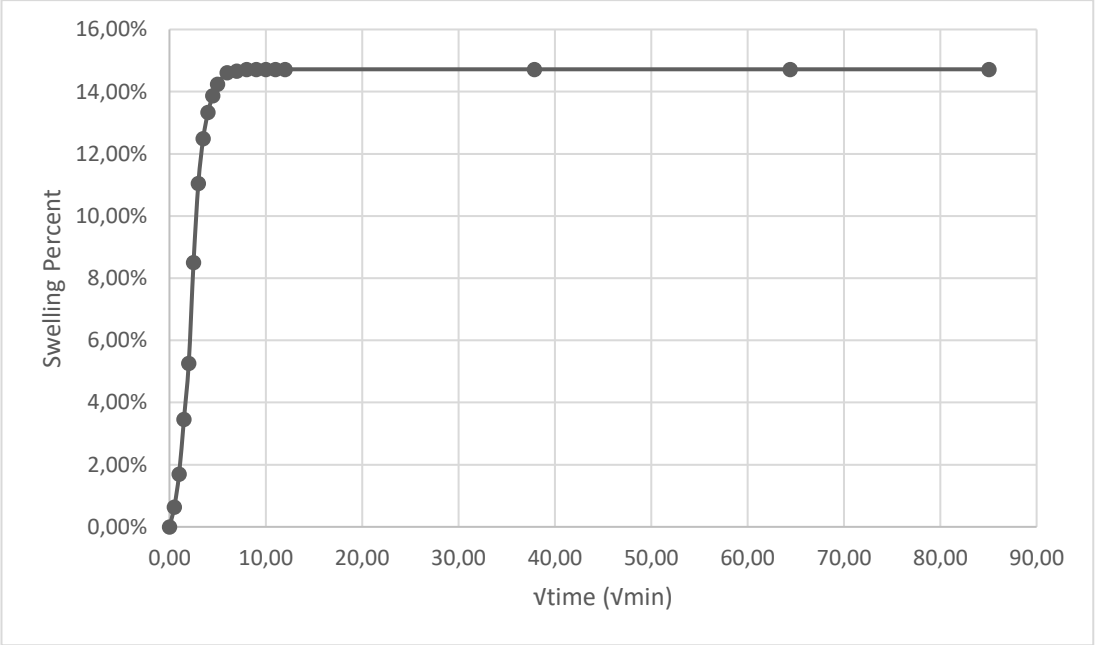

Figure A - 13. Swelling percent versus square root of time graph of 7-day cured Sample #6

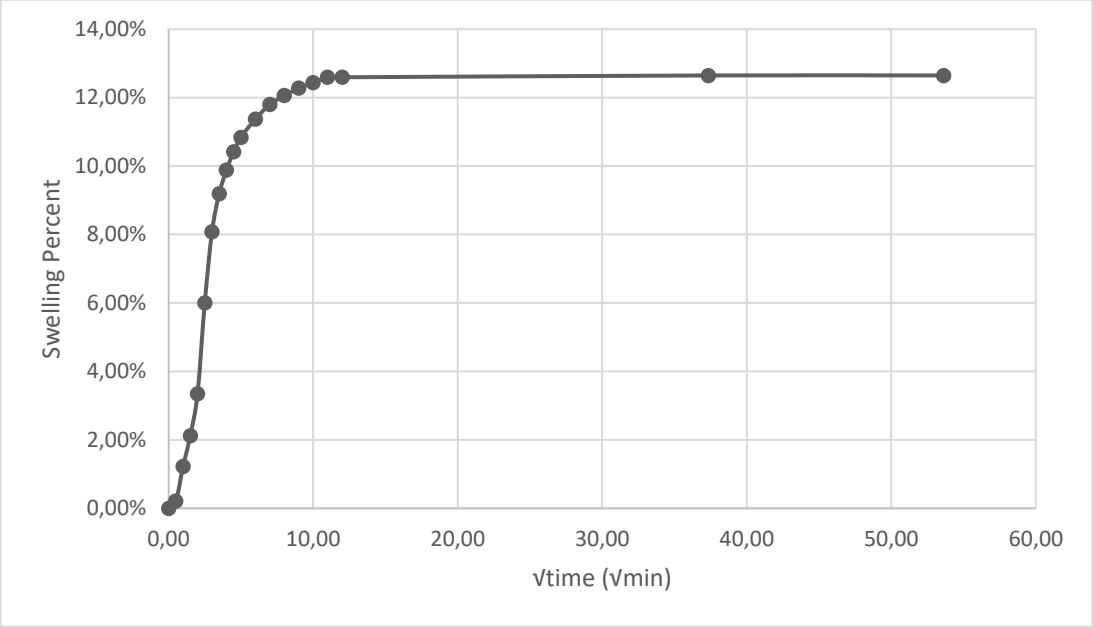

Figure A - 14. Swelling percent versus square root of time graph of 7-day cured Sample #7

The swelling vs square root of time graphs of the 28-day cured samples, which are obtained from the free swell tests, are shown below.

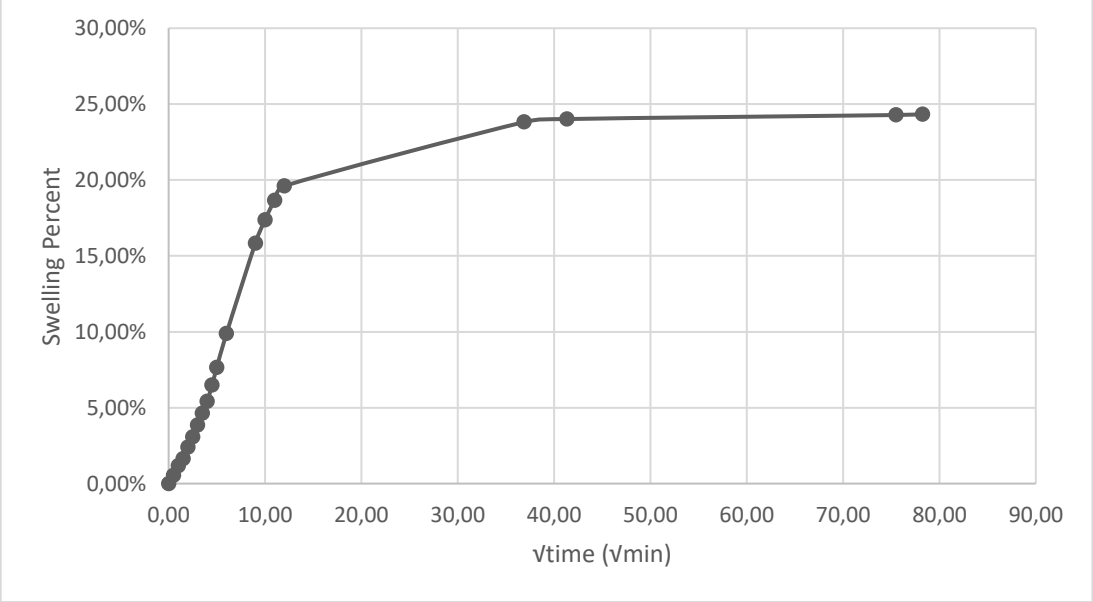

Figure A - 15. Swelling percent versus square root of time graph of 28-day cured Sample #1

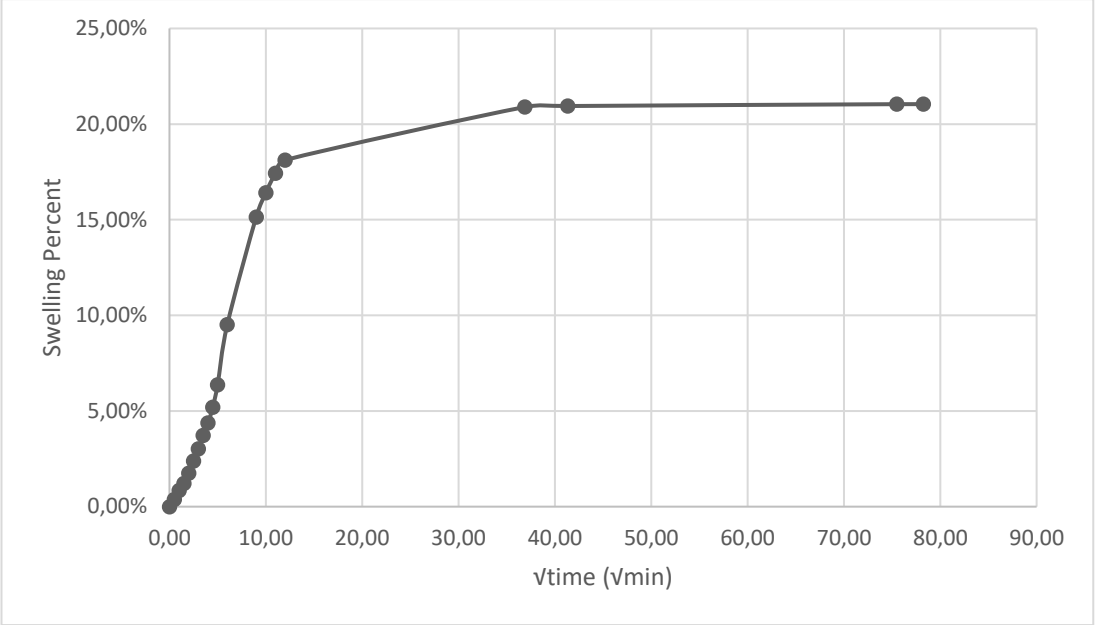

Figure A - 16. Swelling percent versus square root of time graph of 28-day cured Sample #2

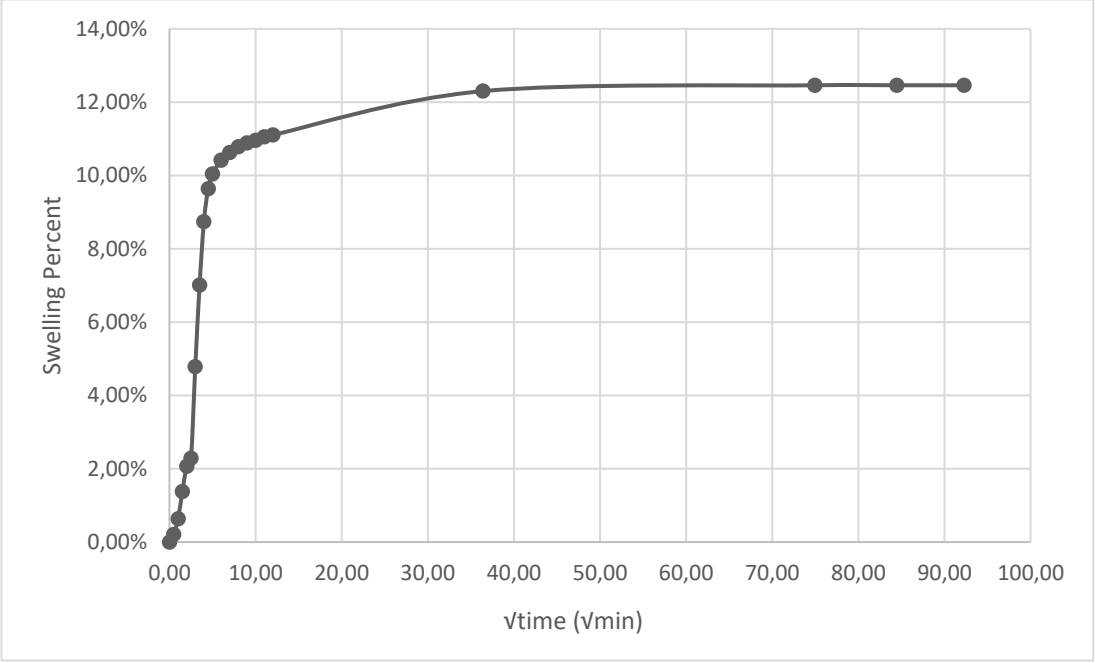

Figure A - 17. Swelling percent versus square root of time graph of 28-day cured Sample #3

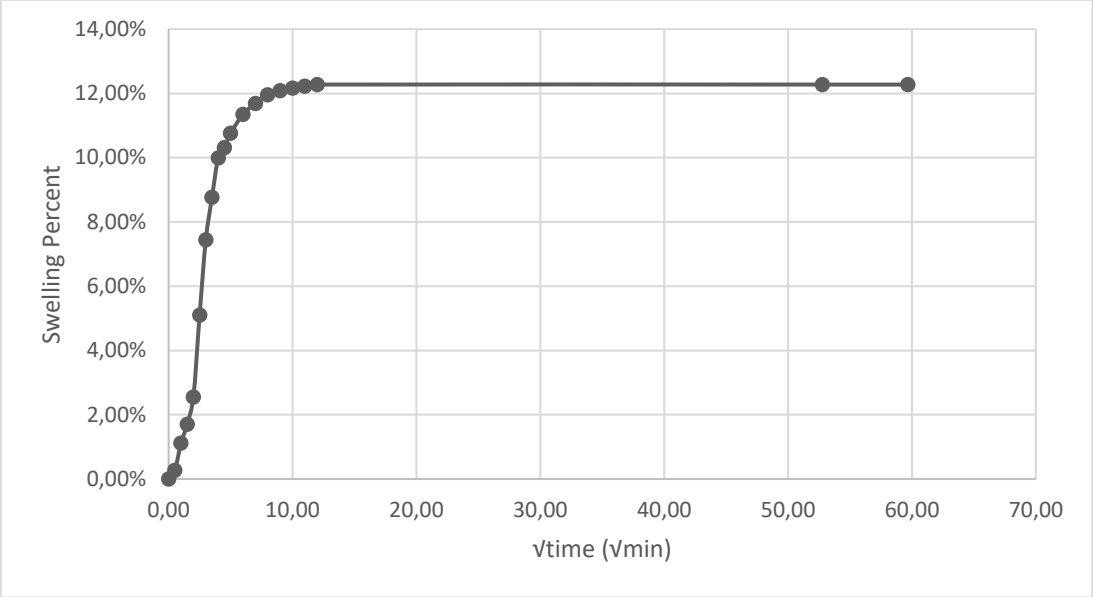

Figure A - 18. Swelling percent versus square root of time graph of 28-day cured Sample #4

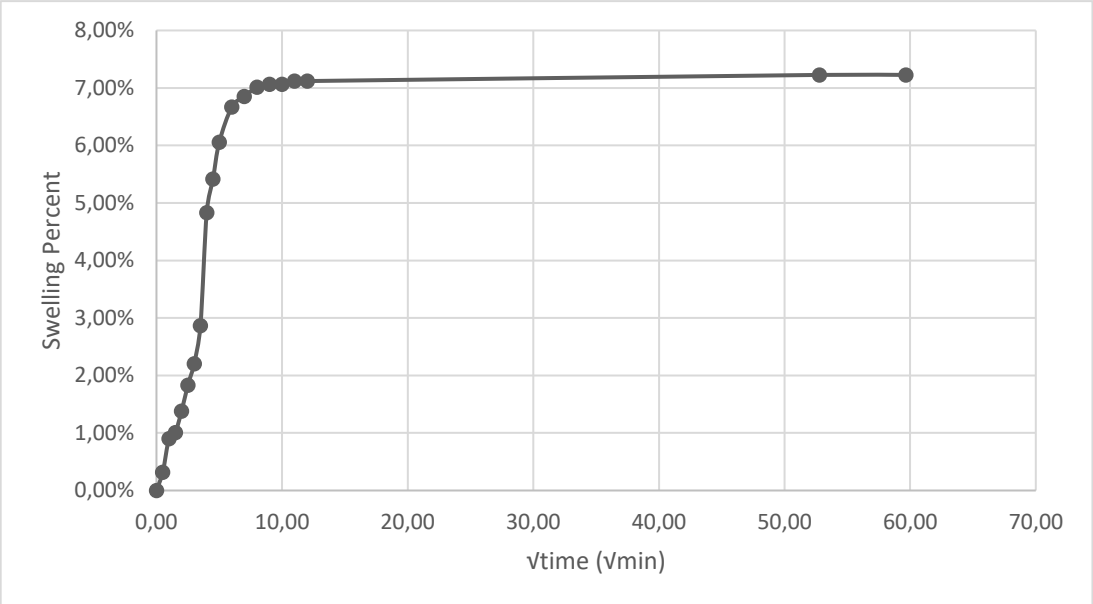

Figure A - 19. Swelling percent versus square root of time graph of 28-day cured Sample #5

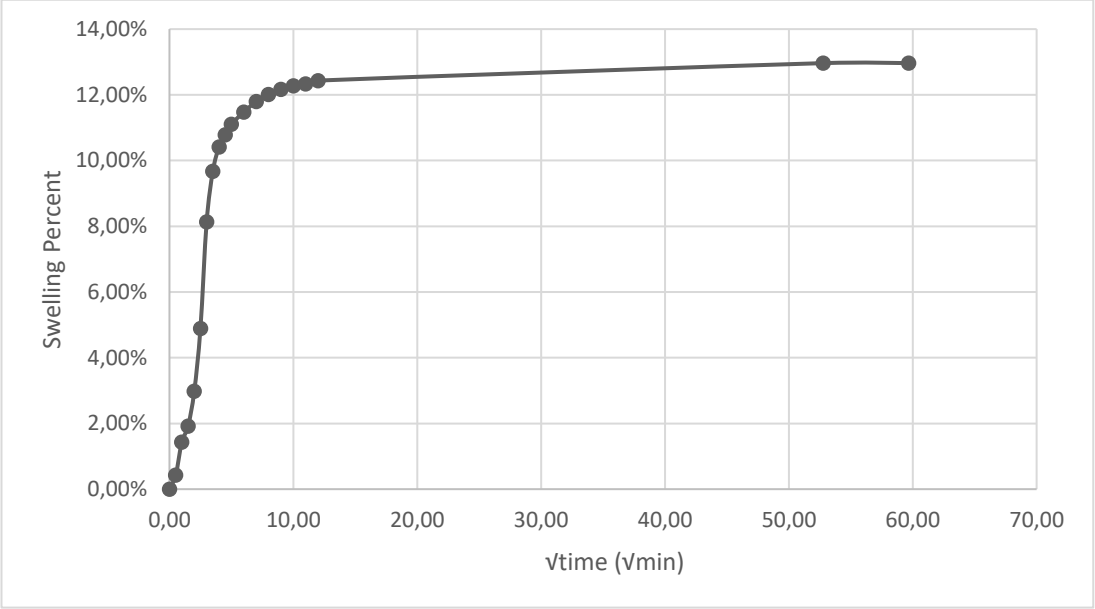

Figure A - 20. Swelling percent versus square root of time graph of 28-day cured Sample #6

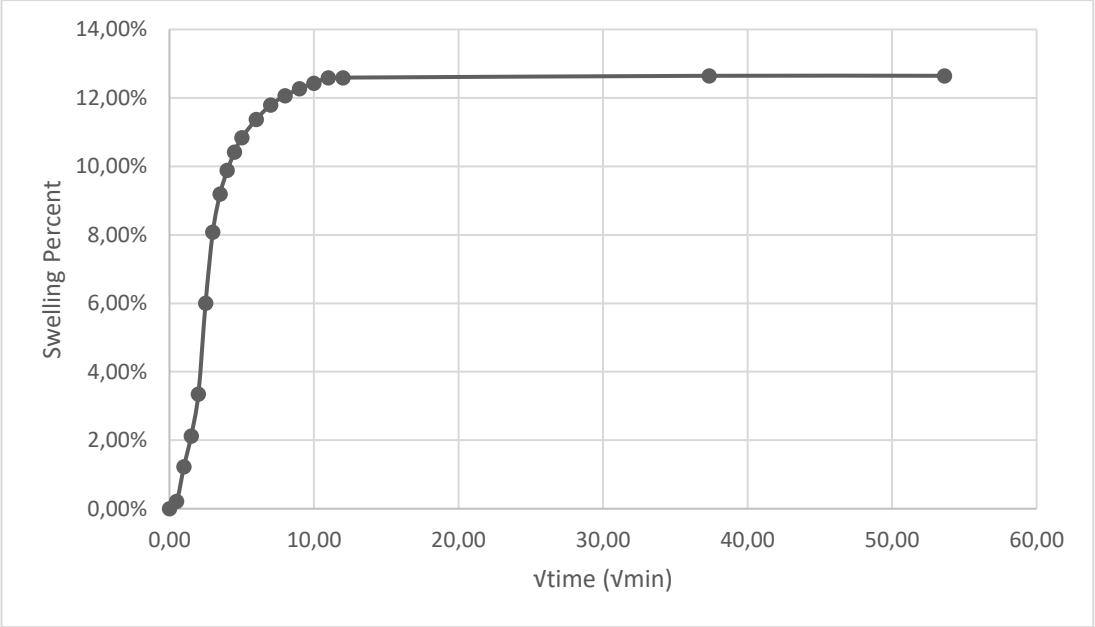

Figure A - 21. Swelling percent versus square root of time graph of 28-day cured Sample #7

B. Proctor Test Graphs of the Samples

The density vs. moisture content graphs of the samples are shown below.

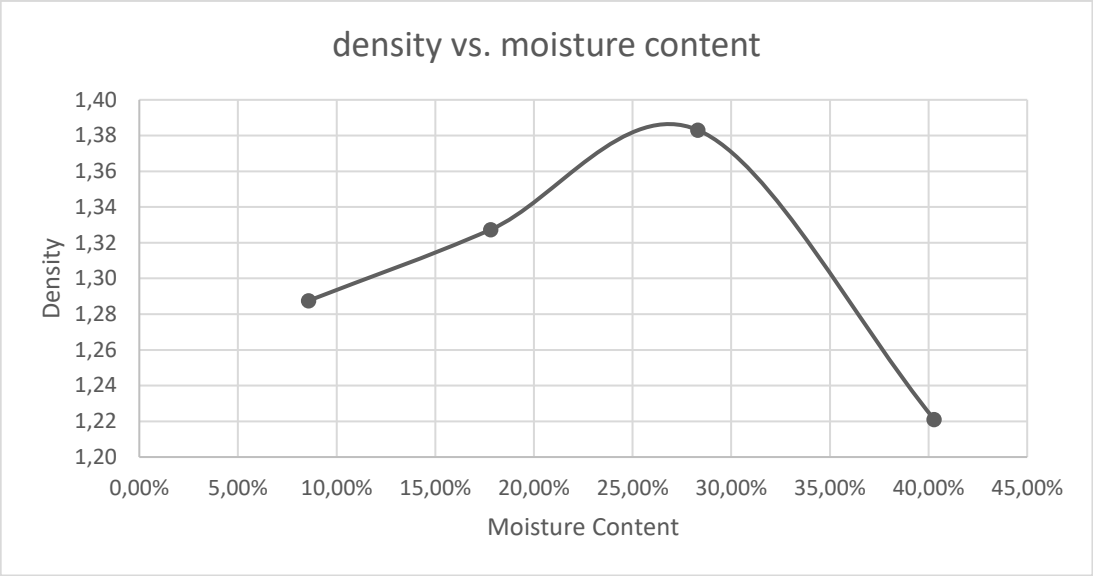

Figure B - 1. Density vs. moisture content graph of Sample #1

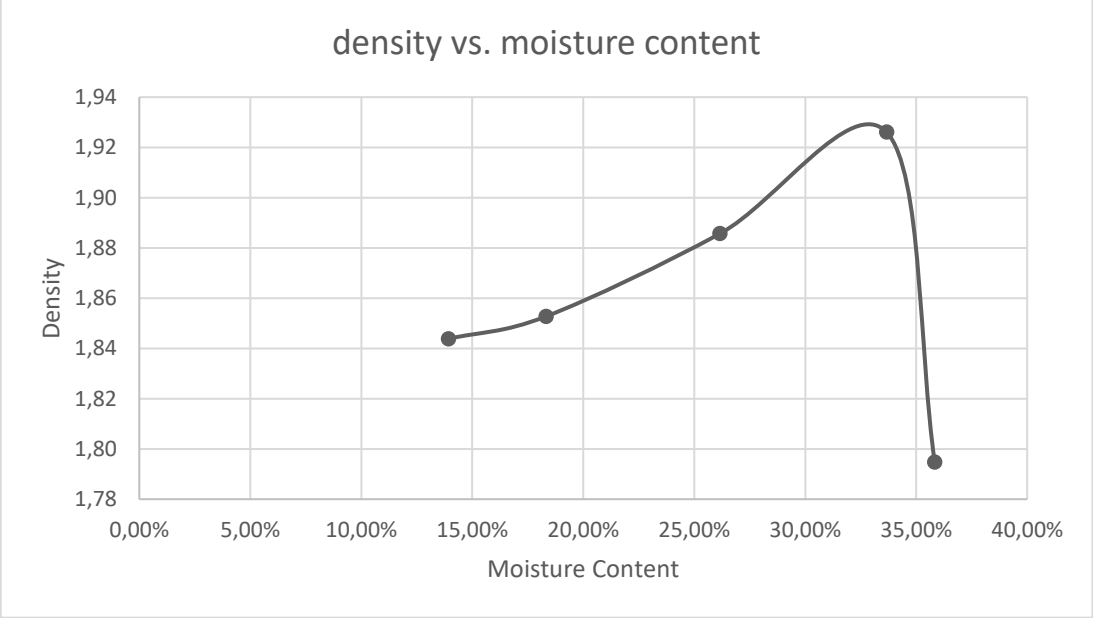

Figure B - 2. Density vs. moisture content graph of Sample #2

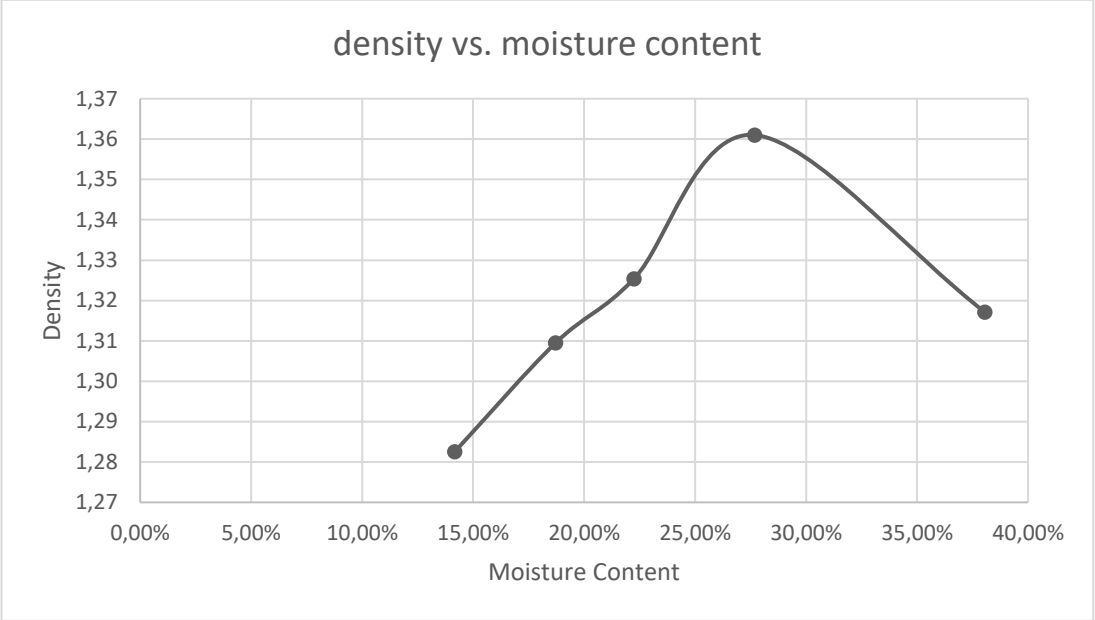

Figure B - 3. Density vs. moisture content graph of Sample #3

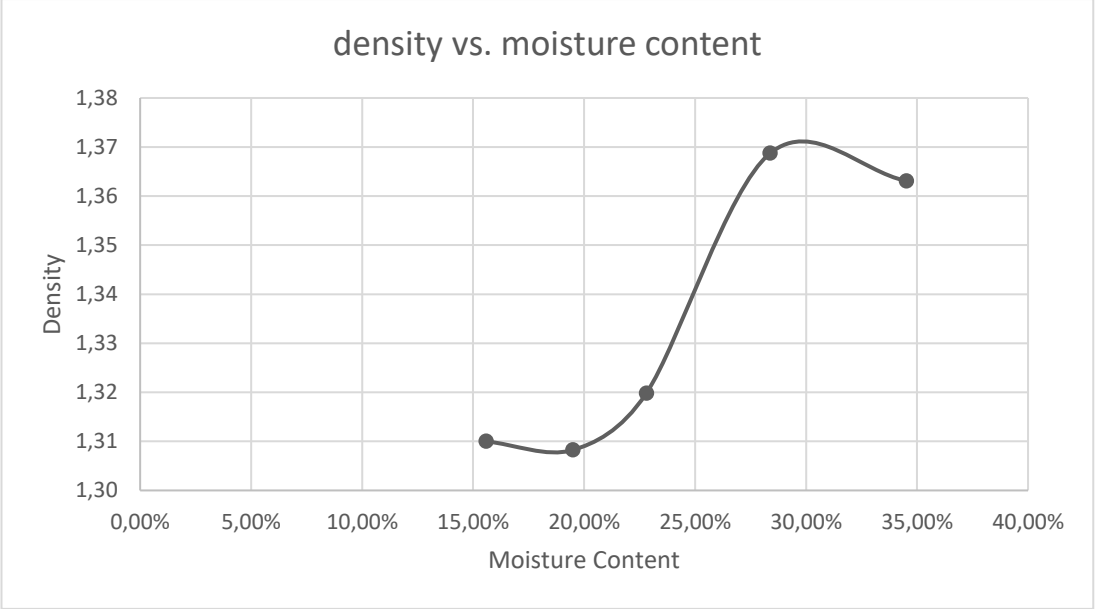

Figure B - 4. Density vs. moisture content graph of Sample #4

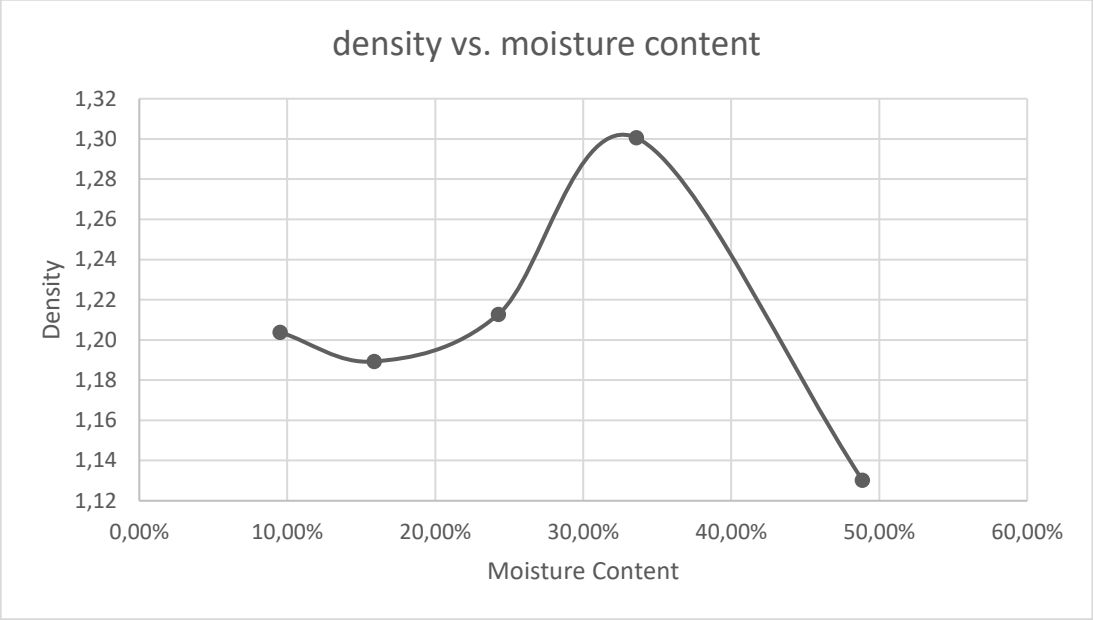

Figure B - 5. Density vs. moisture content graph of Sample #5

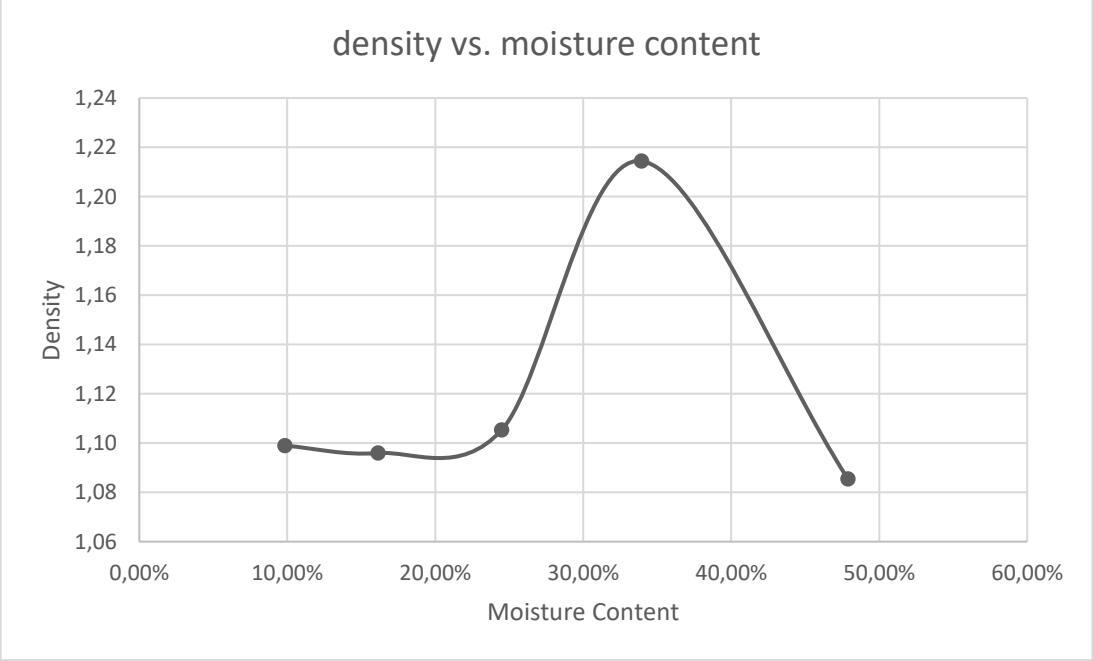

Figure B - 6. Density vs. moisture content graph of Sample #6

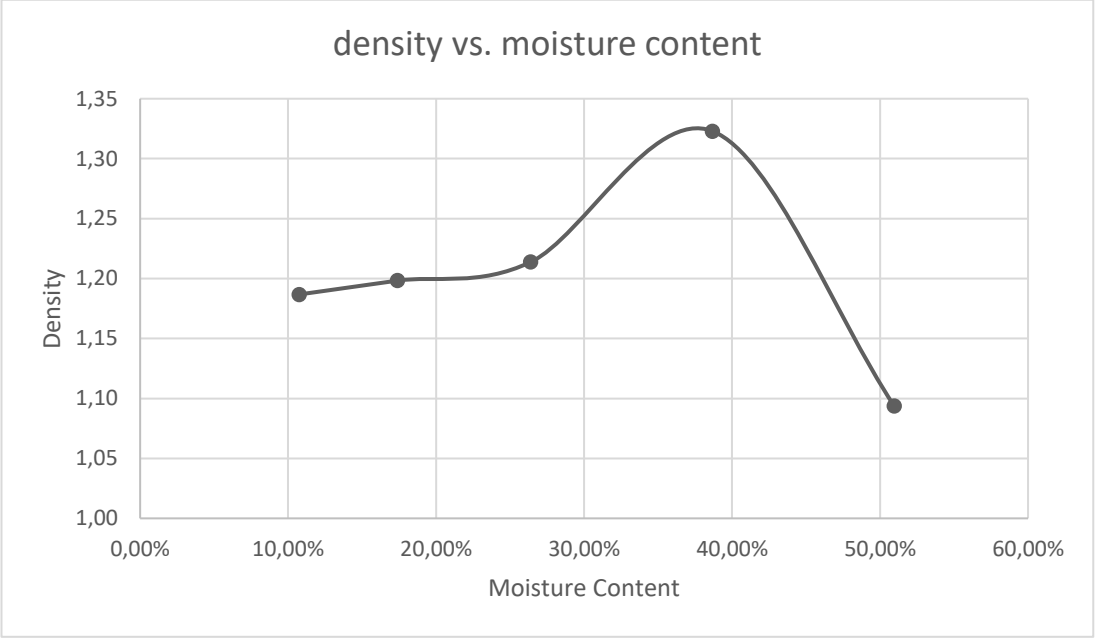

Figure B - 7. Density vs. moisture content graph of Sample #7

C. Bar Graphs of Swell Percentages and Rates of the Specimens

The swell percentage graphs of the non-cured, 7-day cured, and 28-day cured specimens are shown below.

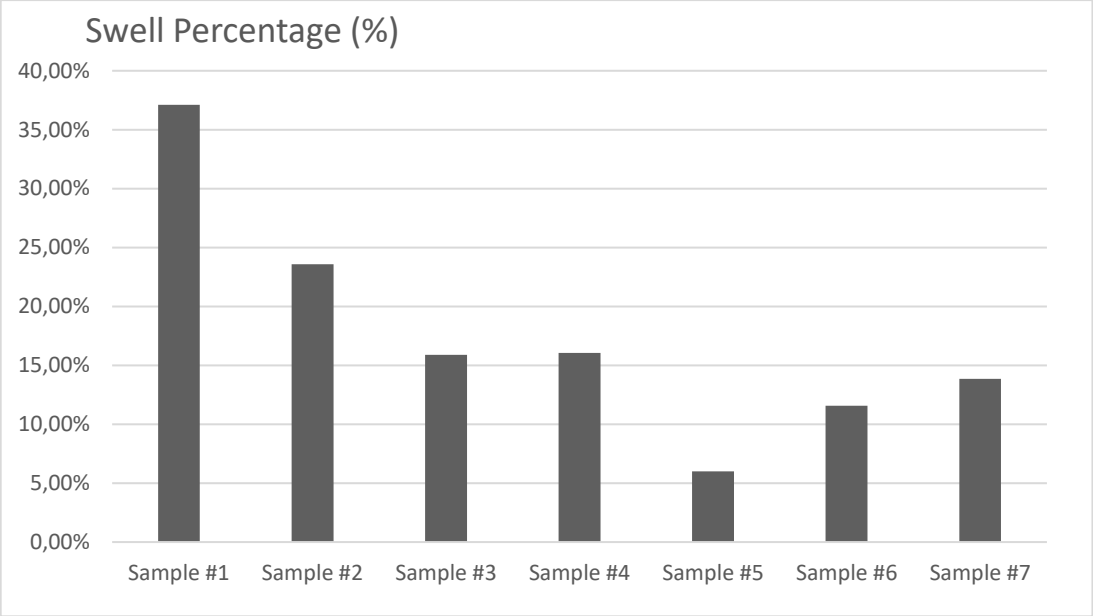

Figure C - 1. Swell percentage of the non-cured specimens

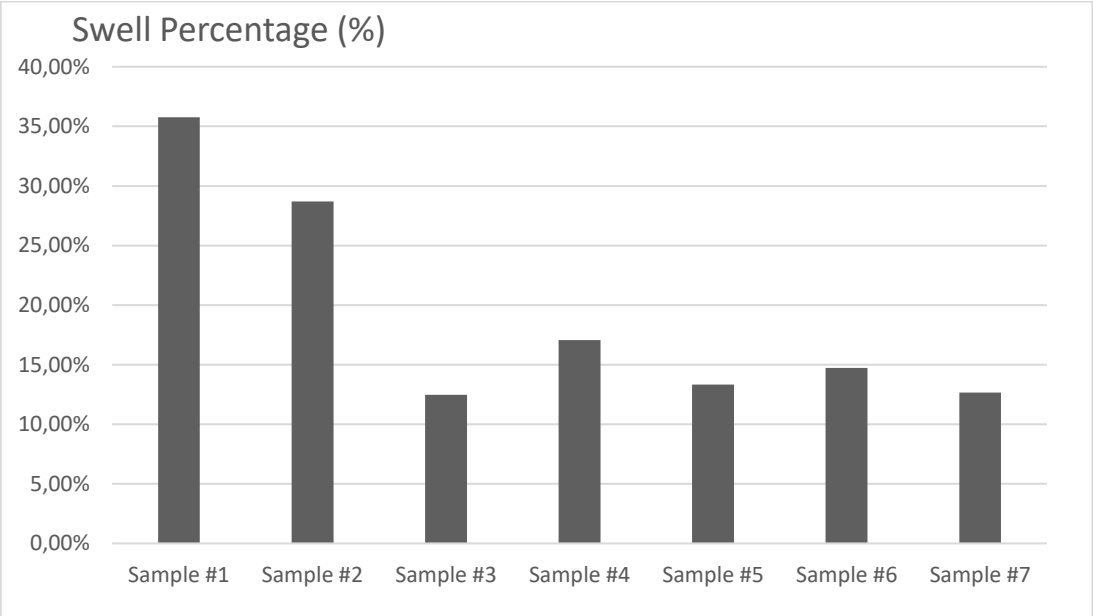

Figure C - 2. Swell percentage of the 7-day cured specimens

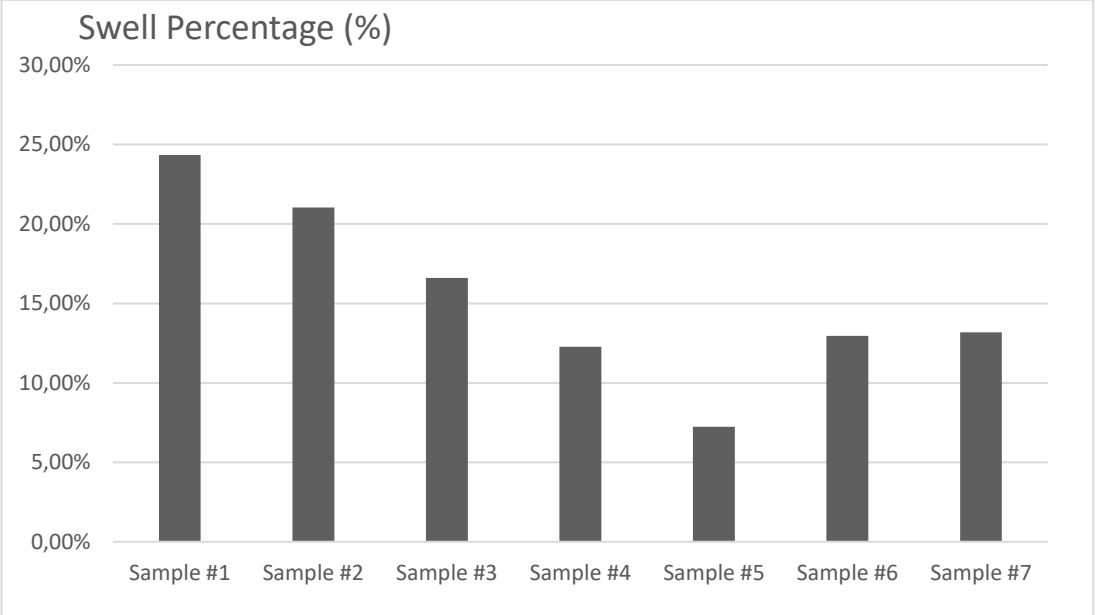

Figure C - 3. Swell percentage of the 28-day cured specimens

The swell rate graphs of the non-cured, 7-day cured, and 28-day cured specimens are shown below.

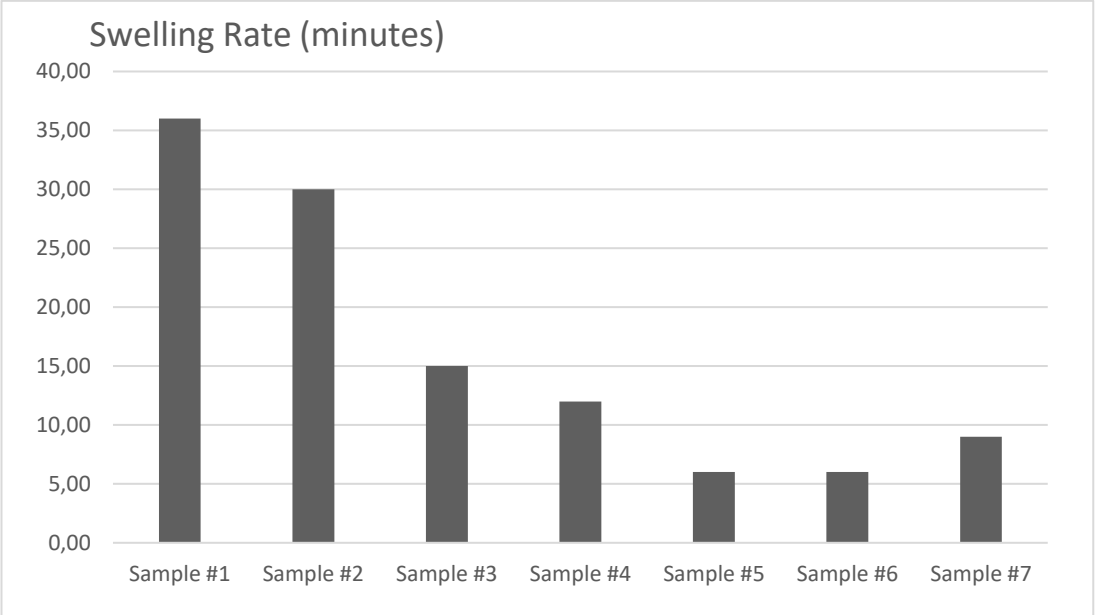

Figure C - 4. Swell rates of the non-cured specimens

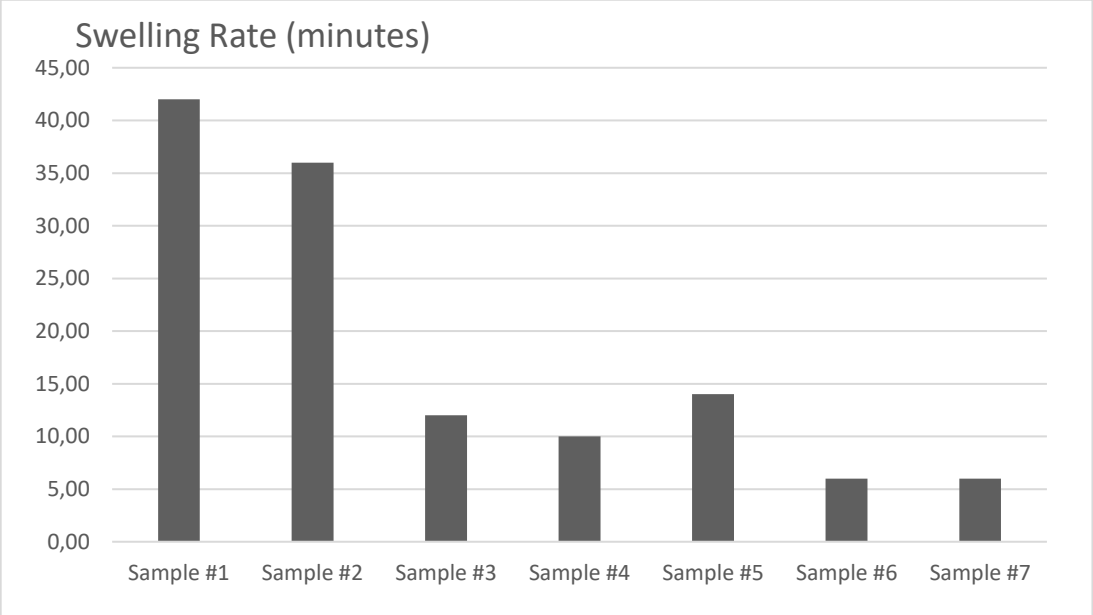

Figure C - 5. Swell rates of the 7-day cured specimens

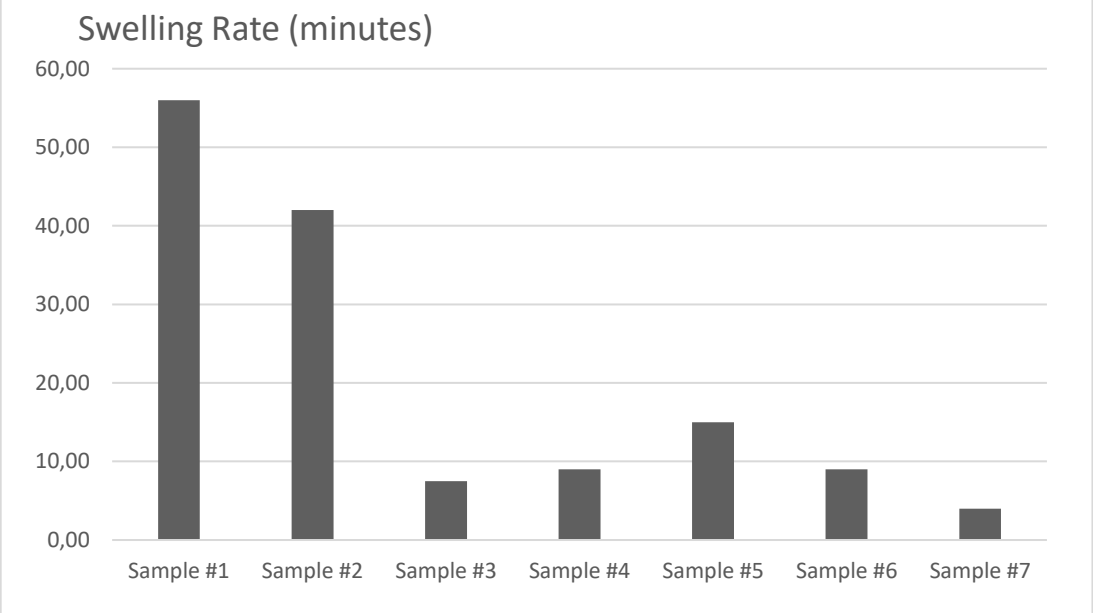

Figure C - 6. Swell rates of the 28-day cured specimens

D. Bar Graphs of Undrained Shear Strengths of the Specimens

The undrained shear strength graphs of the non-cured, 7-day cured, and 28-day cured specimens are shown below.

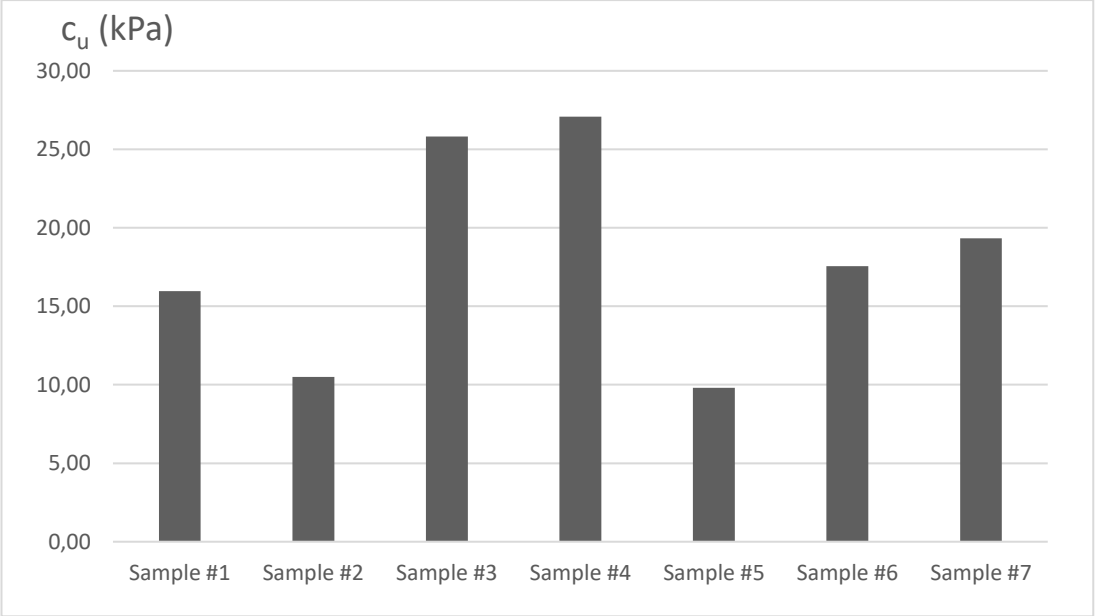

Figure D - 1. Undrained shear strengths of the non-cured specimens

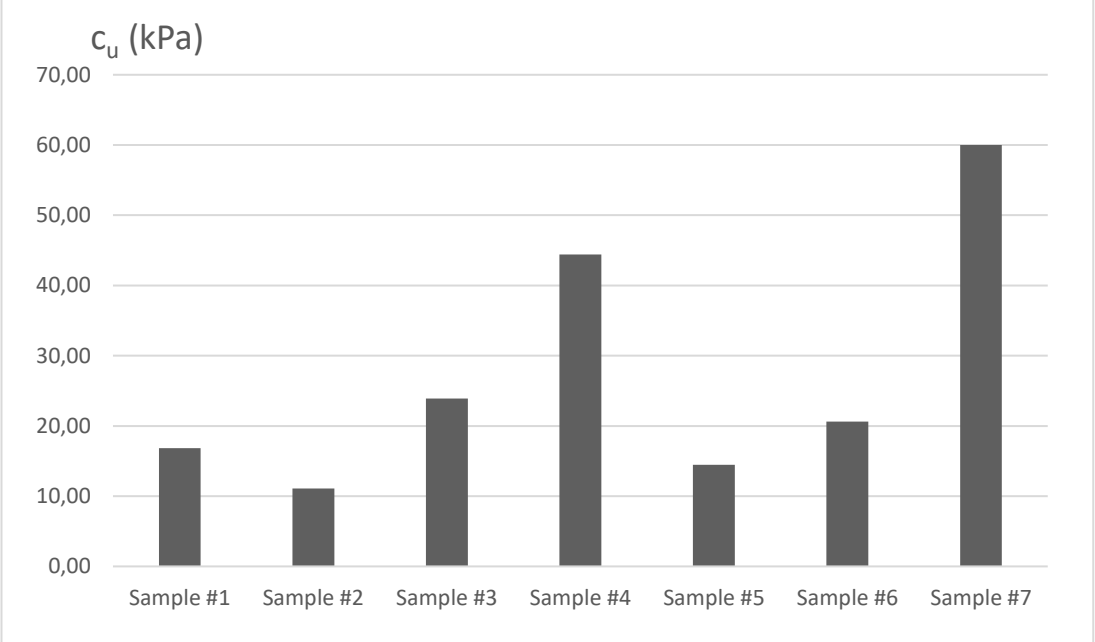

Figure D - 2. Undrained shear strengths of the 7-day cured specimens

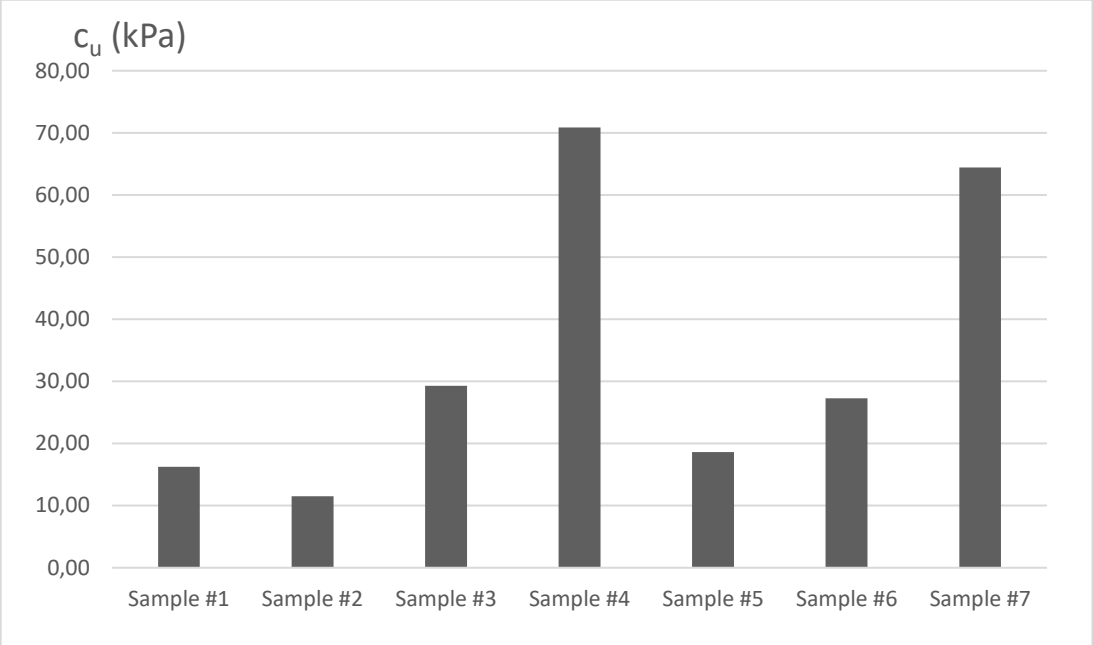

Figure D - 3. Undrained shear strengths of the 28-day cured specimens

E. Bar Graphs of Tensile Strength of the Specimens

The tensile strength graphs of the non-cured, 7-day cured, and 28-day cured specimens from direct tensile strength tests are shown below.

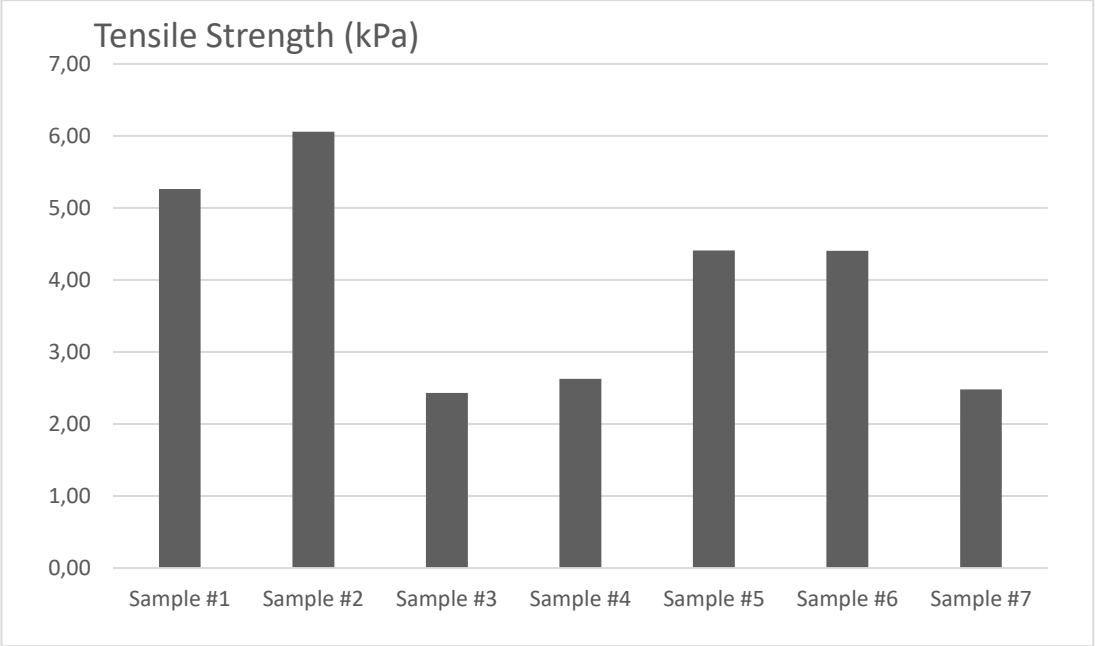

Figure E - 1. Tensile strengths of the non-cured specimens from direct tensile strength tests

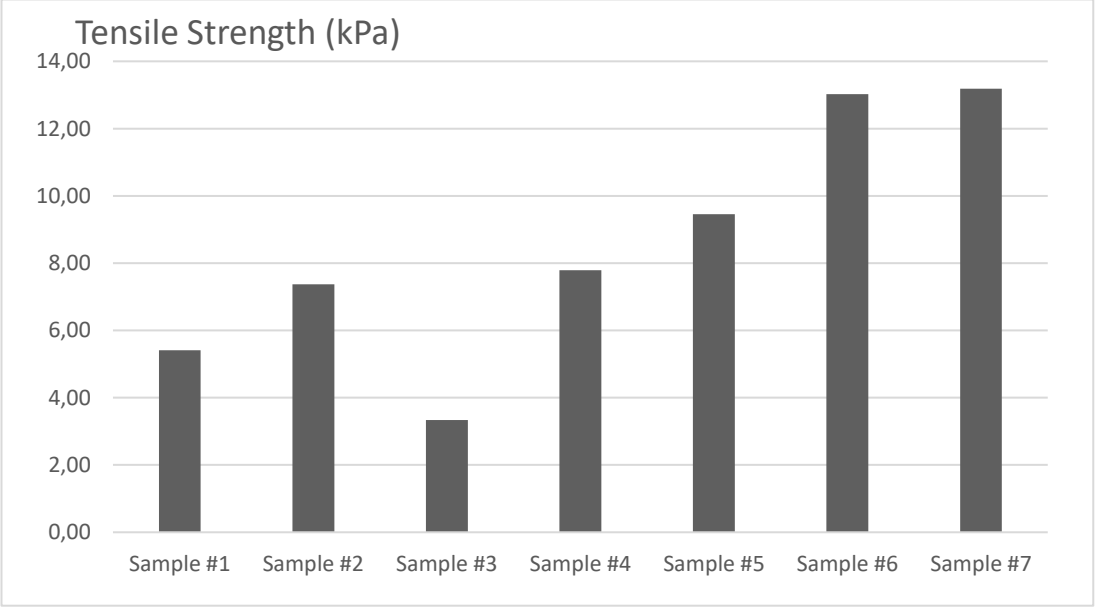

Figure E - 2. Tensile strengths of the 7-day cured specimens from direct tensile strength tests

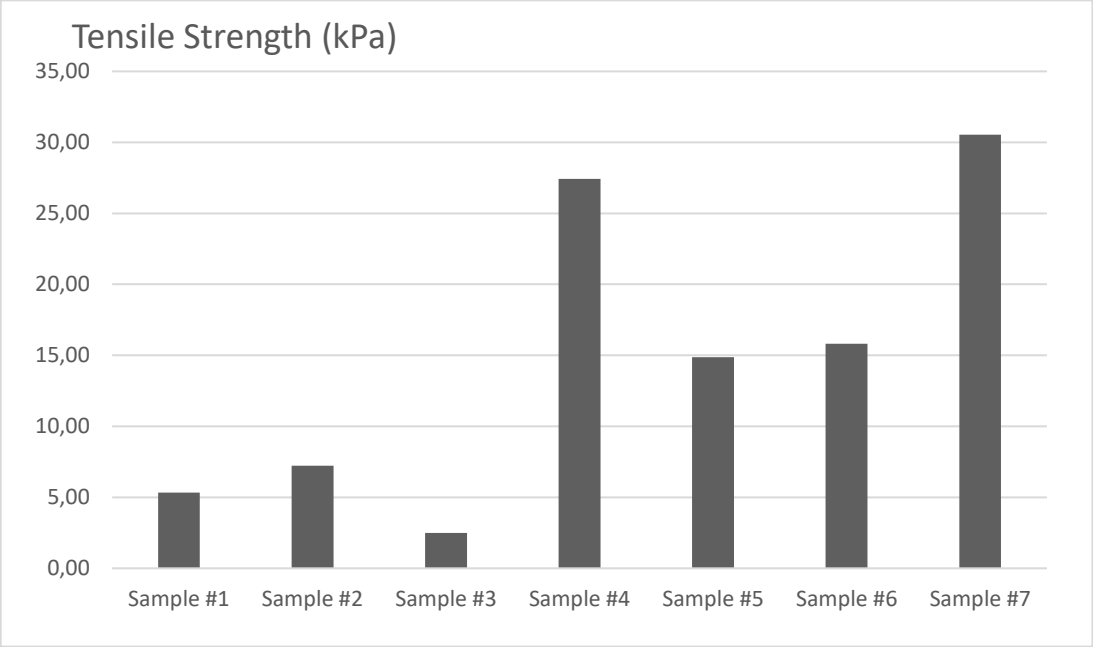

Figure E - 3. Tensile strengths of the 28-day cured specimens from direct tensile strength tests

The tensile strength graphs of the non-cured, 7-day cured, and 28-day cured specimens from split tensile strength tests are shown below.

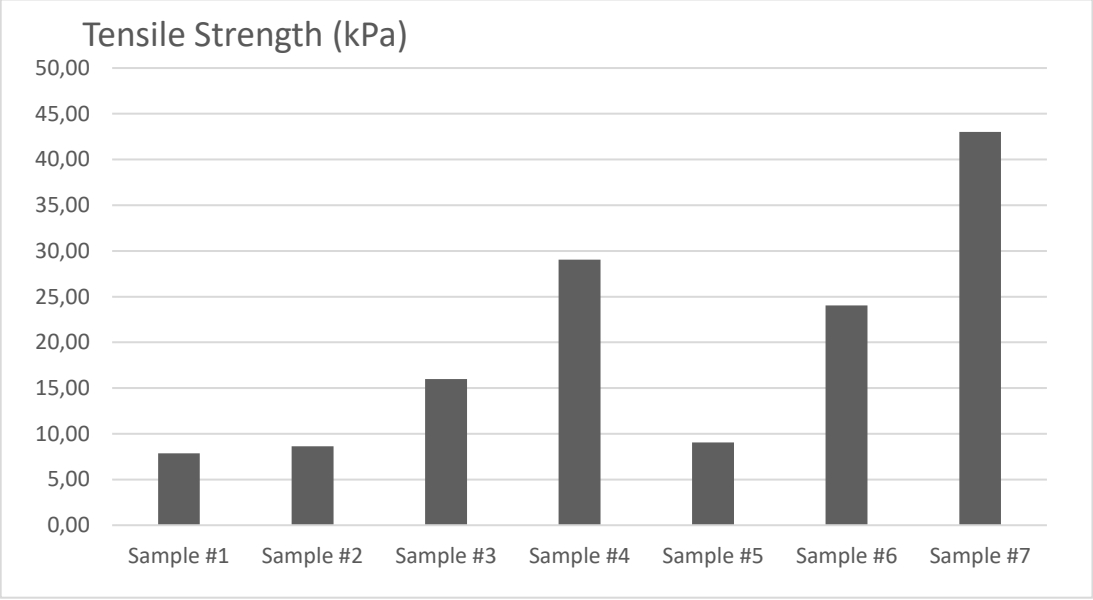

Figure E - 4. *Tensile strengths of the non-cured specimens from split tensile strength tests*

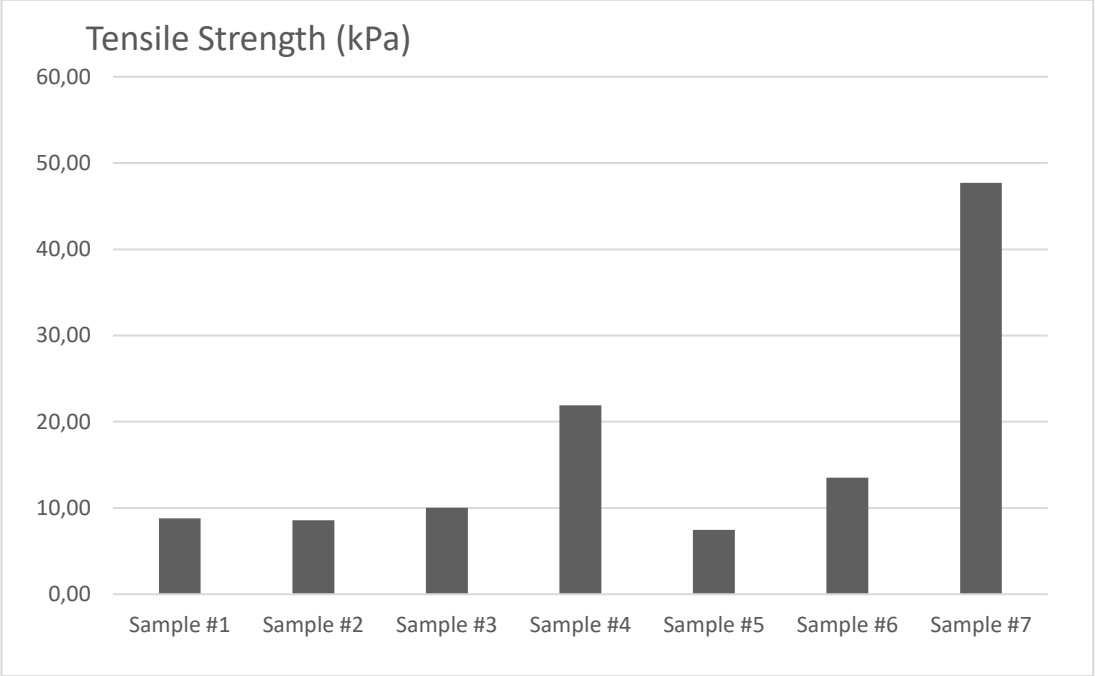

Figure E - 5. *Tensile strengths of the 7-day cured specimens from split tensile strength tests*

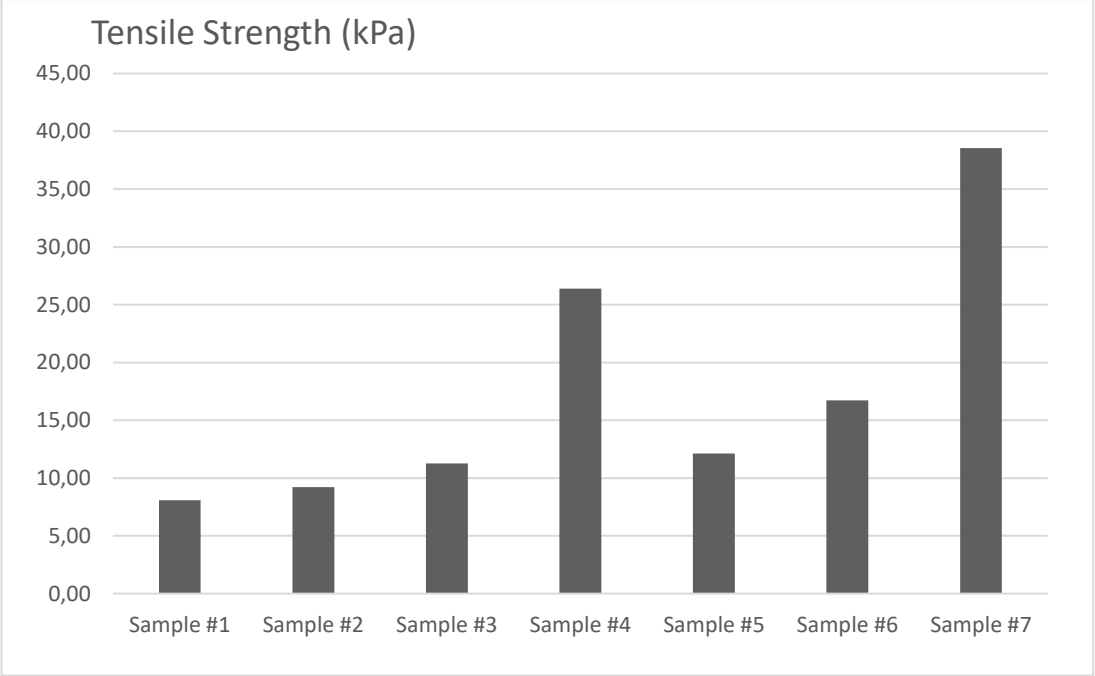

Figure E - 6. *Tensile strengths of the 28-day cured specimens from split tensile strength tests*

F. Bayer Process

The following figures have been taken from different internet websites and combined together.

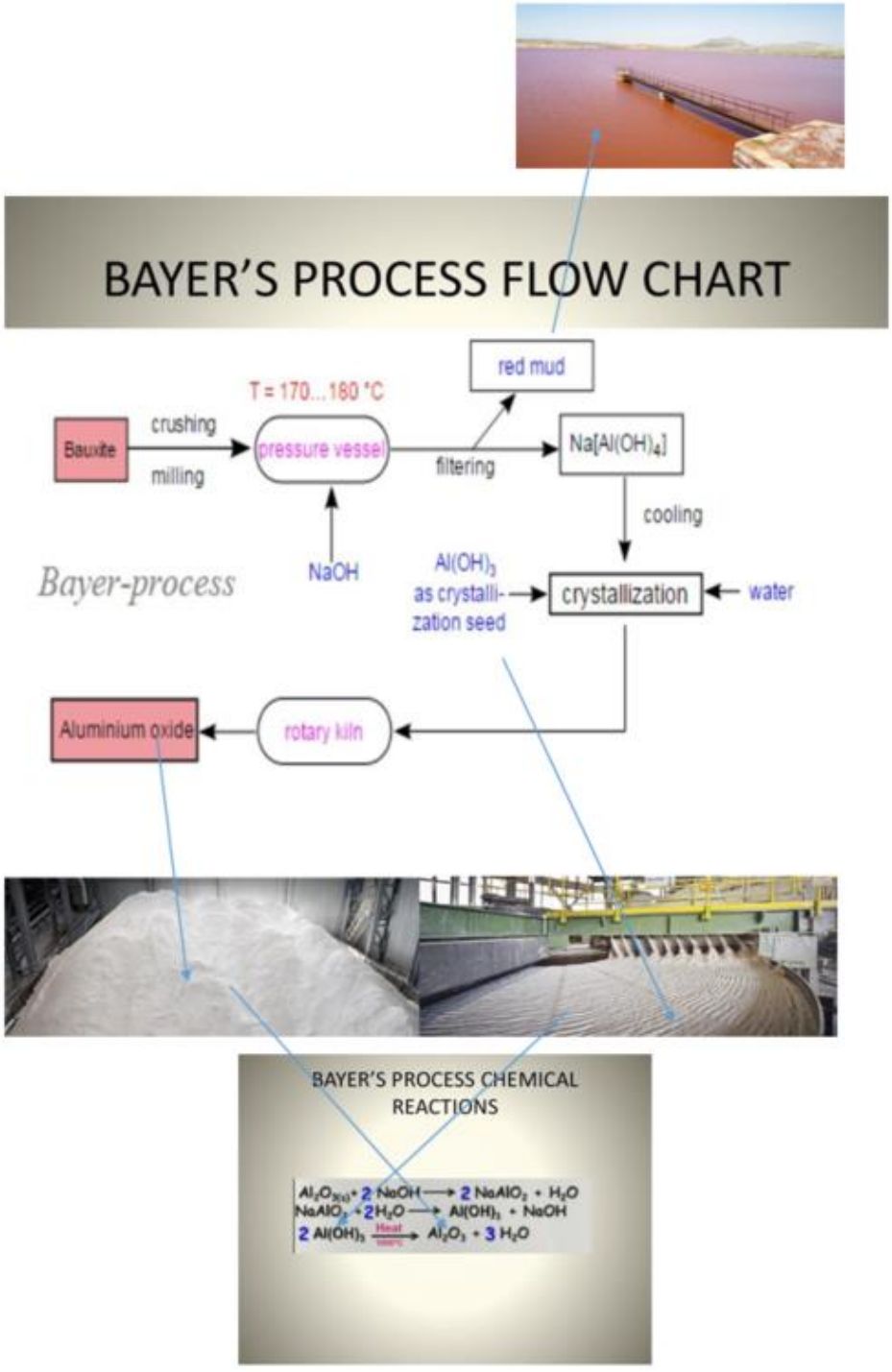

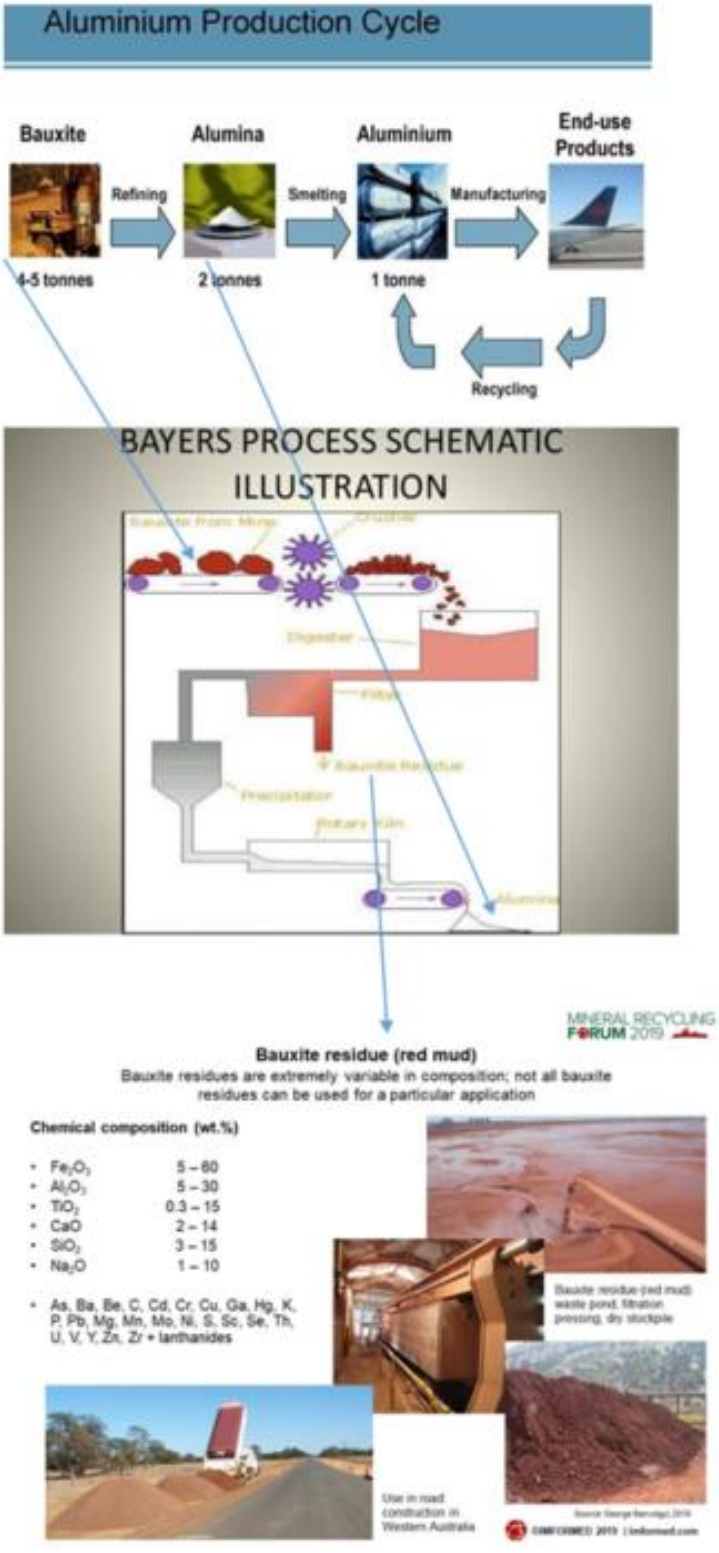
Aluminium Production Cycle
Bauxite
Alumina
Aluminium
End-use Products
Refining
Smelting
Manufacturing
4-5 tonnes
2 tonnes
1 tonne
Recycling
BAYERS PROCESS SCHEMATIC ILLUSTRATION
MINERAL RECYCLING FORUM 2019
Bauxite residue (red mud)
Bauxite residues are extremely variable in composition; not all bauxite residues can be used for a particular application
Chemical composition (wt.%)
• Fe_2O_3 5 – 60
• Al_2O_3 5 – 30
• TiO_2 0.3 – 15
• CaO 2 – 14
• SiO_2 3 – 15
• Na_2O 1 – 10
• As, Ba, Be, C, Cd, Cr, Cu, Ga, Hg, K, P, Pb, Mg, Mn, Mo, Ni, S, Sc, Se, Th, U, V, Y, Zn, Zr + lanthanides
Use in road construction in Western Australia